– **Typeset by GMNI &** FoilTEX –

SHARK-FV 2015 Conference
SHARING HIGHER-ORDER ADVANCED RESEARCH KNOW-HOW on FINITE VOLUME
Ofir, Portugal
May 18 - 22, 2015

# HIGHER-ORDER FINITE VOLUME METHODS WITH MOVING LEAST SQUARES APPROXIMATIONS


X. Nogueira[a], L. Ramírez[a], S. Khelladi[b],
J.C Chassaing[c], I. Colominas[a]

a: Dept. of Applied Mathematics
Civil Engineering School
University of A Coruña, Spain

b:Arts et Métiers Paris Tech
151 Boulevard de l'Hôpital
75013 Paris, France

c:Institute Jean Le Rond d'Alembert
Case 162, 4 Place Jussieu
75252 Paris, France

e-mail: xnogueira@udc.es
web page: http://caminos.udc.es/gmni

# Outline

- Introduction
- The FV-MLS method
- Multiscale properties of MLS: MLS-based shock detection
- A formulation for all-speed flows
- A MLS-based sliding mesh technique
- Application to Navier-Stokes-Korteweg equations
- Conclusions

# Outline

- Introduction
- The FV-MLS method
- Multiscale properties of MLS: MLS-based shock detection
- A formulation for all-speed flows
- A MLS-based sliding mesh technique
- Application to Navier-Stokes-Korteweg equations
- Conclusions

# A Coruña...OK. But... where is it?

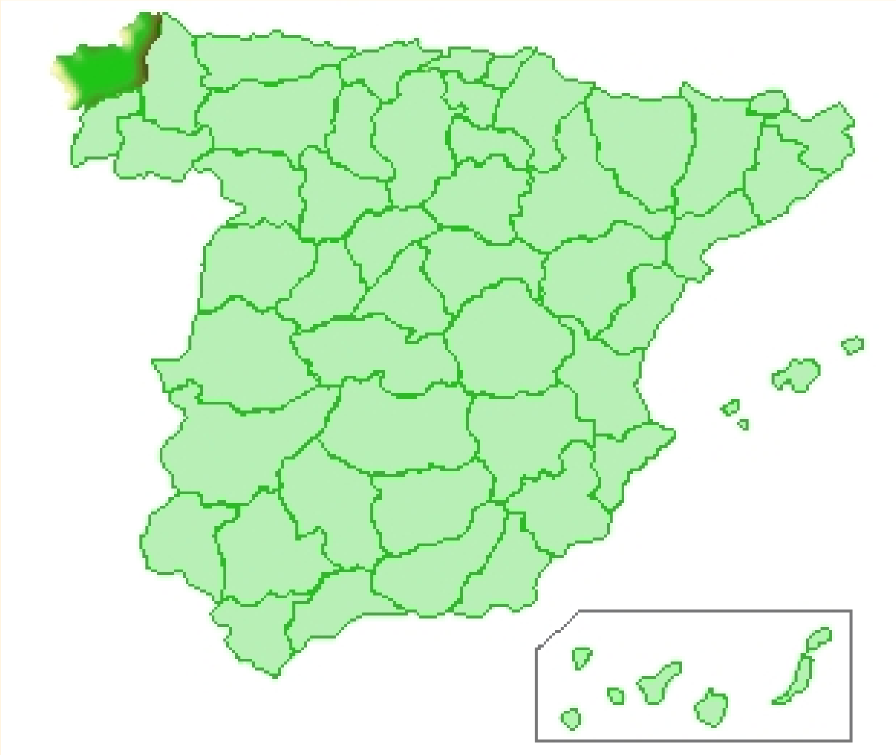

# A Coruña...OK. But... where is it?



# A Coruña...OK. But... where is it?



# It's in Galicia

SHARK-FV 2015 Conference
SHARING HIGHER-ORDER ADVANCED RESEARCH KNOW-HOW on FINITE VOLUME
Ofir, Portugal
May 18 - 22, 2015

# It's in Galicia

# It's in Galicia

# It's in Galicia

# Introduction



- Origin of this research:
  - Development of more accurate numerical methods for turbomachinery.
  - Standard industrial codes: $2^{nd}$ order.
  - We need high-resolution schemes for unstructured grids.
  - Turbomachinery $\Rightarrow$ Relative motion rotor/stator.

# Introduction

- It is not straightforward to obtain finite volume methods with order higher than two on unstructured grids.
- One of the main difficulties is the computation of high-order derivatives.

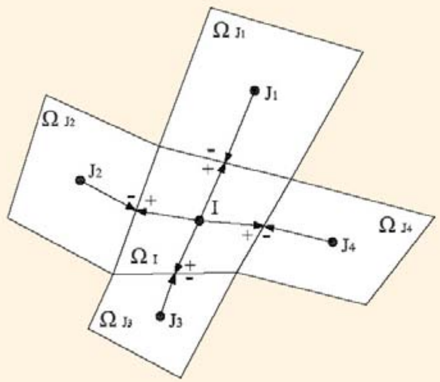

# Outline

- Introduction
- The FV-MLS method
- Multiscale properties of MLS: MLS-based shock detection
- A formulation for all-speed flows
- A MLS-based sliding mesh technique
- Application to Navier-Stokes-Korteweg equations
- Conclusions

# The MLS method in a nutshell

- MLS is an approximation method very used by the meshless community.
- MLS performs a reconstruction of $\mathrm{u}(\boldsymbol{x})$ at a point $\boldsymbol{x}$ by using a weighted LS approximation in the vicinity of $\boldsymbol{x}$.
- The approximation is written in terms of MLS shape functions.

$$\boxed{\hat{u}(\boldsymbol{x}) = \sum_{j=1}^{n_{\mathrm{x}}} N_j(\boldsymbol{x}) u_j}$$

- The approximation basically depends on a kernel and a basis function.

# Kernel functions

- Many functions used as kernels: splines, gaussians
- An example, the cubic spline:

$$W_j(\boldsymbol{x}) = W(\boldsymbol{x}-\boldsymbol{x}_j, h) = \frac{\alpha}{h^\nu}\begin{cases} 1-\frac{3}{2}s^2+\frac{3}{4}s^3 & s \leq 1 \\ \frac{1}{4}(2-s)^3 & 1 < s \leq 2 \\ 0 & s > 2 \end{cases}$$

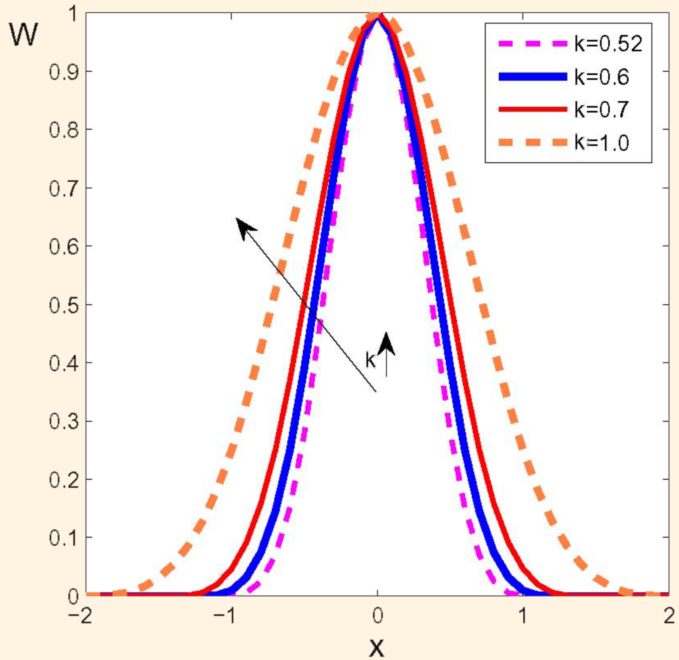


$$s = \frac{\|\boldsymbol{x}-\boldsymbol{x}_j\|}{h}$$

$$h = k\max\left(\|\boldsymbol{x}-\boldsymbol{x}_j\|\right)$$

# Kernel functions

- Many functions used as kernels: splines, gaussians
- An example, the cubic spline:

$$W_j(\boldsymbol{x}) = W(\boldsymbol{x} - \boldsymbol{x}_j, h) = \frac{\alpha}{h^\nu} \begin{cases} 1 - \frac{3}{2}s^2 + \frac{3}{4}s^3 & s \le 1 \\ \frac{1}{4}(2-s)^3 & 1 < s \le 2 \\ 0 & s > 2 \end{cases}$$

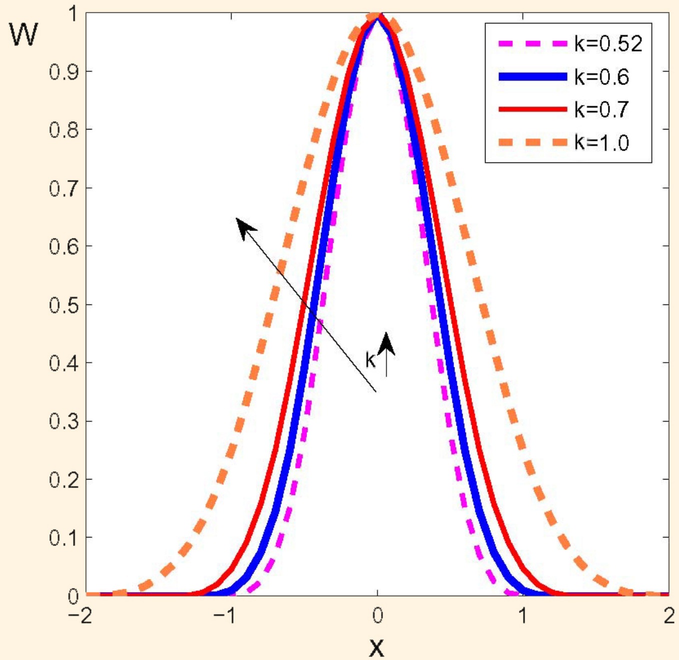


$$s = \frac{\|\boldsymbol{x} - \boldsymbol{x}_j\|}{h}$$

$$h = \boldsymbol{k} \max\left(\|\boldsymbol{x} - \boldsymbol{x}_j\|\right)$$

## Kernel functions

- Another example: Exponential Kernel.

$$W(x, x^*, \kappa) = \frac{e^{-\left(\frac{s}{c}\right)^2} - e^{-\left(\frac{dm}{c}\right)^2}}{1 - e^{-\left(\frac{dm}{c}\right)^2}}$$

$$s = |x - x^*|\,, d_m = 2\max\left(|x_j - x^*|\right), c = \frac{d_m}{2\kappa}$$

- A 2D kernel is obtained by multiplying two 1D kernels:

$$W_j(\boldsymbol{x}, \boldsymbol{x}^*, \kappa_x, \kappa_y) = W_j(x, x^*, \kappa_x) W_j(y, y^*, \kappa_y)$$

- Another example: Exponential Kernel.

$$W(x, x^*, \boldsymbol{\kappa}) = \frac{e^{-\left(\frac{s}{c}\right)^2} - e^{-\left(\frac{dm}{c}\right)^2}}{1 - e^{-\left(\frac{dm}{c}\right)^2}}$$

$$s = \left|x - x^*\right|, d_m = 2\max\left(\left|x_j - x^*\right|\right), c = \frac{d_m}{2\boldsymbol{\kappa}}$$

- A 2D kernel is obtained by multiplying two 1D kernels:

$$W_j(\boldsymbol{x}, \boldsymbol{x}^*, \kappa_x, \kappa_y) = W_j(x, x^*, \kappa_x) W_j(y, y^*, \kappa_y)$$

# Kernel functions



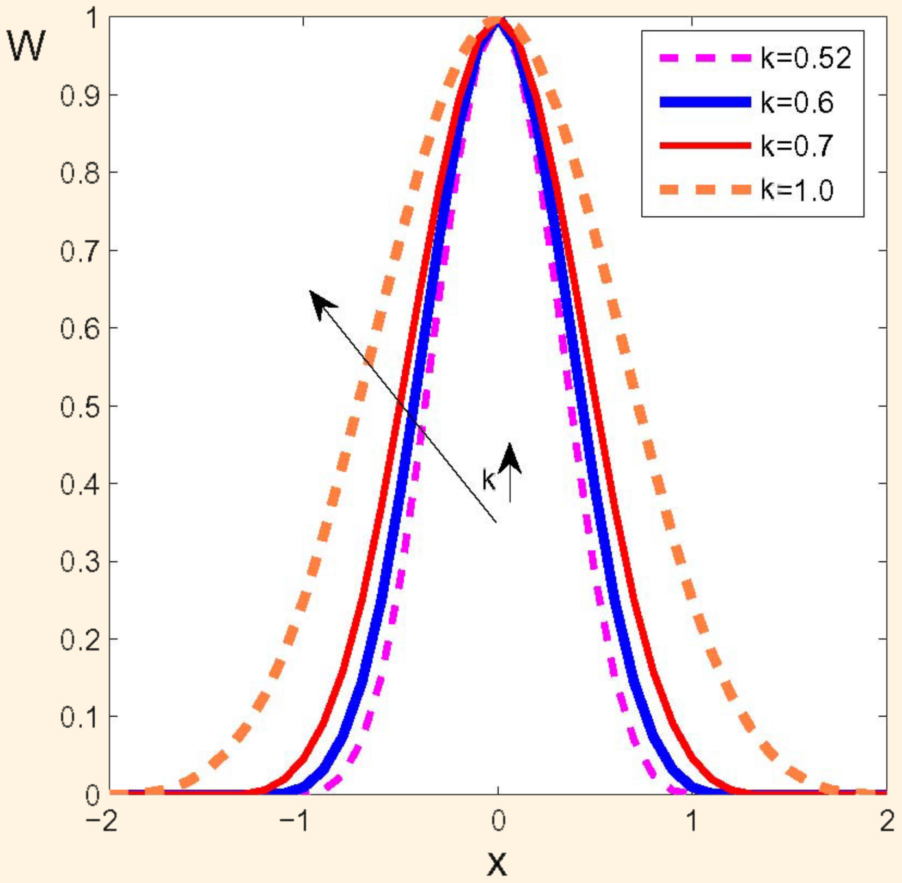


CUBIC SPLINE

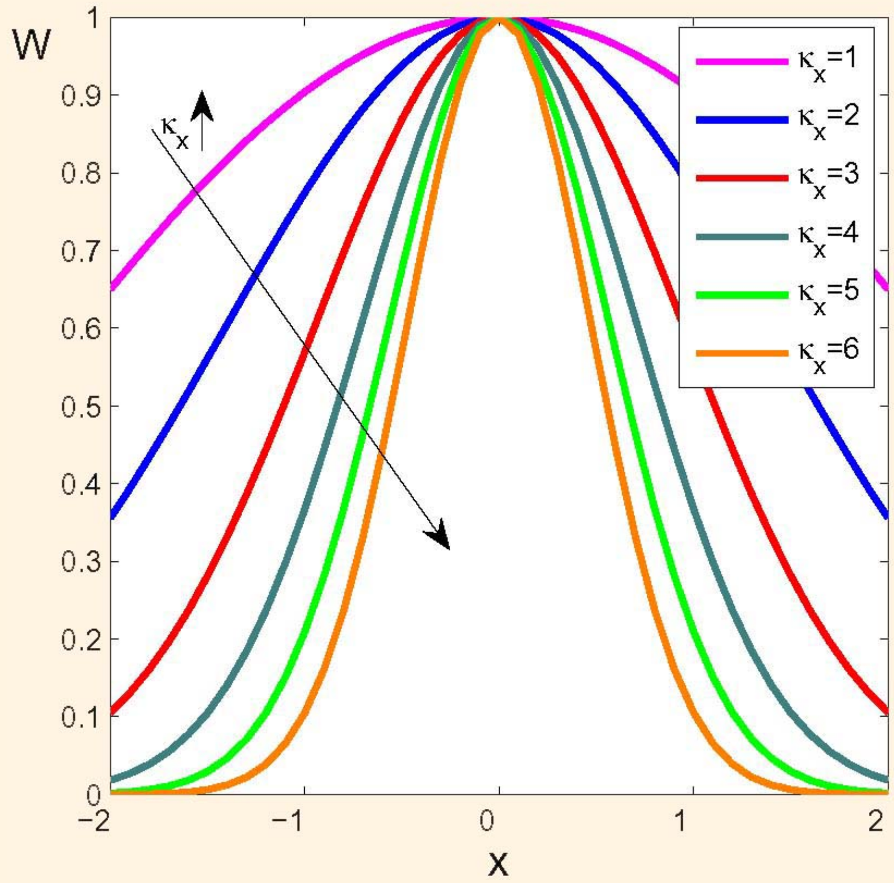


EXPONENTIAL KERNEL

# A practical note

- Vertices and/or centroids of the control cells are the "particles" to perform the MLS approximation.
- We need to define stencils to "mark" the neighbor particles that define the cloud of points.

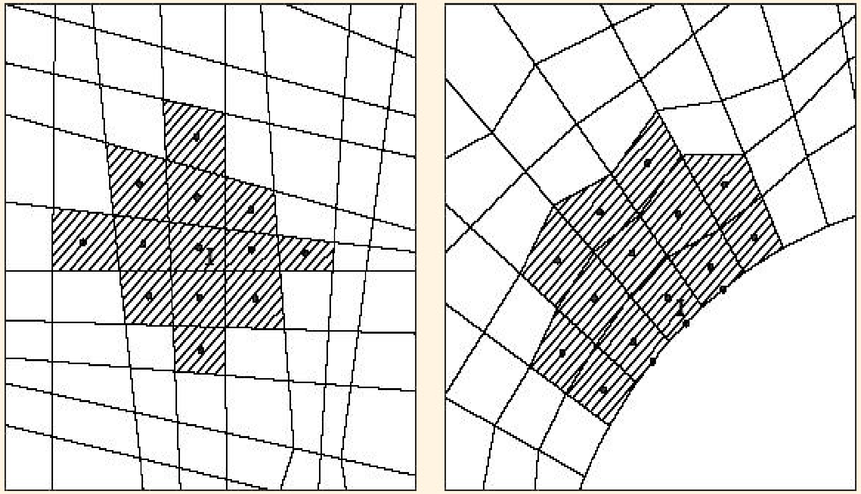

- We use a polynomial cubic basis in all the computations.

# The FV-MLS method



- In order to develop high-order finite volume schemes:
  - Compute fluxes more accurately.
  - Improve function reconstruction at an integration point $\boldsymbol{x}$ placed at the interface between elements.

$$\boldsymbol{U}(x) = \boldsymbol{U_I} + \nabla \boldsymbol{U_I} \cdot (\boldsymbol{x} - \boldsymbol{x_I}) + \frac{1}{2}(\boldsymbol{x} - \boldsymbol{x_I})^T \boldsymbol{H_I}(\boldsymbol{x} - \boldsymbol{x_I}) + \ldots$$

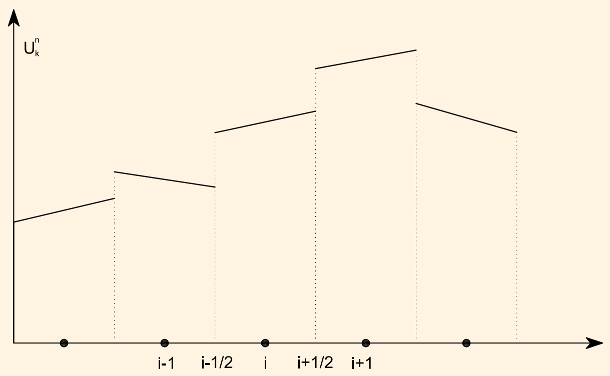


Piece-wise linear reconstruction of a function.

# The FV-MLS method

- Computation of high-order derivatives:
  - Easy on structured grids.
  - Unstructured grids⇒PROBLEM.

- We propose:
  - The use of Moving Least Squares (MLS) to obtain an accurate and multidimensional approximation of derivatives on unstructured grids.

# The FV-MLS method

- This scheme acknowledge the different nature of convective and diffusive terms.
- We start from a high-order, continuous MLS approximation of the solution:
- Convective terms discretization:
  - Breaks the continuous representation of the MLS approximation.
  - Obtains a continuous representation of the variables inside each cell.
- Diffusive terms discretization is:
  - Centered.
  - Continuous.
  - Highly accurate.

# Outline

- Introduction
- The FV-MLS method
- Multiscale properties of MLS: MLS-based shock detection
- A formulation for all-speed flows
- A MLS-based sliding mesh technique
- Application to Navier-Stokes-Korteweg equations
- Conclusions

# MLS-based shock detection




Mach cone. (Source: www.airliners.net)

# MLS-based shock detection

- Slope limiters are used to design TVD schemes.
  - A slope limiter limits the Taylor reconstruction of a high-order finite volume scheme as follows:

$$\boldsymbol{U}(\boldsymbol{x}) = \boldsymbol{U}_I + \chi_I \nabla \boldsymbol{U}_I \cdot (\boldsymbol{x} - \boldsymbol{x}_I)$$

    - $\chi_I = 0 \Rightarrow$ First-order scheme
    - $\chi_I = 1 \Rightarrow$ No limitation
  - Slope limiters present some drawbacks.
    - They avoid the convergence of the numerical method.
    - They may be active in cells where the flow is smooth.
    - Straightforward application to higher-order schemes is not obvious.

# MLS-based filtering (I)

- We propose to use the MLS multiresolution properties to detect shock waves[1]. (Generalization of the work of Sjögreen and Yee [2] for unstructured grids)
- The use of the Reproducing Kernel Particle Method as a filter for turbulence problems was proposed in 2000 by Wagner and Liu.
- MLS approximation of a variable can be seen as a low-pass filtering.

$$\boxed{\overline{\Phi_I} = \sum_{j=1}^{n} N_j(\boldsymbol{x})\Phi_j}$$

[1] X. Nogueira, L. Cueto-Felgueroso, I. Colominas, F. Navarrina, M. Casteleiro, *A new shock-capturing technique based on moving least squares for higher-order numerical schemes on unstructured grids*, CMAME, 2010

[2] Sjögreen, B., Yee, H. C., *Multiresolution wavelet based adaptive numerical dissipation control for high order methods*, Journal of Scientific Computing, *20*:211-255, 2004.

- The filter properties are analyzed by the study of its transfer function

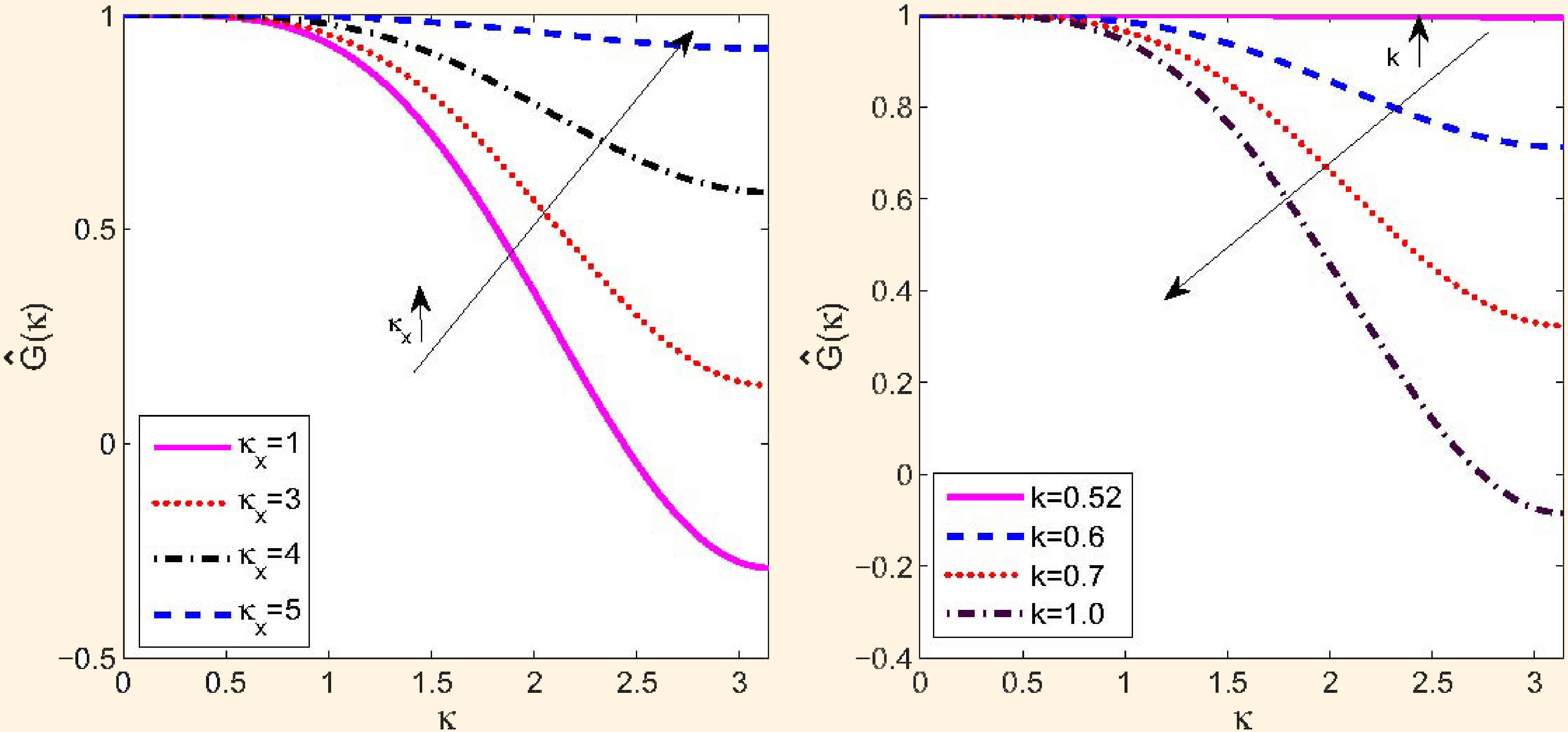


Transfer function for the exponential (left) and for the cubic (right) kernels.

# MLS-based shock detection (II)

- We can decompose a given data series in:

$$u = \hat{u} + u'$$

Raw Data ($u$)

Low frequencies ($\hat{u}$)

High frequencies ($u'$)

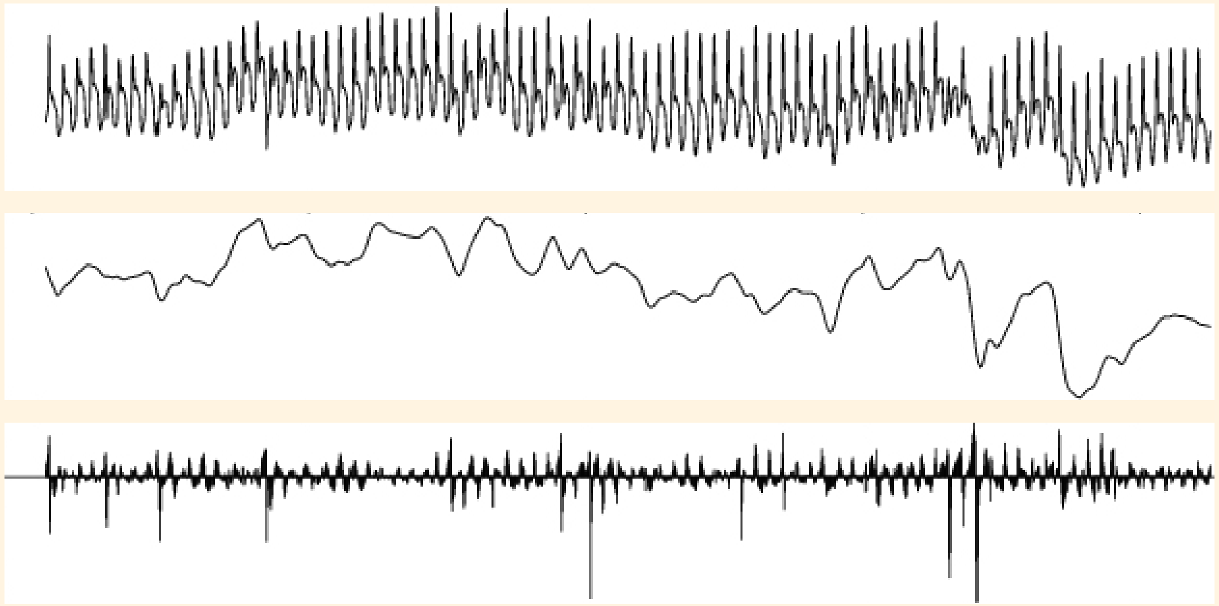

- The cut frequency of the filter varies according to its transfer function.

SHARK-FV 2015 Conference
SHARING HIGHER-ORDER ADVANCED RESEARCH KNOW-HOW on FINITE VOLUME
Ofir, Portugal
May 18 - 22, 2015

- Wavelets connection.
  - We define two sets of MLS shape functions, $\mathbf{N}^h(\mathbf{x})$ y $\mathbf{N}^{2h}(\mathbf{x})$, computed with $h$ and $2h$ (Two different cut frequencies).
  - Set of wavelet functions:

$$\mathbf{\Phi^{2h}}(\mathbf{x}) = \mathbf{N^h}(\mathbf{x}) - \mathbf{N^{2h}}(\mathbf{x})$$

    - h (smoothing length) is the scale parameter of the wavelet function.
    - We can do the same procedure with $\kappa_x$ and exponential kernels.
  - h-scale solution is the sum of the low-scale part and its complementary high-scale part:

$$u_h(\mathbf{x}) = u_{2h}(\mathbf{x}) + \mathbf{\Psi}(\mathbf{x})$$

$$\mathbf{\Psi}(\mathbf{x}) = \sum_{j=1}^{n} \mathbf{u_j} \mathbf{\Phi_j^{2h}}(\mathbf{x}) = \sum_{j=1}^{n} \mathbf{u_j}(\mathbf{N^h}(\mathbf{x}) - \mathbf{N^{2h}}(\mathbf{x}))$$

# MLS-based shock detection

- MLS-based selective limiting:
  - $\Psi \Rightarrow$ indicates the smoothness of the solution.
  - We use $\Psi$ to decide if a slope limiter algorithm is activated or not.
  - We select the density as the reference variable.
  - We need to define a threshold value for the function $\boldsymbol{\Psi}_\rho(\mathbf{x})$.
    - We propose a possible choice, that depend on a parameter $C_{lc}$:
      - $T_v$ defined from the gradient of the reference variable in cell $I$.

$$T_v = \frac{C_{lc} \left|\nabla \rho\right|_I A_I^{\frac{1}{d}}}{M}$$

$A_I$ is the size (area in 2D) of the control volume $I$, $d$ is the number of spatial dimensions and $M$ is the Mach number

# MLS-based shock detection

- The slope limiter is active when:

$$\boxed{|\Psi_\rho| = \left| \sum_{j=1}^{n_I} \rho_j \left( \mathbf{N}^h(\mathbf{x}) - \mathbf{N}^{2h}(\mathbf{x}) \right) \right| > T_v}$$

- MLS-based detection method can be applied to structured and unstructured grids.
- This selective limiting allows the extension of slope limiters to higher-order schemes.
- It avoids the limitation of smooth extrema.
- It improves the convergence of the numerical method.

# MLS-based shock detection. A first 1D test (I)



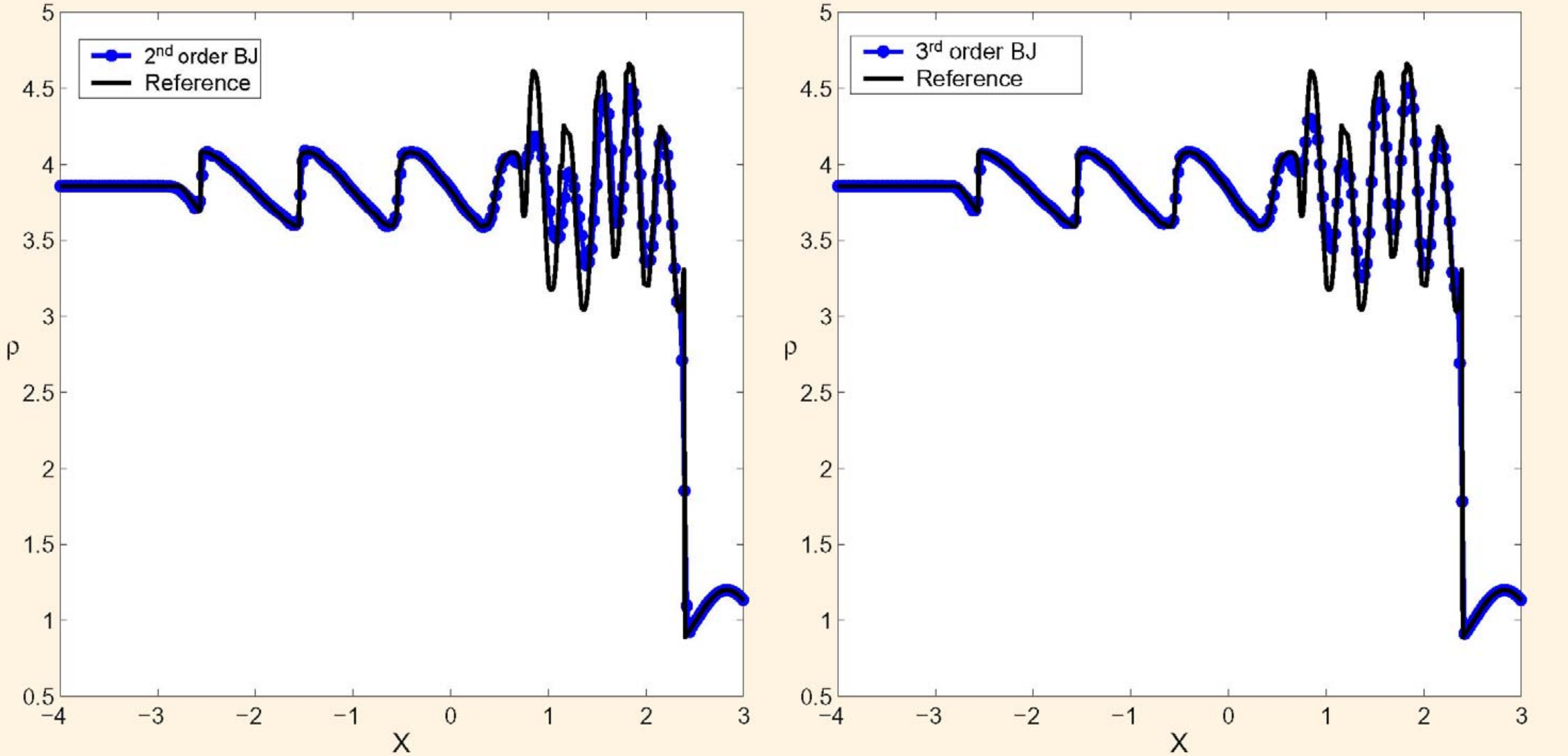


Linear reconstruction (left) and quadratic reconstruction (right) with the BJ limiter for the 1D Shu-Osher problem.

# MLS-based shock detection. A first 1D test (II)

SHARK-FV 2015 Conference
SHARING HIGHER-ORDER ADVANCED RESEARCH KNOW-HOW on FINITE VOLUME
Ofir, Portugal
May 18 - 22, 2015

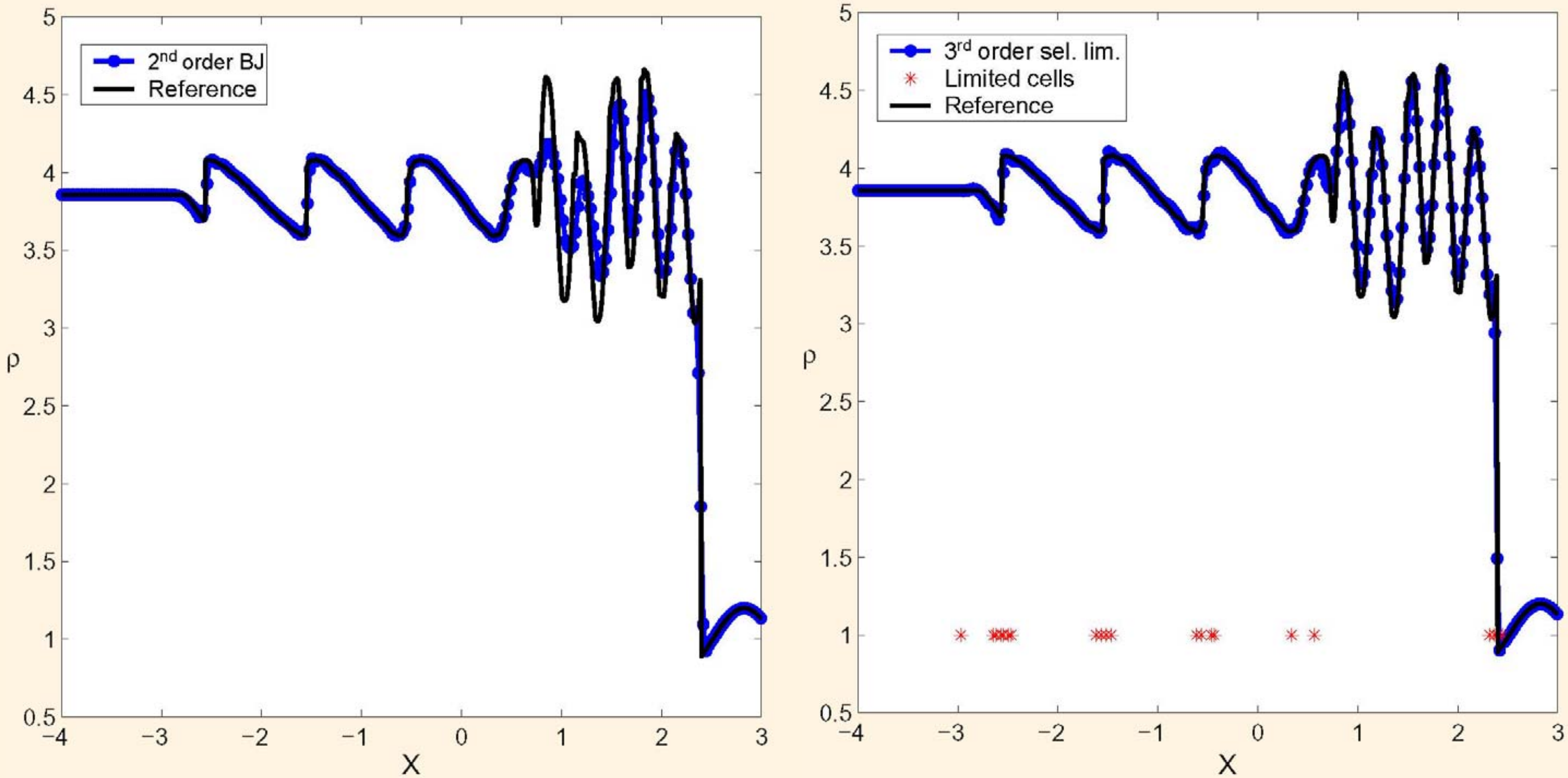


Quadratic reconstruction without detector (left) and with detector (right) for the 1D Shu-Osher problem.

- $\Psi \Rightarrow$ indicates the smoothness of the solution.

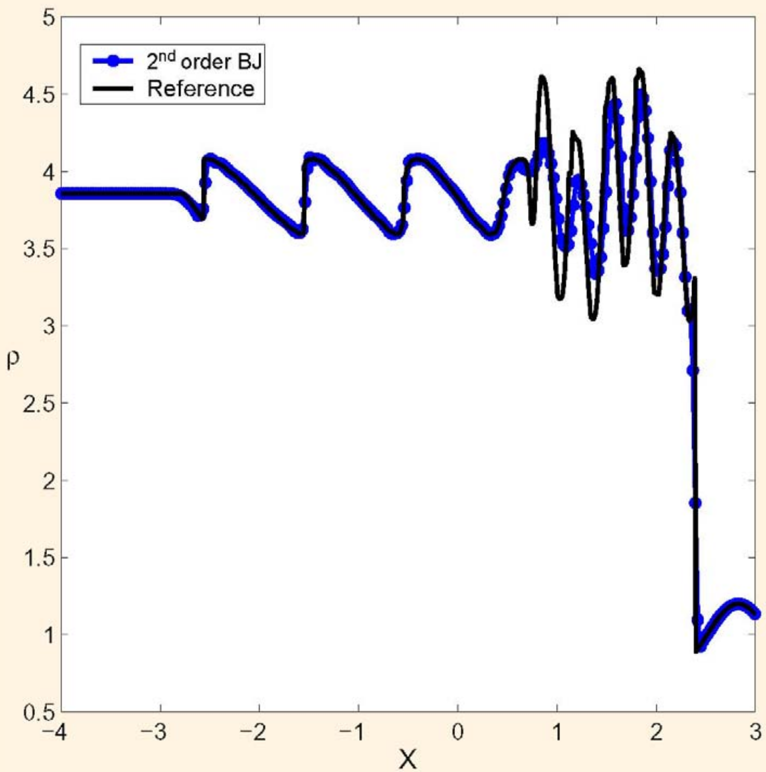


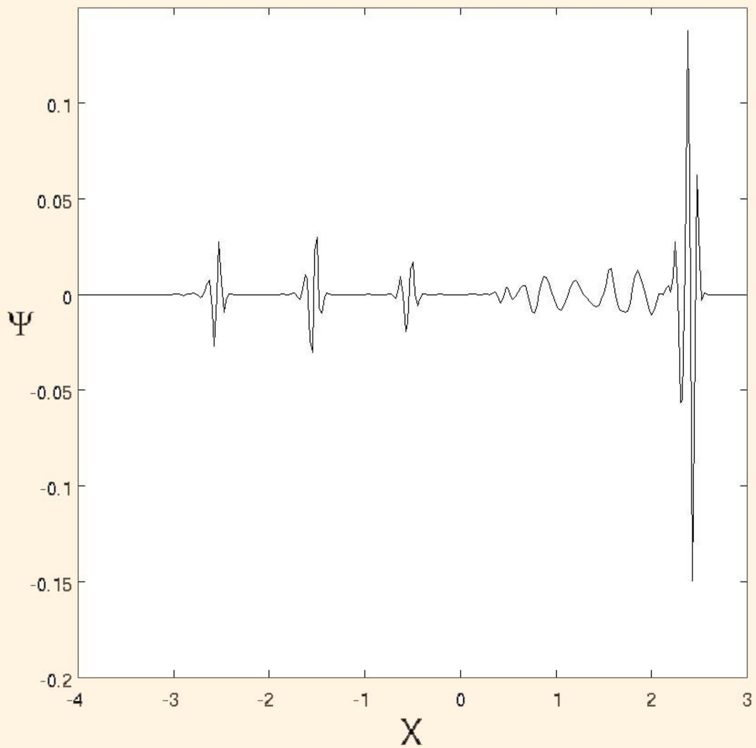


Shape of $\Psi$ for the 1D Shu-Osher problem.

## Multiple dimensions detection test



- We test the ability of the proposed method to detect shock waves in a multidimensional data distribution.

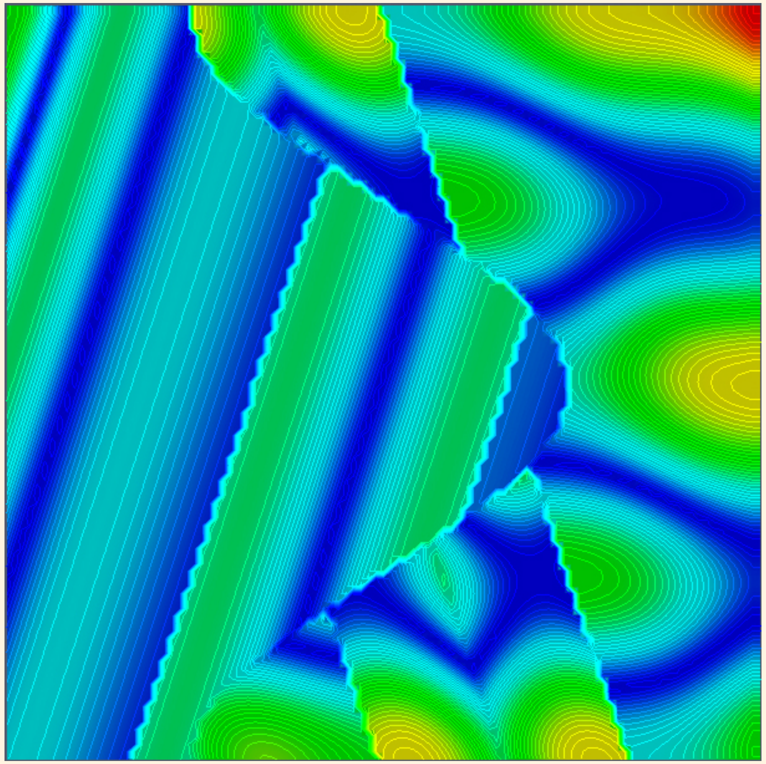

Abgrall function for the multidimensional detection test.

# Multiple dimensions detection test



- We test the ability of the proposed method to detect shock waves in a multidimensional data distribution.

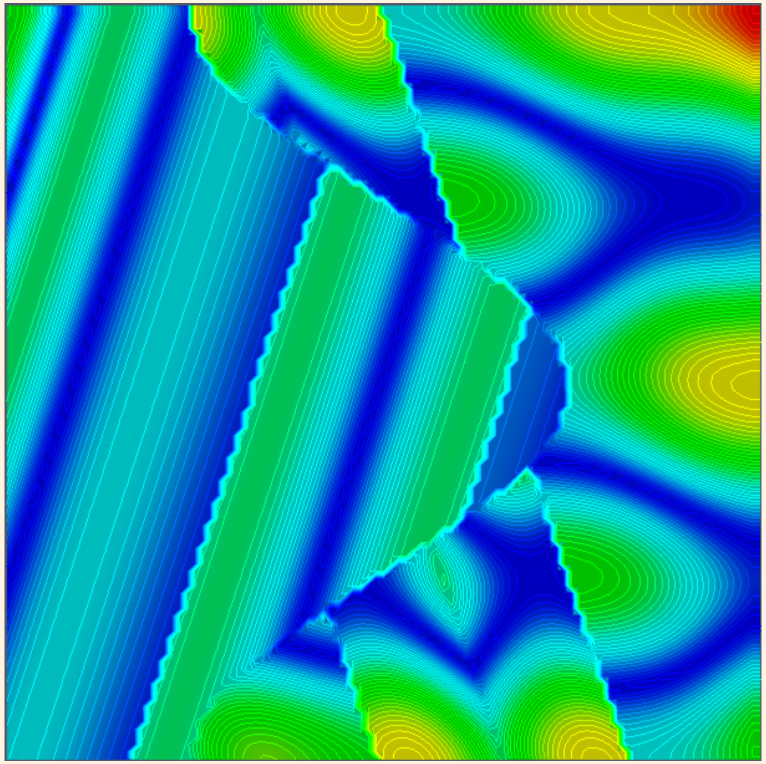

Abgrall function for the multidimensional detection test.

# Multiple dimensions detection test.



$C_{lc} = 0.2$

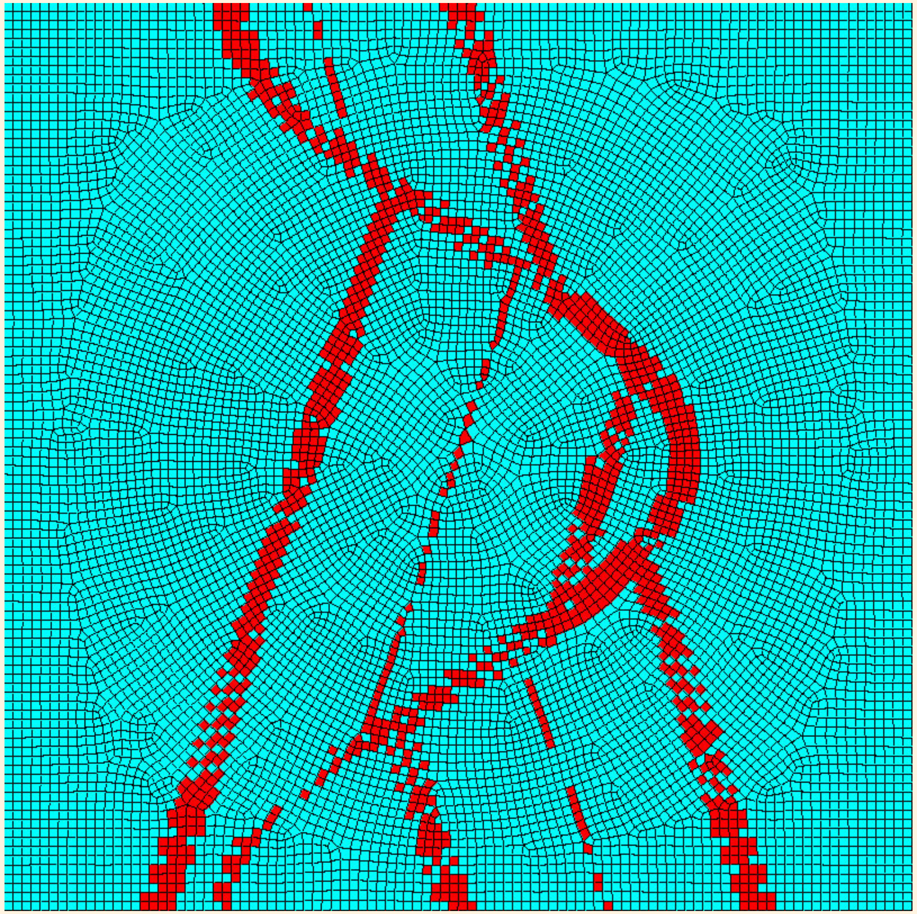

$C_{lc} = 0.4$

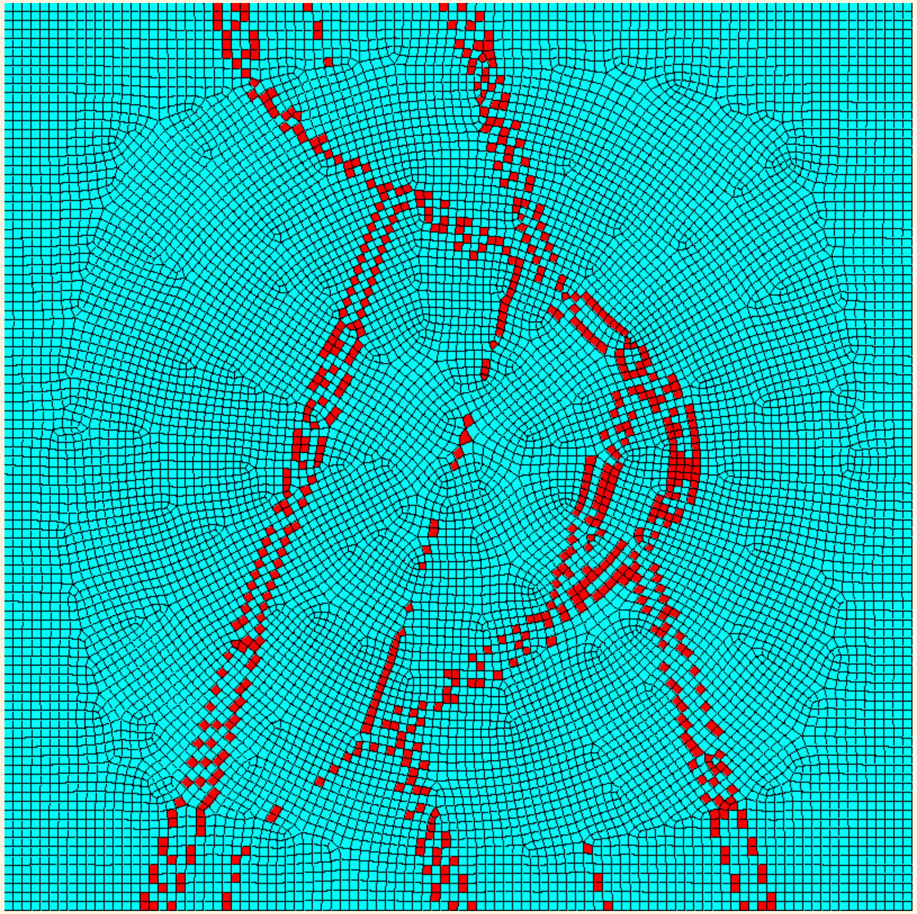

## Multiple dimensions detection test.

- General grids ⇒ this approach may become unstable.
- Solution: If the slope limiter is activated in a cell it is activated in the whole stencil of that cell.
- We choose a less restrictive parameter for the detection ⇒ $C_{lc2} = 0.32$.

# Multiple dimensions detection test. Unstructured grid



$$C_{lc2} = 0.32$$

Detection results for the Abgrall function with the methodology for general grids.

## 2D Examples. A subsonic case

- Slope limiters may limit even for smooth flows
- Slope limiters may difficult to achieve convergence
- MLS-based selective limiting alleviate these problems.
- We check these effects by solving the subsonic flow past a NACA 0012 profile
  - Mach number=0.63, Angle of attack=$2^{o}$

# 2D Examples. A subsonic case

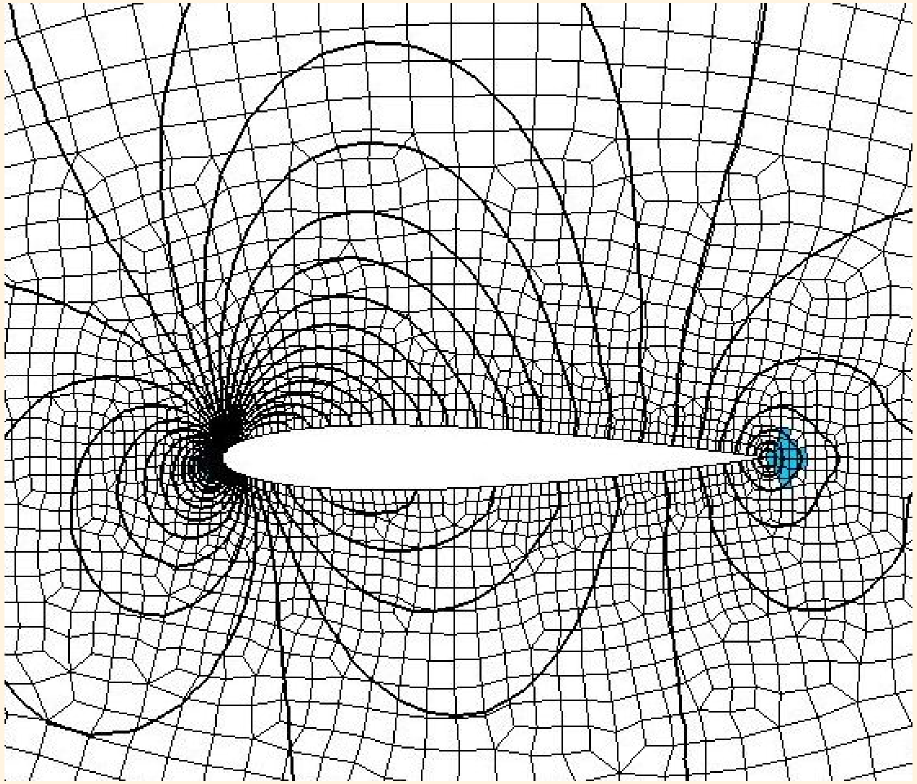


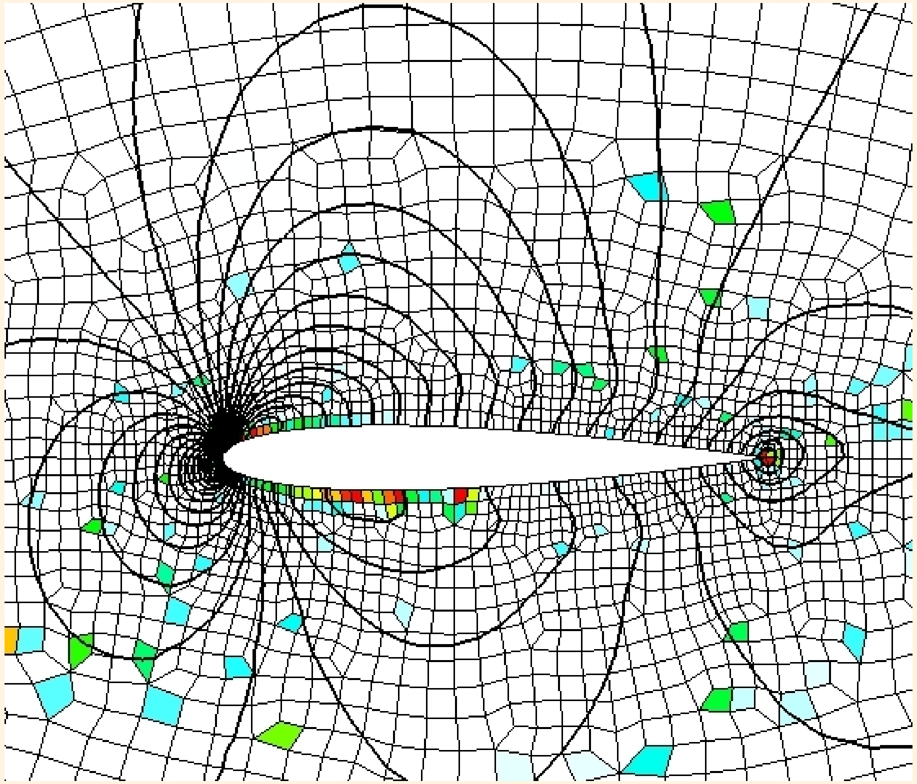

# 2D Examples. A subsonic case

| Numerical Scheme | $C_L$ | $C_D$ |
|---|---|---|
| Hodography method | 0.335 | 0 |
| FV-MLS $3^{rd}$ order + BJ | 0.318 | 5.29E-03 |
| FV-MLS $3^{rd}$ order BJ + selective limiting | 0.328 | 1.24E-03 |

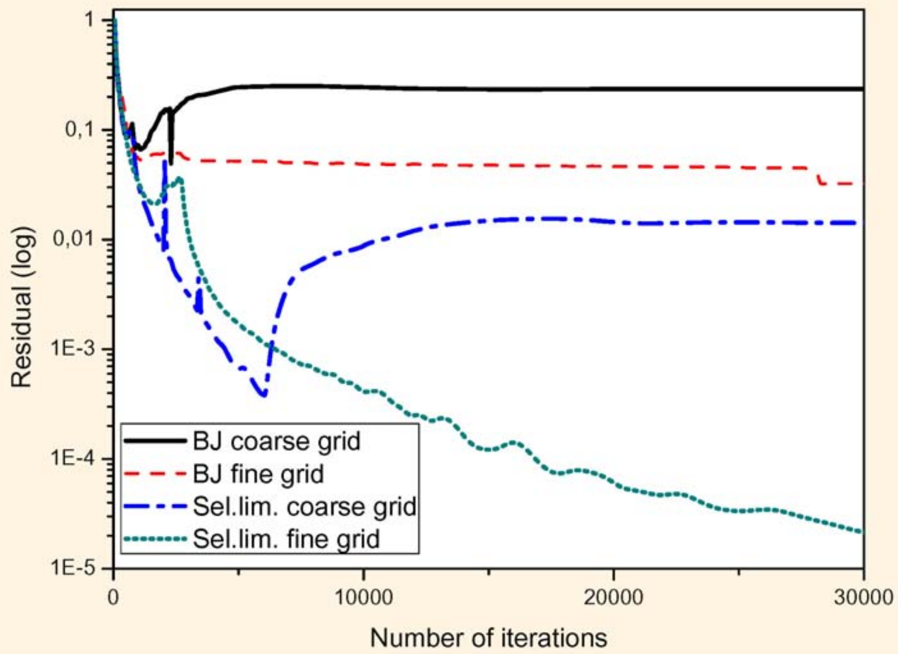

# 2D Examples. Transonic flow past a NACA 0012



Mach number=0.8, Angle of attack=1.25$^{o}$

Selective limiting

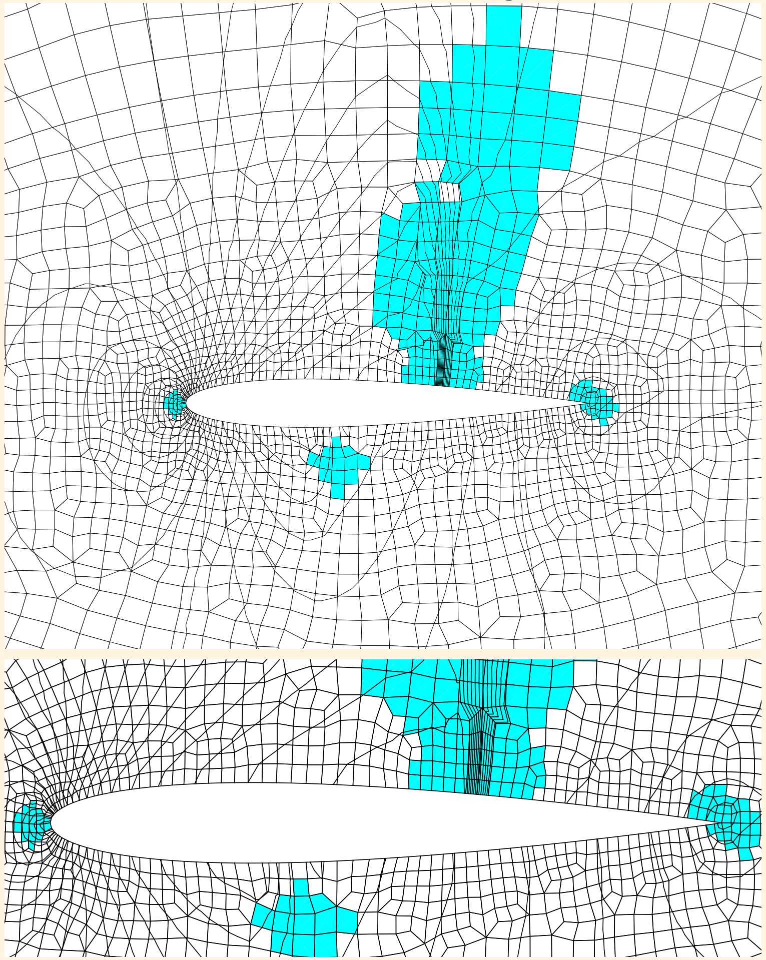

BJ limiter

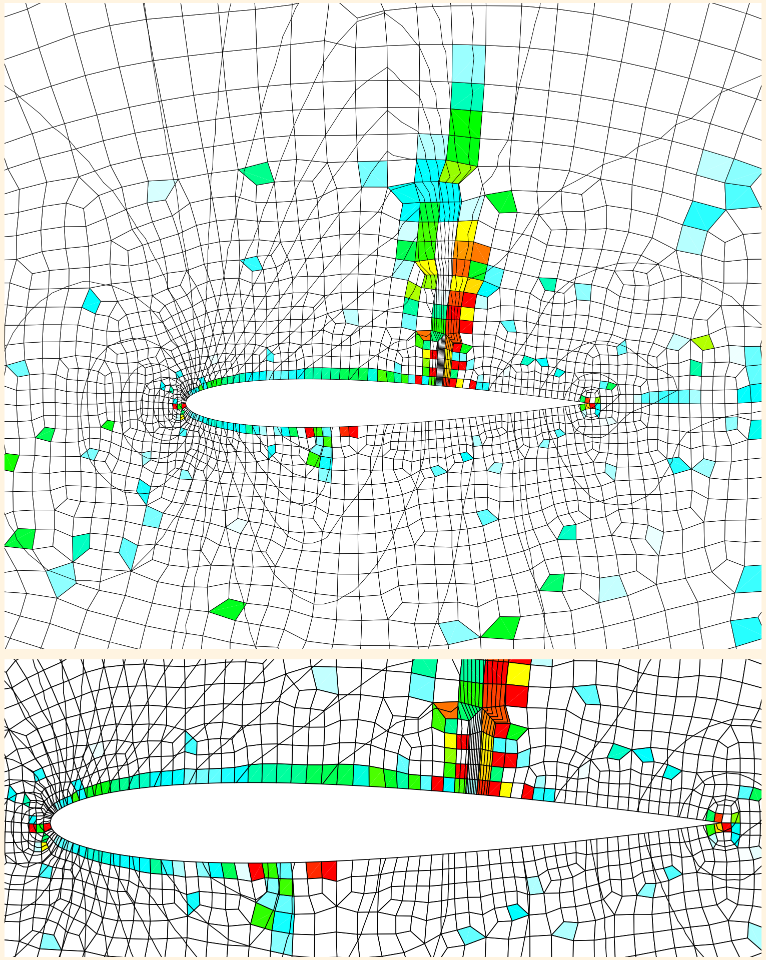

# 2D Examples. Transonic flow past a NACA 0012

| Numerical Scheme | $C_L$ | $C_D$ |
|---|---|---|
| FV-MLS $2^{nd}$ order + BJ | 0.341 | 2.465E-02 |
| FV-MLS $4^{th}$ order + BJ | 0.342 | 2.486E-02 |
| FV-MLS $4^{th}$ order BJ + selective limiting | 0.343 | 2.317E-02 |
| AGARD Reference | 0.347 | 2.221E-02 |

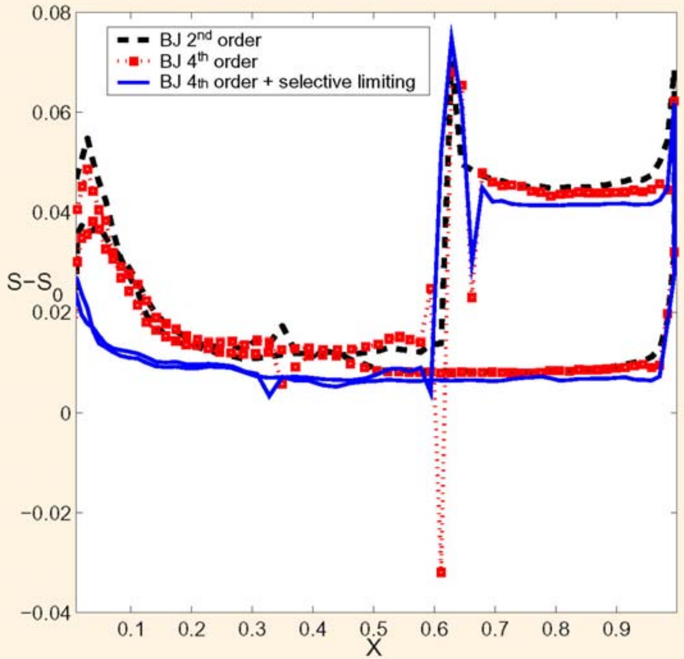

Shock-wave-vortex Interaction.
$M_v = 0.4$, $M_s = 1.2$, $200 \times 200$ grid
Third-order FV-MLS scheme, Barth-Jespersen limiter

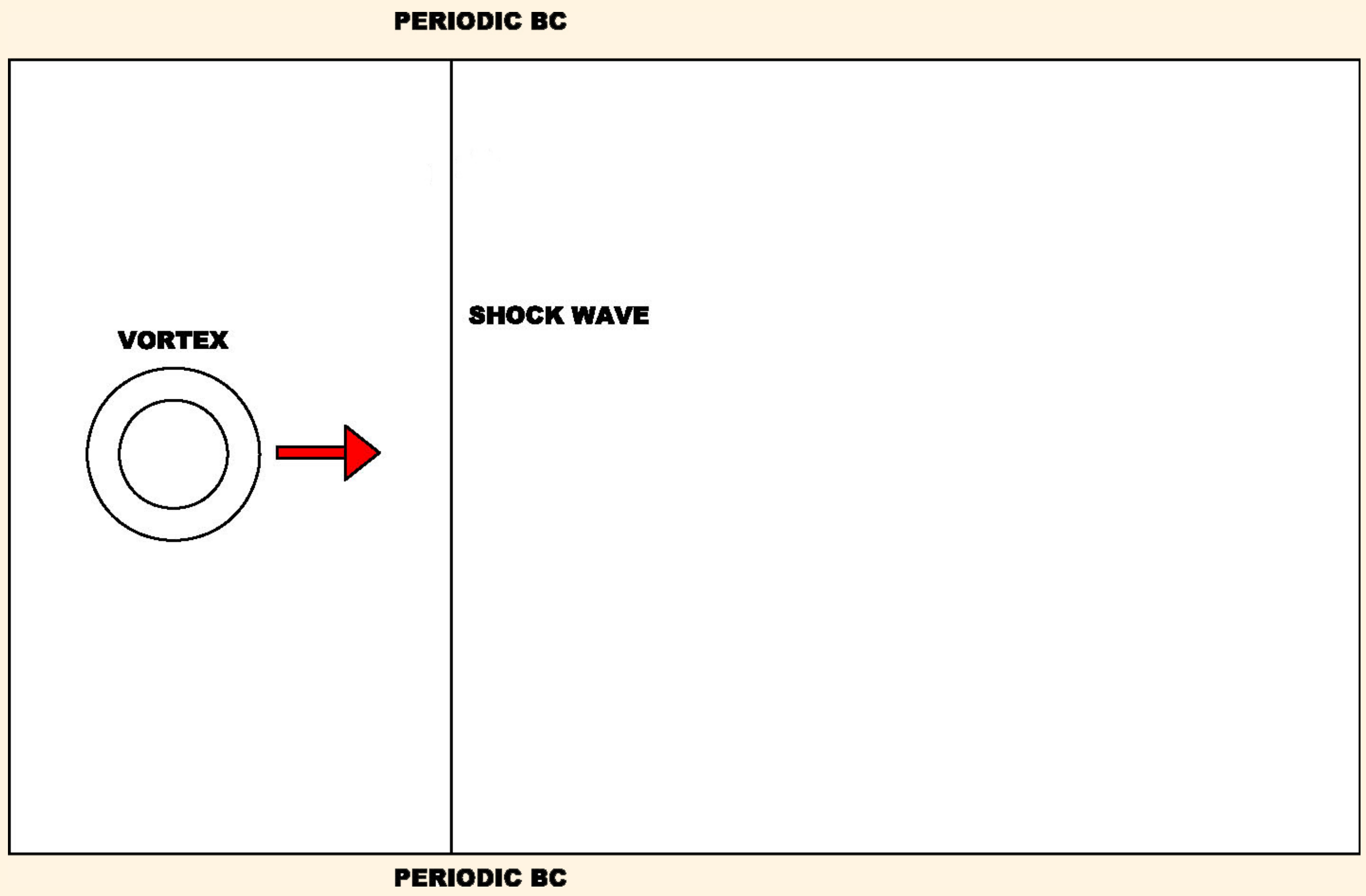

# 2D Examples. Shock-wave-vortex Interaction

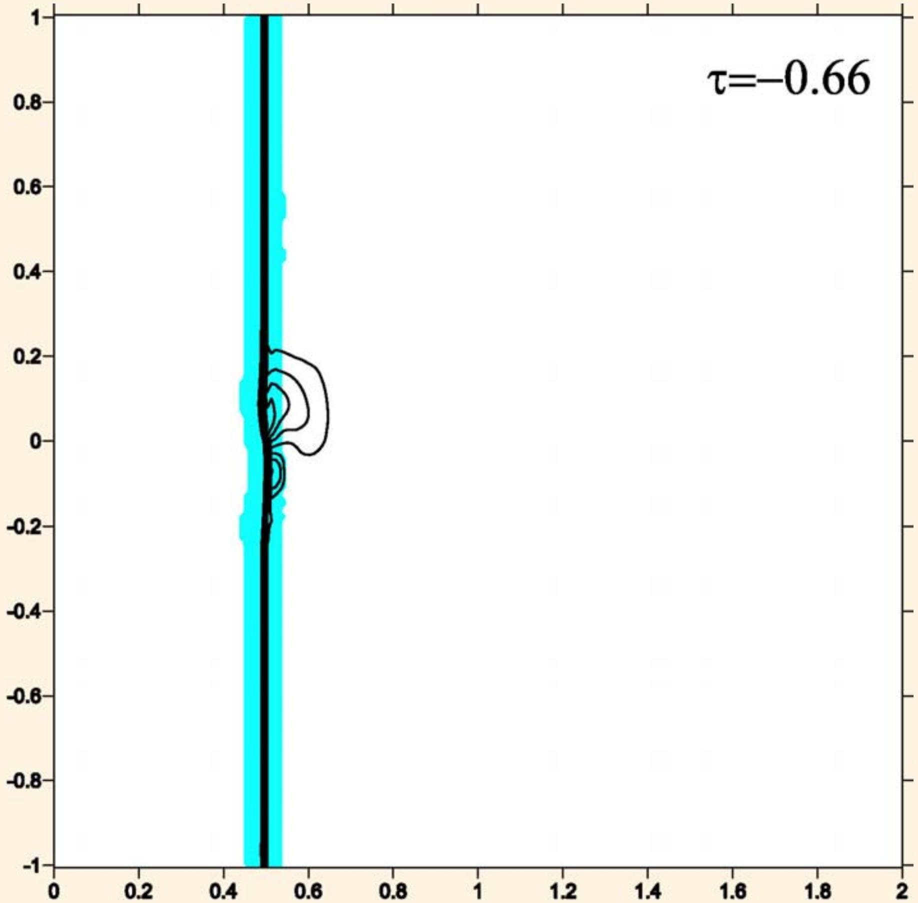


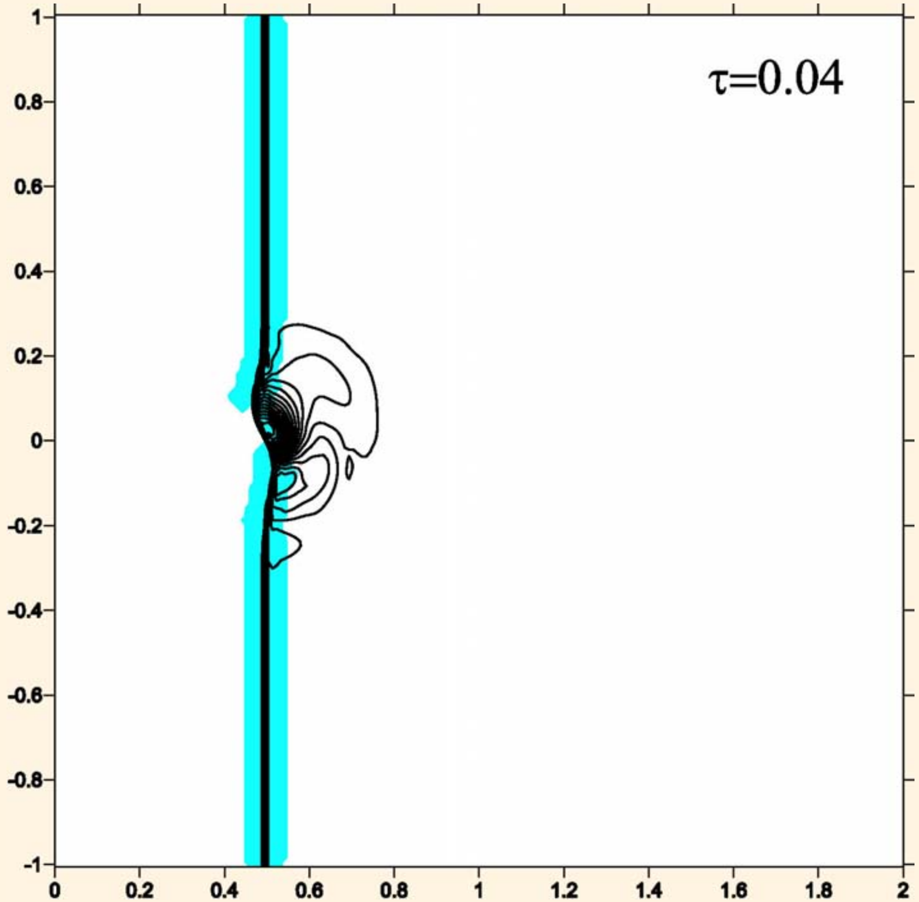

# 2D Examples. Shock-wave-vortex Interaction

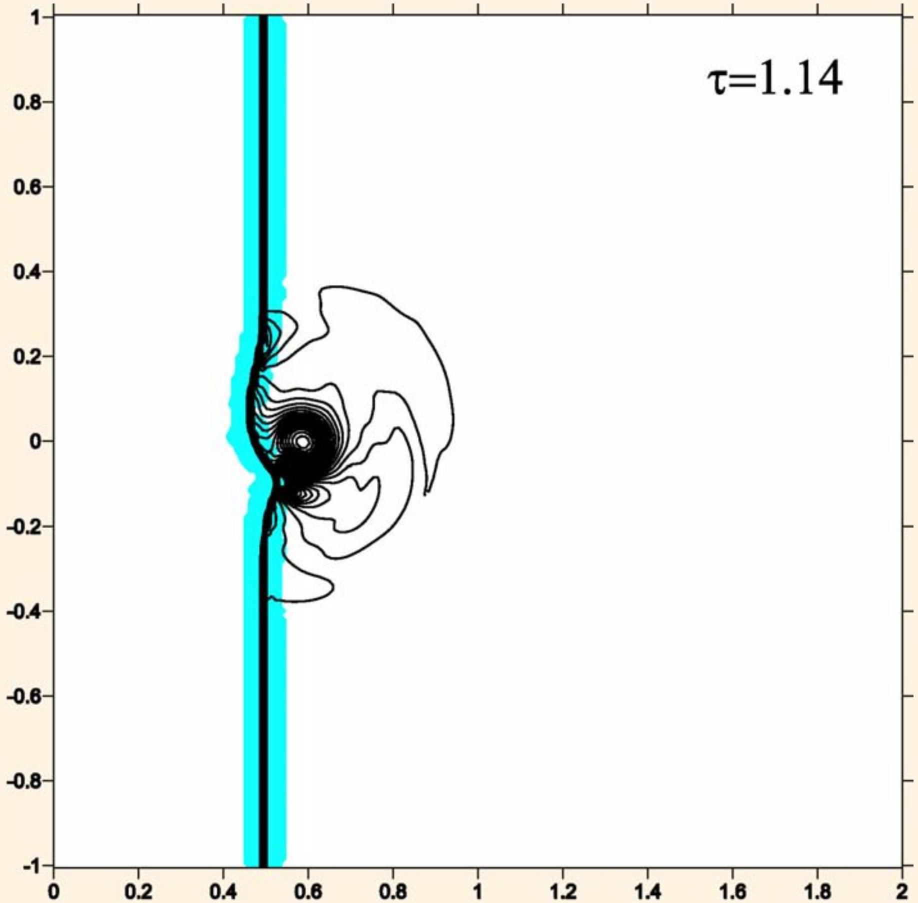


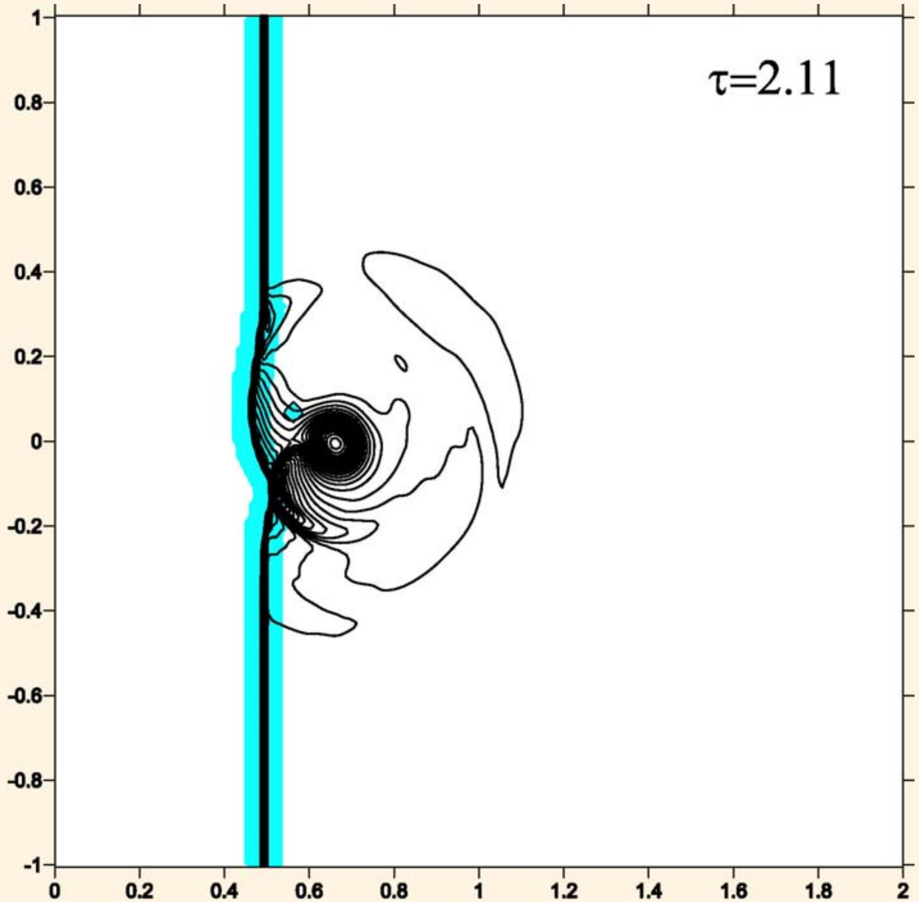

# 2D Examples. Shock-wave-vortex Interaction

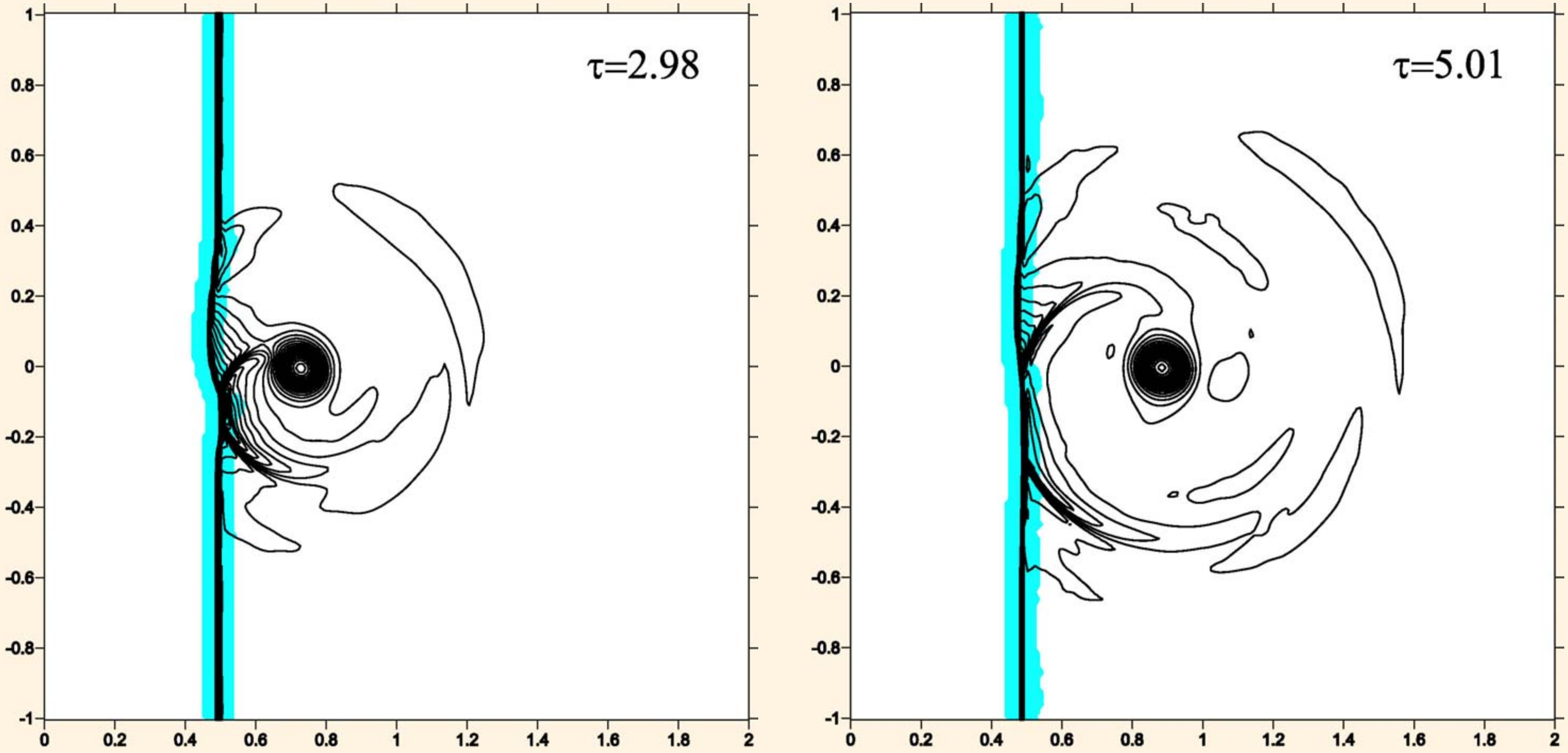

# 2D Examples. Double Mach Reflection

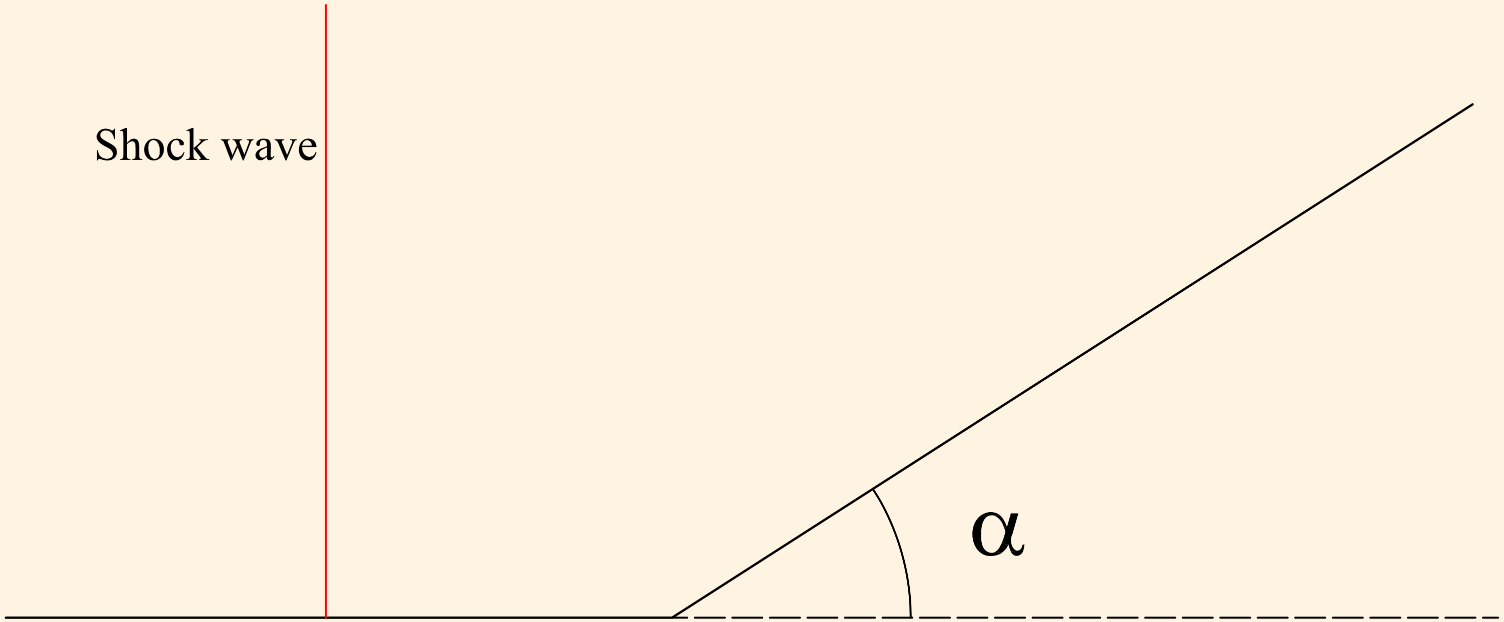


Schematic representation of the Double Mach reflection problem.

- The size of the elements is $\Delta x = \Delta y = \frac{1}{200}$
- Mach 10 right-moving shock
- $\alpha = 60$ degrees
- Third-order FV-MLS scheme, Van Albada limiter

# 2D Examples. Double Mach Reflection

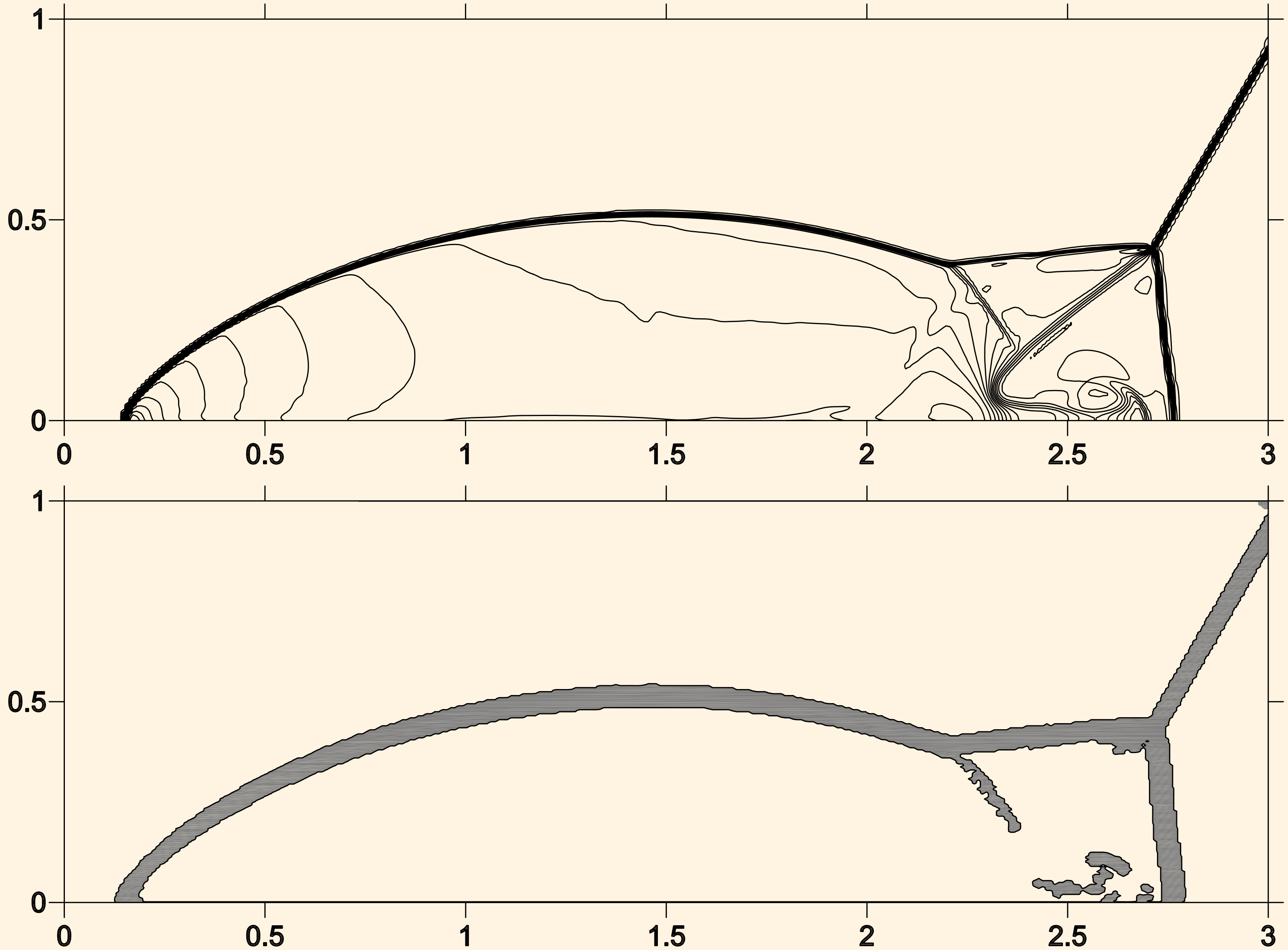

# Double Mach Reflection. Detail of the Mach stems region



Present Approach

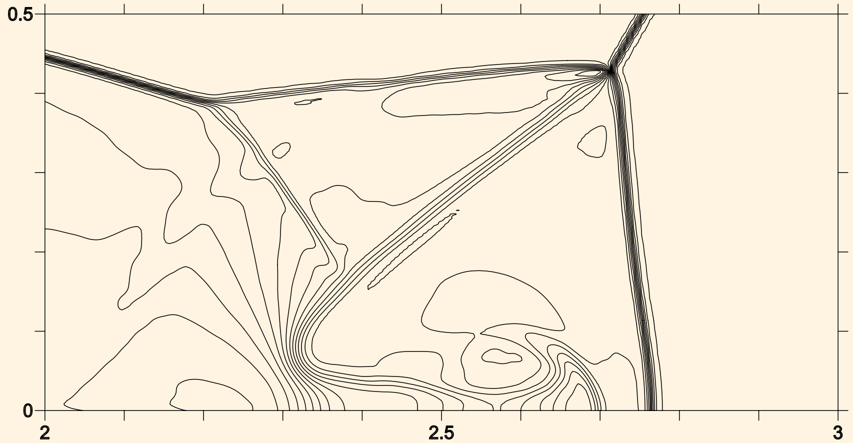


WENO (Shu, JCP,150 (1999))

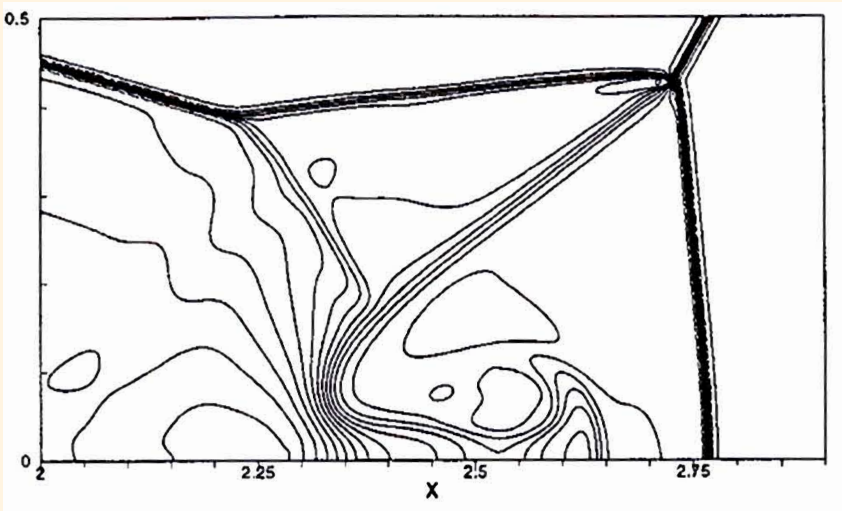

# 2D Examples. Mach 3 Forward step

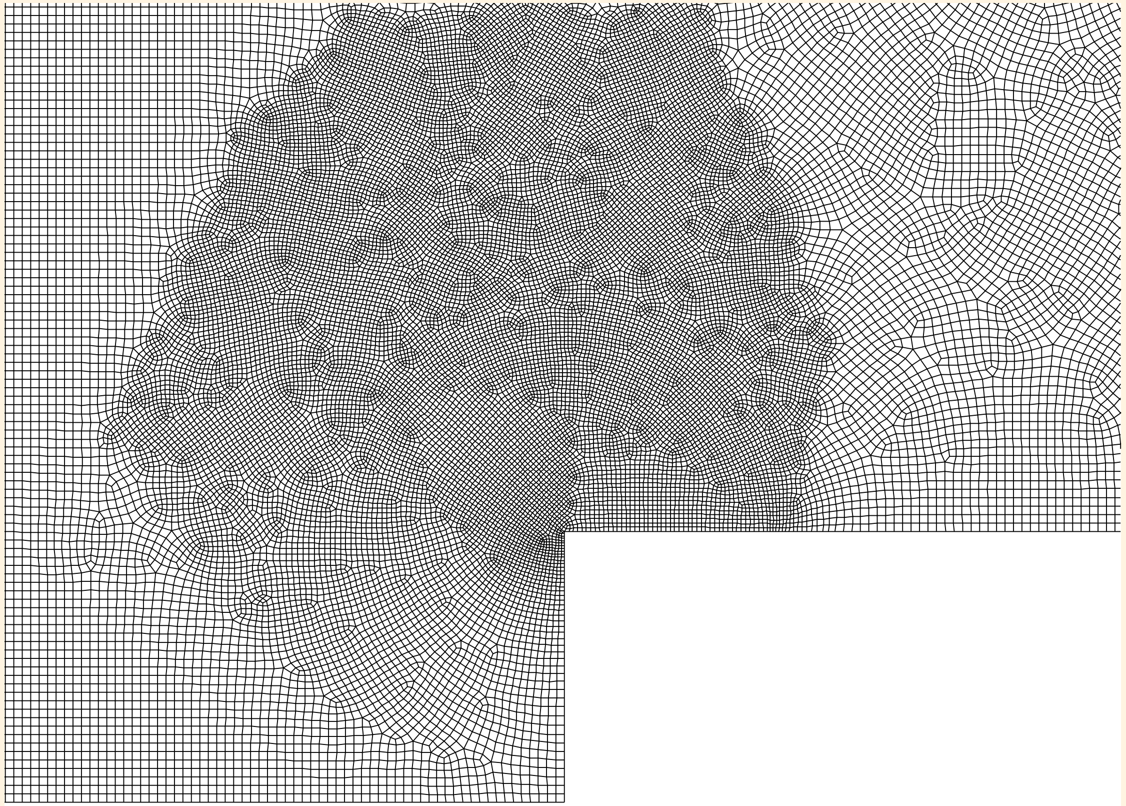

Detail of the mesh in the corner region.

- The size of the elements away from the corner is $(\Delta x = \Delta y = \frac{1}{160})$. Size of elements near the corner is one-half that.
- Third-order FV-MLS scheme, Jawahar limiter

# 2D Examples. Mach 3 Forward step



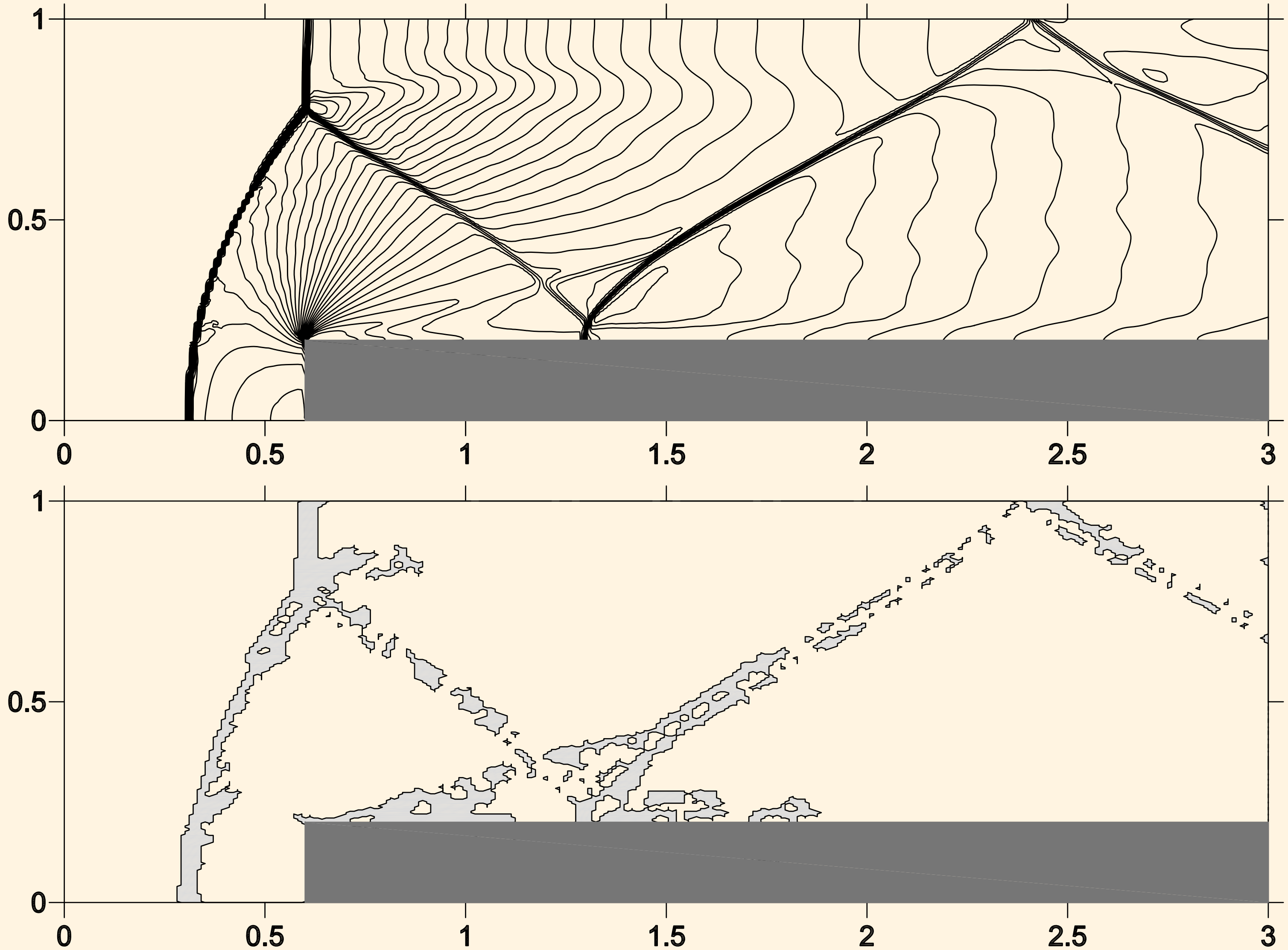

# 2D Examples. Mach 3 Forward step



Present Approach

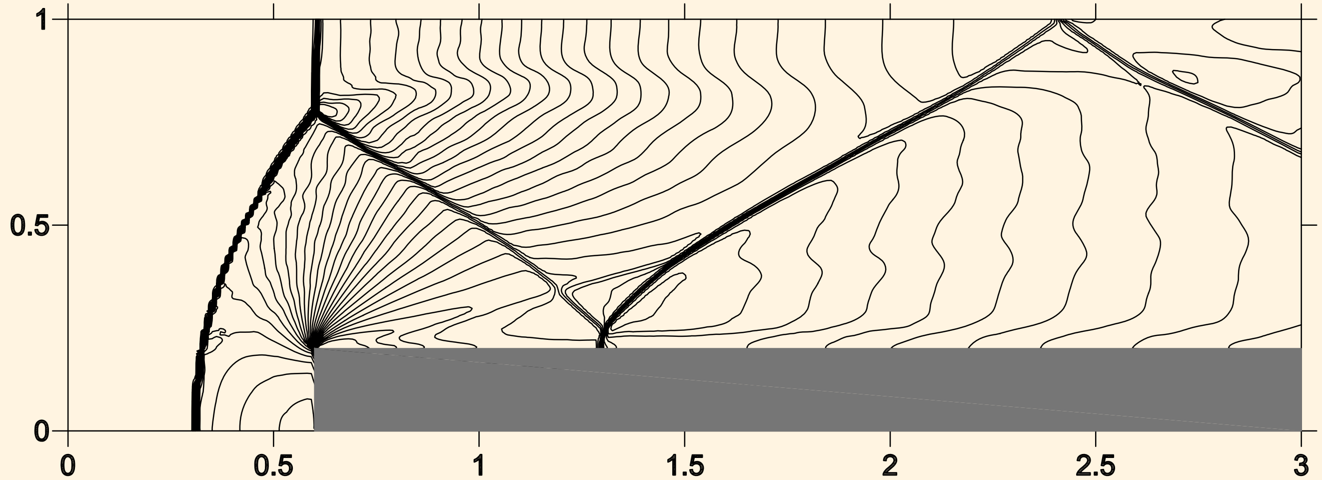


WENO (Shu, JCP,150 (1999))

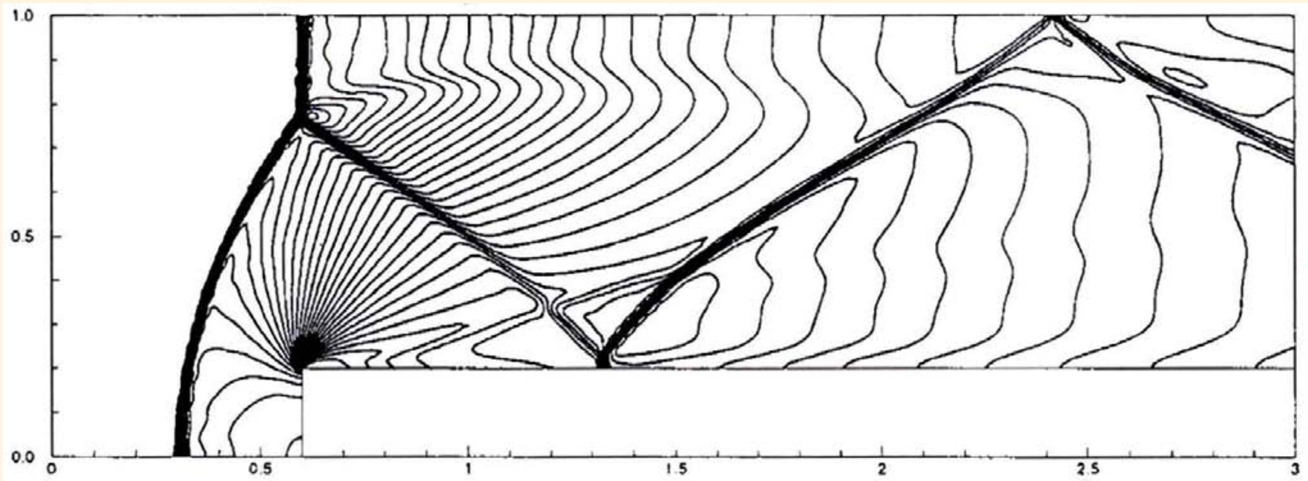

# A high-order formulation for all-speed flows

- Two families of FV schemes:
  - Density-based solvers$\Rightarrow$ Compressible flows
  - Pressure-based solvers$\Rightarrow$ Incompressible flows
- The difference is in the computation of pressure field, and in the density.

Compressible Flow

Incompressible Flow

# A high-order formulation for all-speed flows

- Density-based solvers:
  - Density $\Rightarrow$ computed from the continuity equation
  - Pressure $\Rightarrow$ obtained via an EQUATION OF STATE
- Fails to compute low Mach number flows:
  - Discretized equations do not verify the right scaling of the pressure fluctuations with $M^2$

# A high-order formulation for all-speed flows



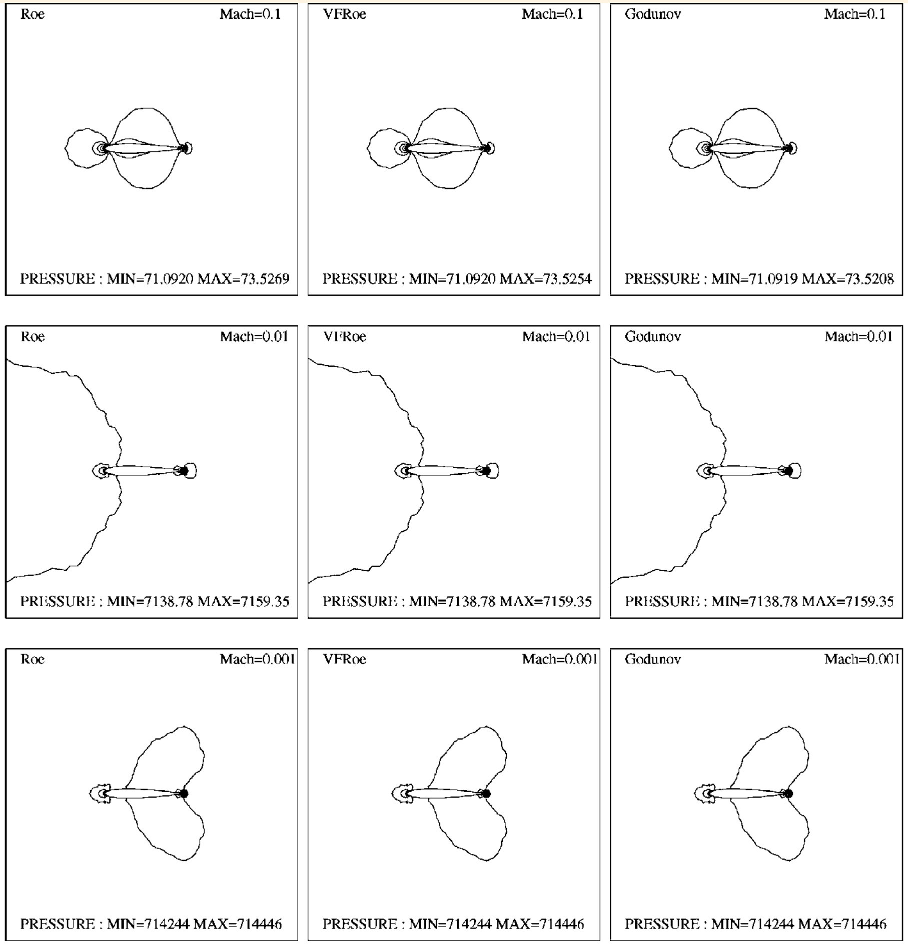


Fig. 1. Isovalues of the pressure, on a 3114 node mesh for $M_\infty = 0.1$ (top), $M_\infty = 0.01$ (middle), $M_\infty = 0.001$ (bottom) and for Roe scheme (left), VFRoe scheme (middle), Godunov scheme (right).

H. Guillard and A.Murrone, Computers & Fluids, 2004

# A high-order formulation for all-speed flows

- Pressure-based solvers:
  - Continuity and momentum equations $\Rightarrow$ Poisson equation
  - Pressure $\Rightarrow$ Solve Poisson equation
- Not well-suited to compute high Mach flows

We want to develop solvers for

ALL THE REGIMES OF A FLOW

# A high-order formulation for all-speed flows

- Conservation laws

$$\frac{\partial \boldsymbol{U}}{\partial t} + \nabla \cdot \left(\boldsymbol{\mathcal{F}}^{\boldsymbol{\mathcal{H}}} - \boldsymbol{\mathcal{F}}^{\boldsymbol{\mathcal{V}}}\right) = \boldsymbol{S} \qquad in \quad \Omega_T$$

- Numerical discretization:

$$\Omega_I \frac{\partial \boldsymbol{U}_I}{\partial t} + \sum_{j=1}^{N_f} \sum_{ig=1}^{N_G} \left[\boldsymbol{\mathcal{H}}(\boldsymbol{U}_j^+, \boldsymbol{U}_j^-, \hat{\boldsymbol{n}}_j) - \boldsymbol{\mathcal{F}}^{\boldsymbol{\mathcal{V}}}{}_j \cdot \hat{\boldsymbol{n}}_j\right]_{ig} \mathcal{W}_{ig} = \int_{\Omega_I} S \, d\Omega$$

  - Time integration $\rightarrow$ $3^{rd}$ order Runge-Kutta of Shu and Osher
  - $\boldsymbol{\mathcal{H}}(\boldsymbol{U}_j^+, \boldsymbol{U}_j^-, \hat{\boldsymbol{n}}_j)$ $\rightarrow$ Numerical flux

# A high-order formulation for all-speed flows

## ▶ Approximate Riemann solvers

- Roe numerical flux

$$\mathcal{H}_j = \frac{1}{2}(\mathcal{F}^{\mathcal{H}}(U_j^+) + \mathcal{F}^{\mathcal{H}}(U_j^-)) \cdot \hat{n} - \frac{1}{2}\sum_{k=1}^{4} \tilde{\alpha}_k |\tilde{\lambda}_k| \tilde{r}_k$$

▷ $\tilde{\lambda} \rightarrow$ eigenvalues

▷ $\tilde{r} \rightarrow$ eigenvectors

$$\begin{aligned}
\tilde{\alpha}_1 &= \tfrac{1}{2\tilde{c}^2}\left[\Delta(p) - \tilde{\rho}\tilde{c}\left(\Delta(u)n_x + \Delta(v)n_y\right)\right] \\
\tilde{\alpha}_2 &= \tfrac{\tilde{\rho}}{\tilde{c}}\left[\Delta(v)n_x - \Delta(u)n_y\right] \\
\tilde{\alpha}_3 &= \tfrac{1}{\tilde{c}^2}\left[\Delta(p) - \tilde{c}^2\Delta(\rho)\right] \\
\tilde{\alpha}_4 &= \tfrac{1}{2\tilde{c}^2}\left[\Delta(p) + \tilde{\rho}\tilde{c}\left(\Delta(u)n_x + \Delta(v)n_y\right)\right]
\end{aligned}$$

- Rusanov numerical flux

$$\mathcal{H}_j = \frac{1}{2}(\mathcal{F}^{\mathcal{H}}(U_j^+) + \mathcal{F}^{\mathcal{H}}(U_j^-)) \cdot \hat{n} - \frac{1}{2}S^+\Delta(U)$$

▷ $S^+ = max(|v^+| + c^+, |v^-| + c^-)$

- Inviscid Flow past a cylinder. $M_\infty = 10^{-3}$

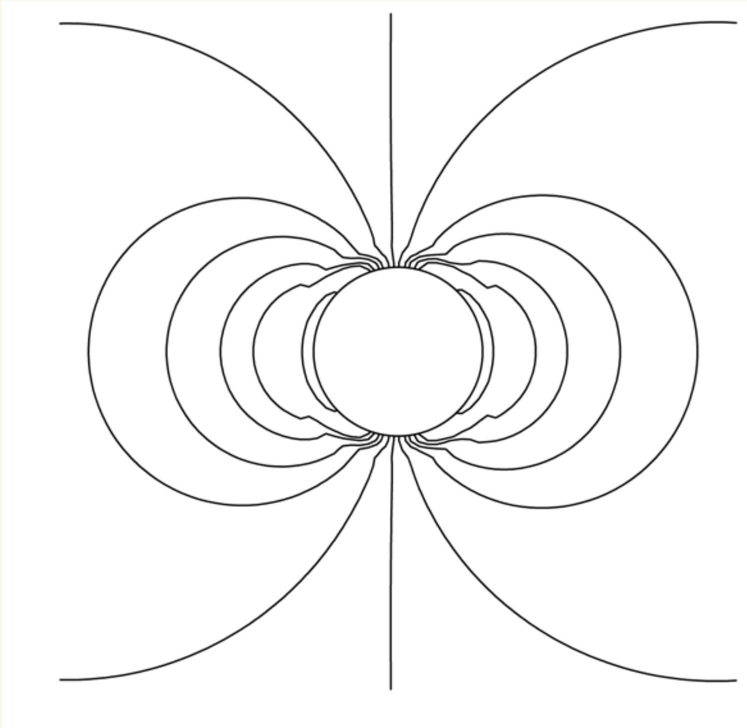

First-order FV

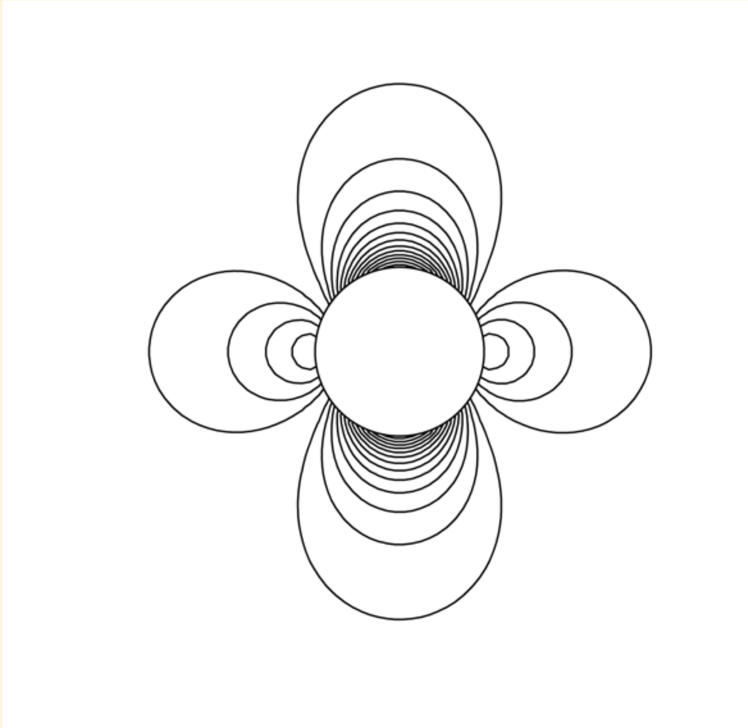

Fourth-order FV-MLS

- Inviscid Flow past a cylinder. $M_\infty = 10^{-3}$

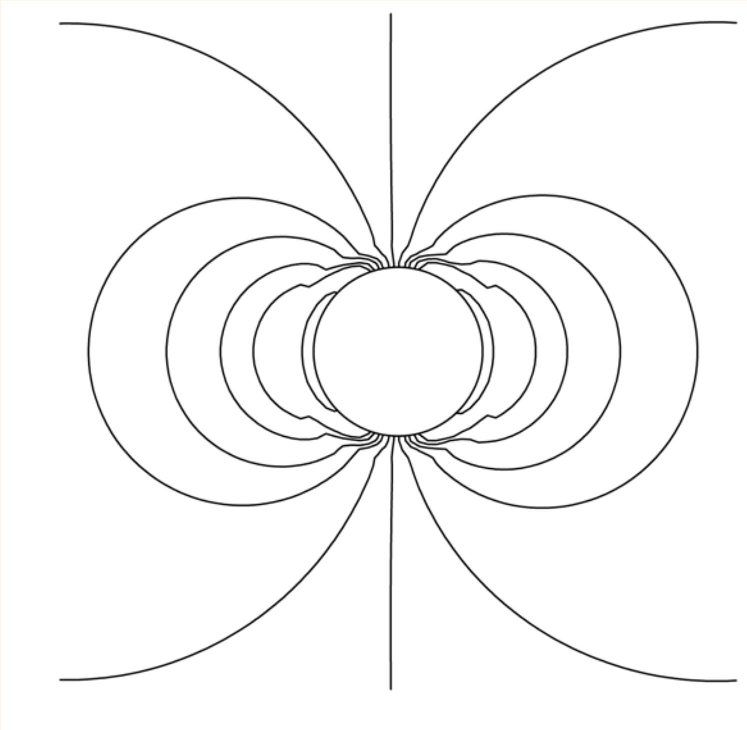

First-order FV

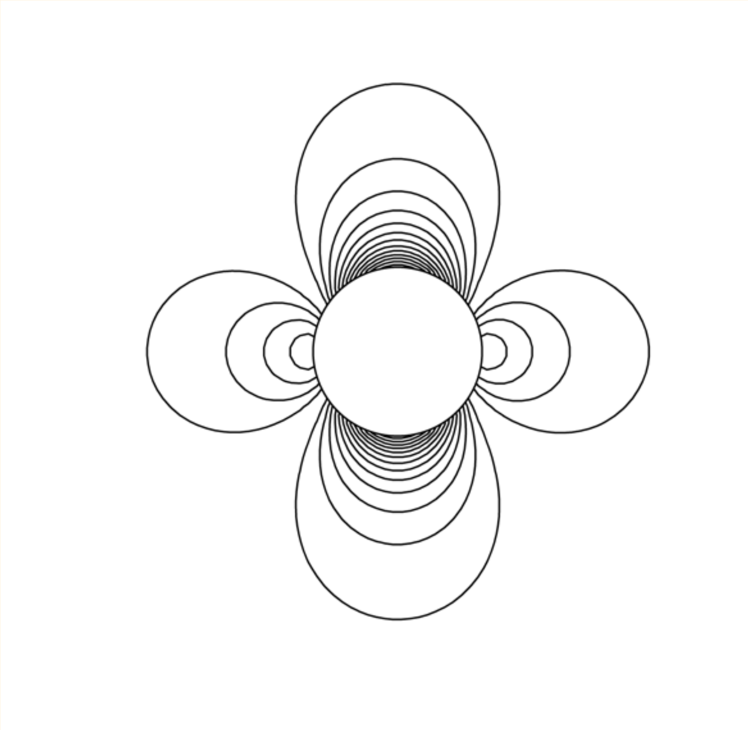

Fourth-order FV-MLS

Unphysical solution!

# Formulation

- Physical solution→Mach,mesh and order dependency

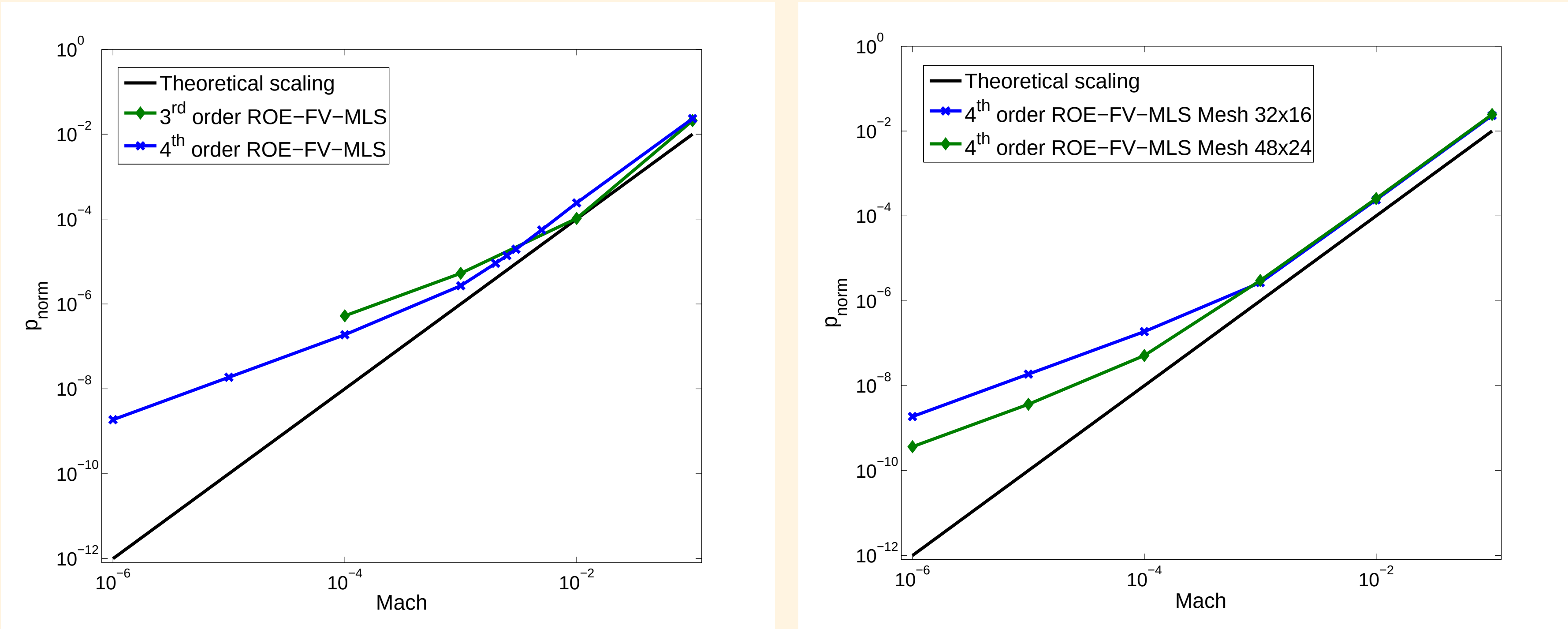


$$p_{norm} = \frac{p_{max} - p_{min}}{p_{max}} \qquad p_{norm} \sim \mathcal{O}(M_\infty^2)$$

# Formulation

- The numerical dissipation of the continuity and momentum equations can always be expressed as:

$$c_u \Delta \boldsymbol{u} + c_p \Delta p$$

  - ▷ $c_u$ and $c_p$ are the coefficients of the velocity difference and pressure difference terms
  - ▷ The accuracy problem is only attributable to $c_u = O(c)$ of the momentum equation
  - ▷ Checkerboard problems are attributable to the order of $c_p$ especially for the contiuity equation. A reasonable interval is $c_p \in [c_p^{-1}, c_p^{0}]$[1]

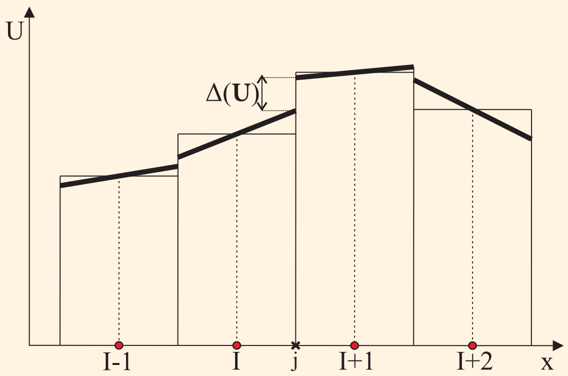


[1] X. -s. Li, C. -w. Gu *Mechanism of Roe-type schemes for all-speed flows and its application*, C&F, 2013

- Rieper's fix for the Roe flux

$$\boldsymbol{\mathcal{H}}_j = \frac{1}{2}(\boldsymbol{\mathcal{F}}^{\boldsymbol{\mathcal{H}}}(\boldsymbol{U}_j^+) + \boldsymbol{\mathcal{F}}^{\boldsymbol{\mathcal{H}}}(\boldsymbol{U}_j^-)) \cdot \hat{\boldsymbol{n}} - \frac{1}{2}\sum_{k=1}^{4} \tilde{\alpha}_k |\tilde{\lambda}_k| \tilde{\boldsymbol{r}}_k$$

$$\tilde{\alpha}_1 = \frac{1}{2\tilde{c}^2}\left[\Delta(p) - \tilde{\rho}\tilde{c} f(M_l)\left(\Delta(u)n_x + \Delta(v)n_y\right)\right]$$

$$\tilde{\alpha}_2 = \frac{\tilde{\rho}}{\tilde{c}}\left[\Delta(v)n_x - \Delta(u)n_y\right]$$

$$\tilde{\alpha}_3 = \frac{1}{\tilde{c}^2}\left[\Delta(p) - \tilde{c}^2\Delta(\rho)\right]$$

$$\tilde{\alpha}_4 = \frac{1}{2\tilde{c}^2}\left[\Delta(p) + \tilde{\rho}\tilde{c} f(M_l)\left(\Delta(u)n_x + \Delta(v)n_y\right)\right]$$

$$f(M_l) = min(M_l, 1) \qquad M_l = \frac{|\tilde{u}|_I + |\tilde{v}|_I}{\tilde{c}_I}$$

▶ Inviscid Flow past a cylinder. $M_\infty = 10^{-2}$

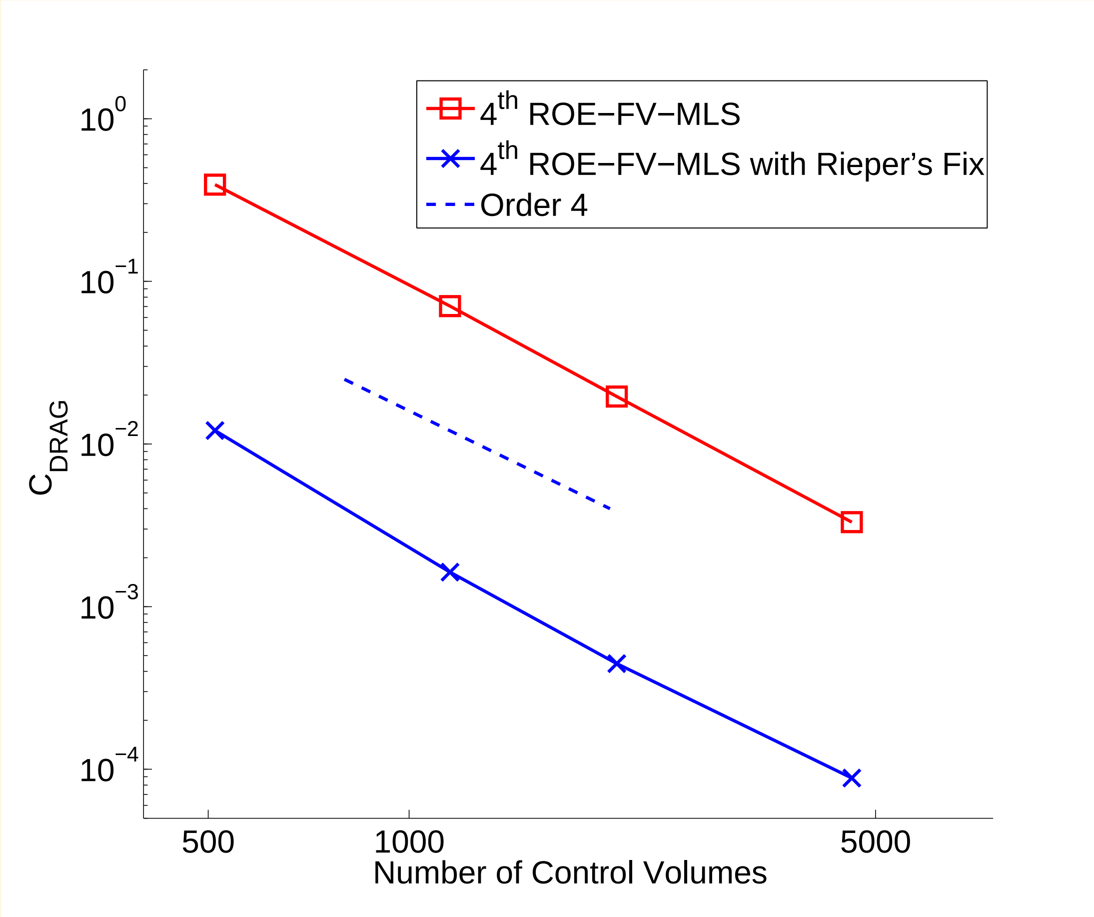


- The formal order of accuracy is recovered

▶ Inviscid Flow past a cylinder. $M_\infty = 10^{-3}$

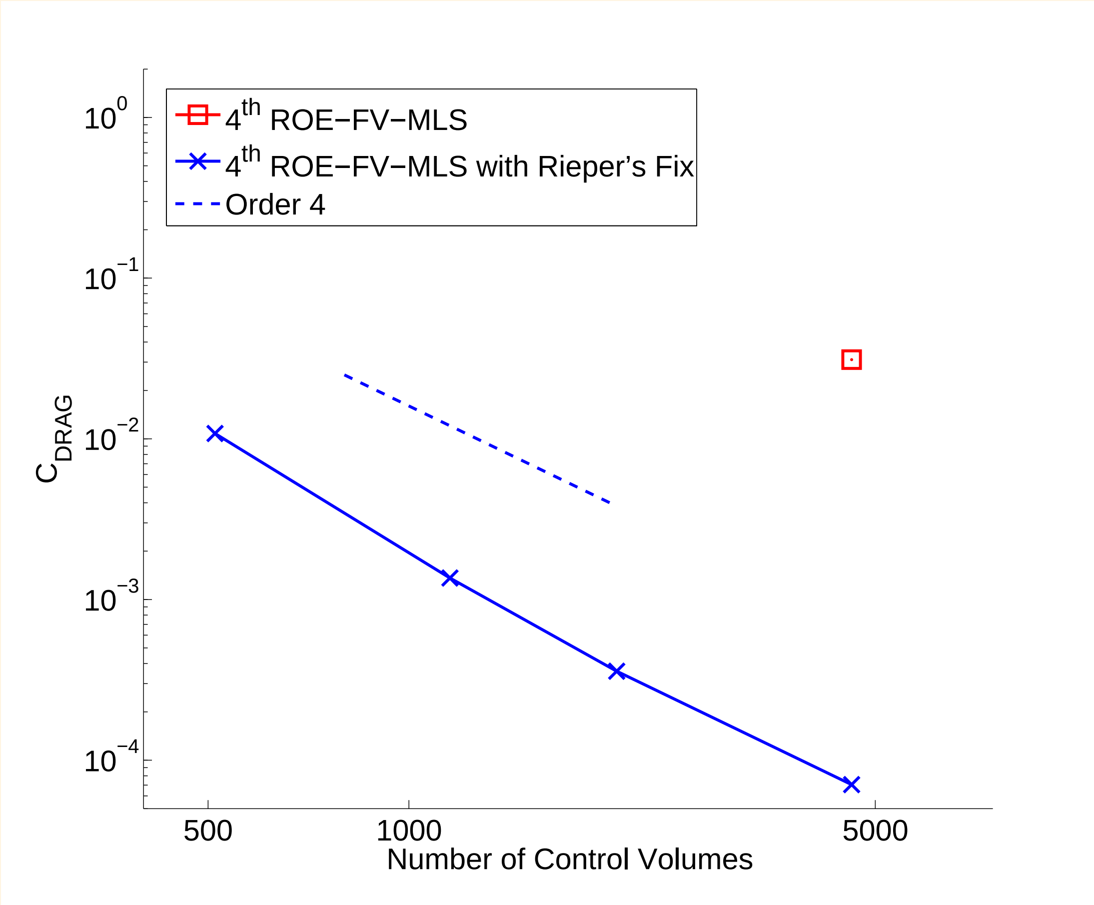


- The formal order of accuracy is recovered with the fix

- Inviscid Flow past a cylinder. $M_\infty = 10^{-6}$.
  - $4^{th}$ ROE-FV-MLS with Rieper's fix
  - $32 \times 16$ grid

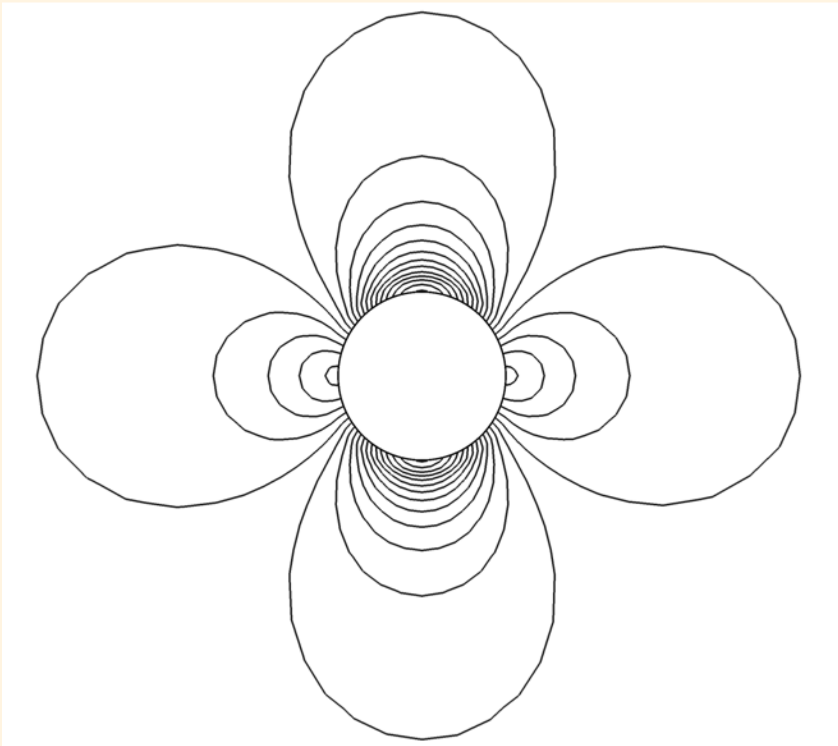

Pressure contours

▶ Li and Gu's fix for the Rusanov flux

$$\boldsymbol{\mathcal{H}}_j = \frac{1}{2}(\boldsymbol{\mathcal{F}}^{\boldsymbol{\mathcal{H}}}(\boldsymbol{U}_j^+) + \boldsymbol{\mathcal{F}}^{\boldsymbol{\mathcal{H}}}(\boldsymbol{U}_j^-)) \cdot \hat{\boldsymbol{n}} - \frac{1}{2}S^+\Delta(\boldsymbol{U})$$

$$S^+ = max(|\boldsymbol{v}^+| + c^+, |\boldsymbol{v}^-| + c^-)$$

$$\Delta(\boldsymbol{U}) = \left\{ \begin{array}{l} \Delta(\rho) \\ f(M_l)\Delta(\rho u) \\ f(M_l)\Delta(\rho v) \\ \Delta(\rho E) \end{array} \right\}$$

$$f(M_l) = min(M_l, 1) \qquad M_l = \frac{|u|_I + |v|_I}{c_I}$$

- Inviscid Flow past a cylinder. $M_\infty = 10^{-2}$

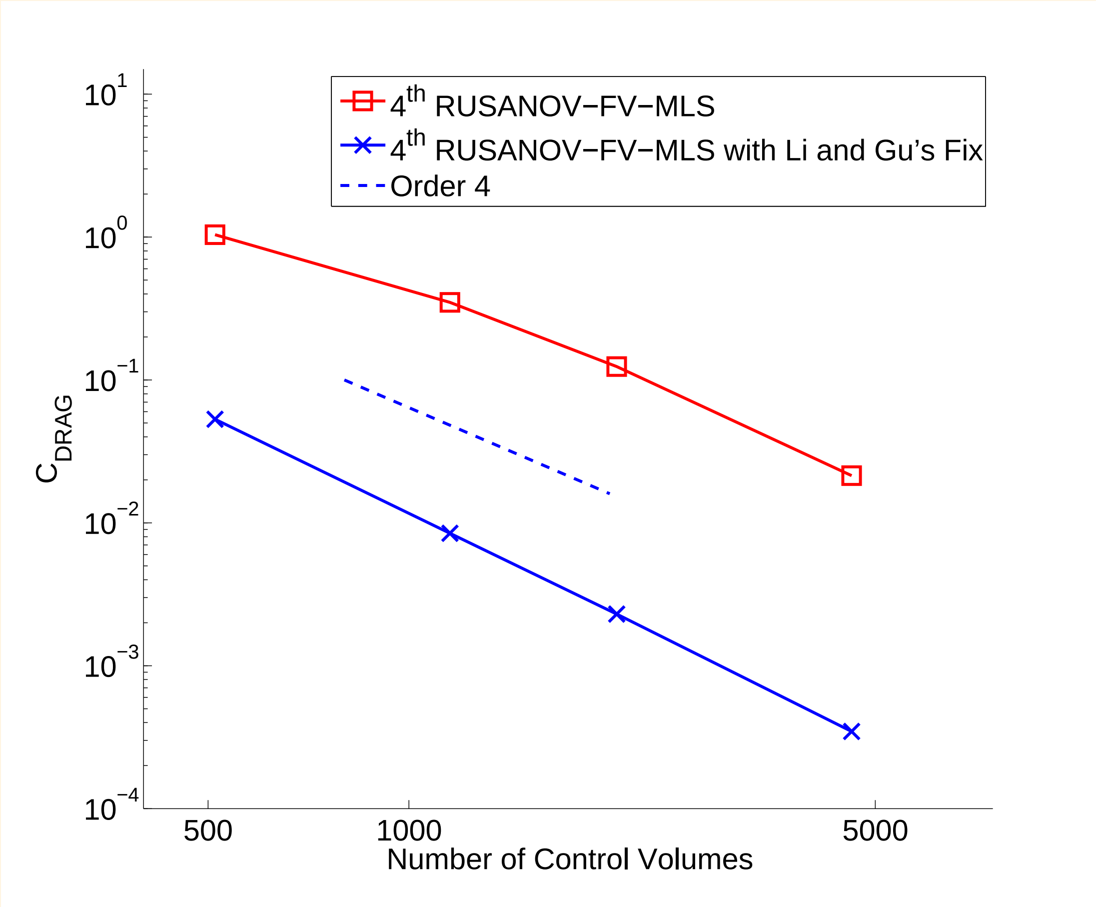


- The formal order of accuracy is recovered

▶ Inviscid Flow past a cylinder. $M_\infty = 10^{-3}$

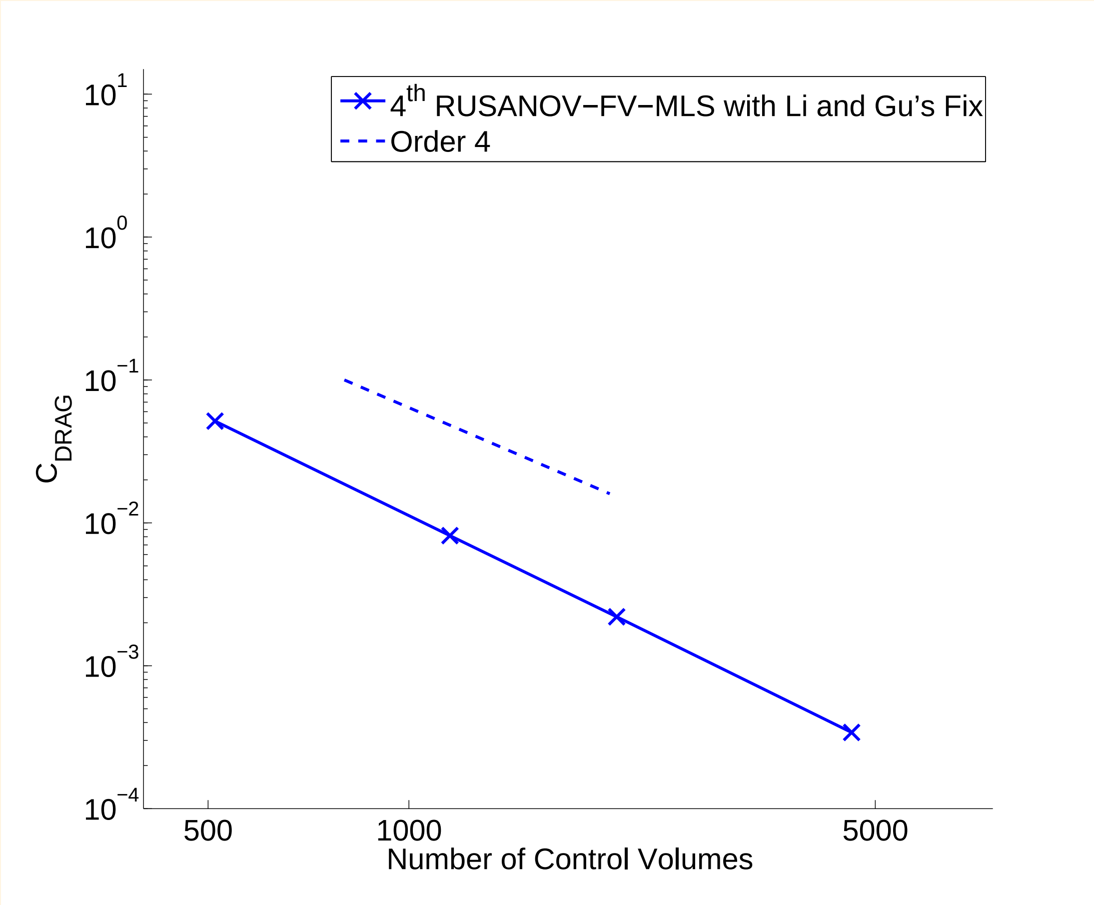


- The formal order of accuracy is recovered with the fix

- Inviscid Flow past a cylinder. $M_\infty = 10^{-2}$.
  - RUSANOV-FV-MLS with Li and Gu's fix
  - $96 \times 48$ grid

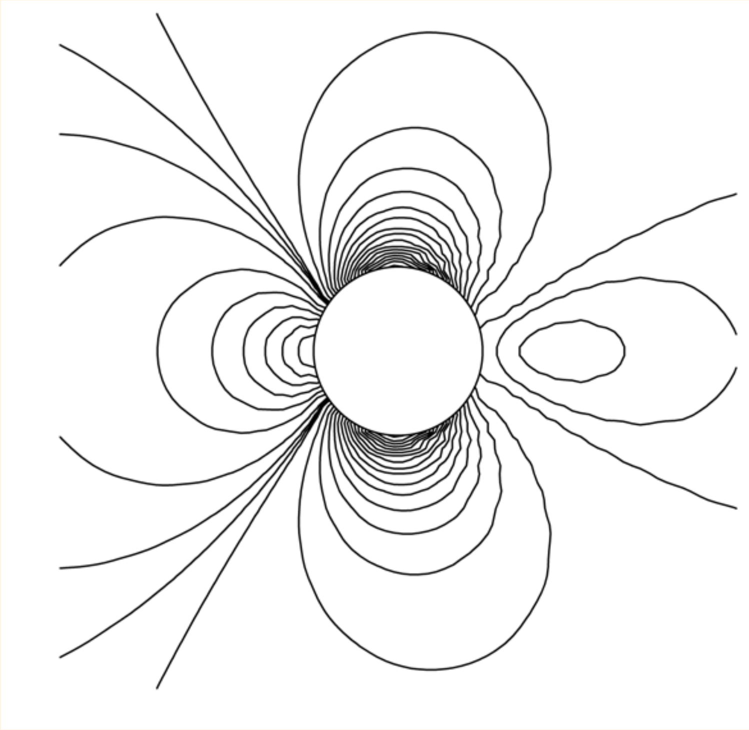

$1^{st}$ order

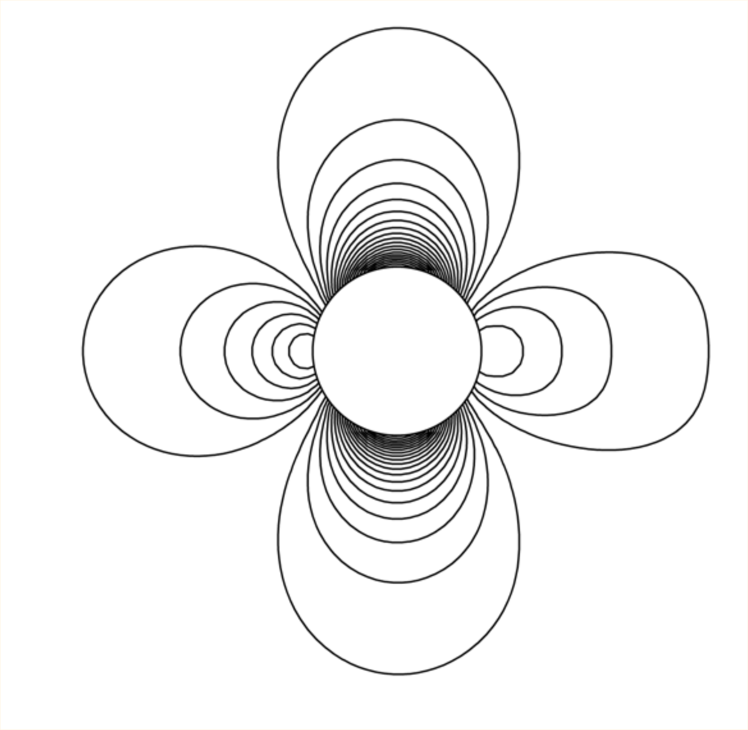

$4^{th}$ order

# A high-order formulation for all-speed flows

- Inviscid Flow past a cylinder. $M_\infty = 10^{-2}$.
  - RUSANOV-FV-MLS with Li and Gu's fix
  - $96 \times 48$ grid

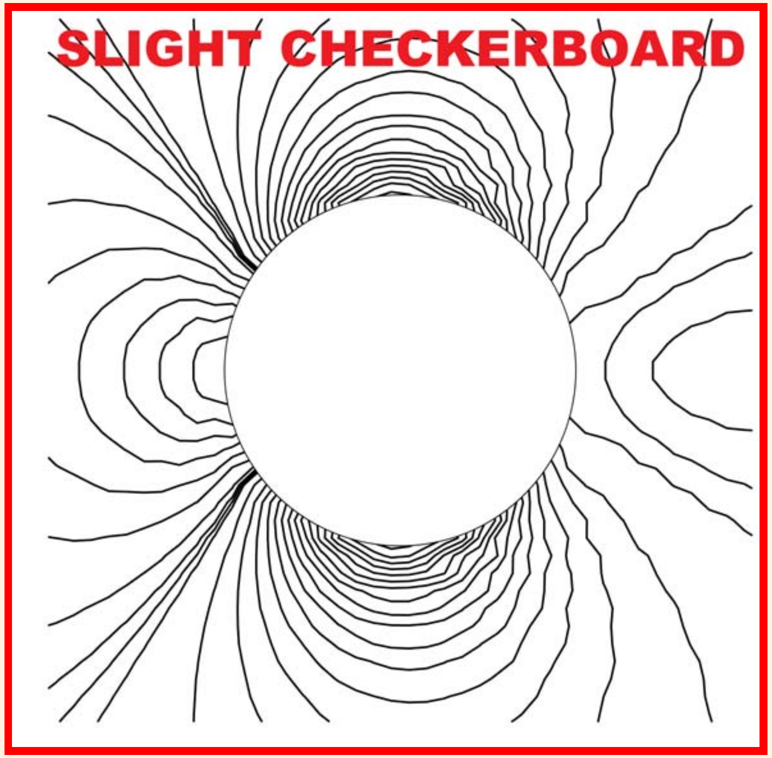


$1^{st}$ order

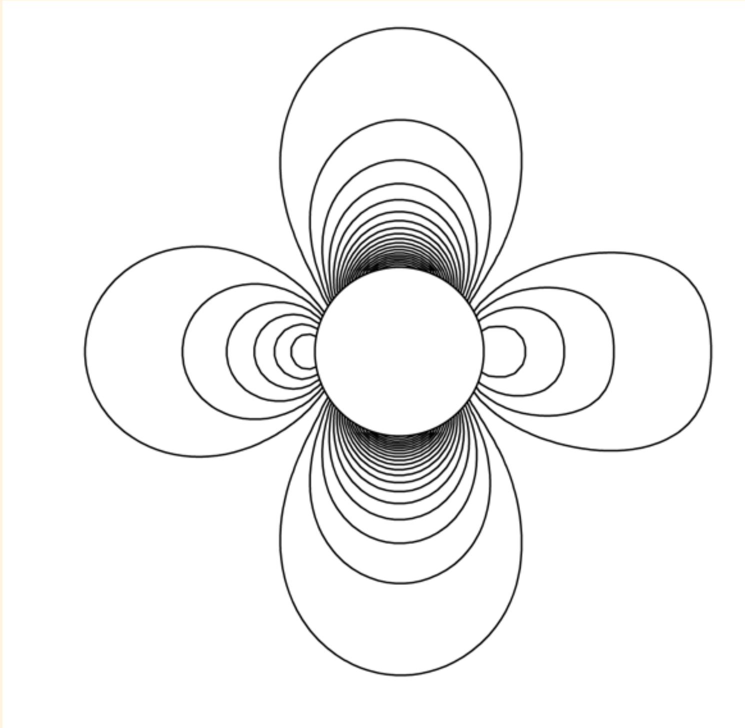

$4^{th}$ order

# Slope limiters

- Slope limiters are used to design TVD schemes.

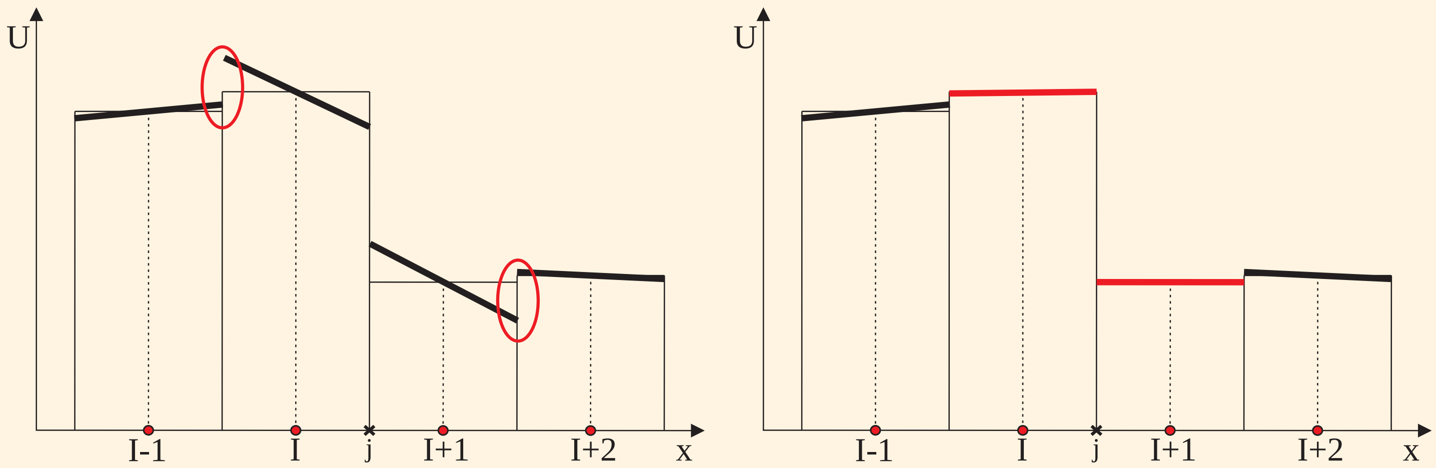


- A slope limiter limits the Taylor reconstruction of a high-order finite volume scheme as follows:

$$\boldsymbol{U}(\boldsymbol{x}) = \boldsymbol{U}_I + \chi_I \nabla \boldsymbol{U}_I \cdot (\boldsymbol{x} - \boldsymbol{x}_I)$$

- $\chi_I = 0 \Rightarrow$ First-order scheme
- $\chi_I = 1 \Rightarrow$ No limitation

- Slope limiters:
  - Barth and Jespersen slope limiter
    - Non-differential limiter
  - Venkatakrishnan slope limiter
    - Differentiable limiter
    - Near strong shocks may introduce deviations from the monotone solution
  - Van-Albada limiter
    - Non-differential limiter

- Inviscid Flow past a cylinder. $M_\infty = 10^{-3}$.
  - $4^{th}$ FV-MLS
  - Unstructured grid of $2320$ elements.

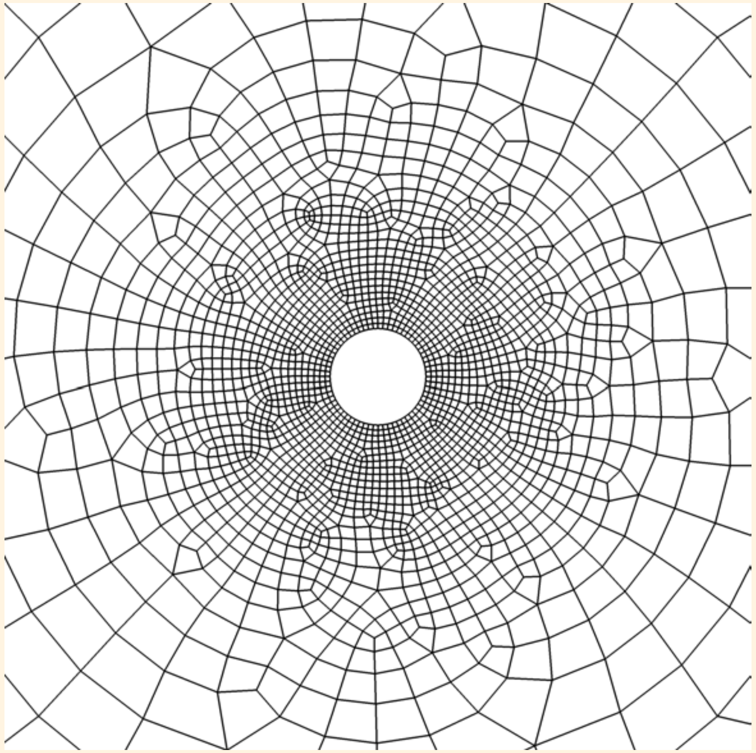

# Slope limiters

- Inviscid Flow past a cylinder. $M_\infty = 10^{-3}$.

| Method | Barth-Jespersen | Van Albada | Venkatakrishnan |
|---|---|---|---|
| $4^{th}$ROE+ Rieper's fix | 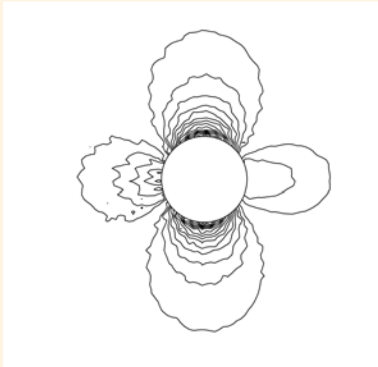 | 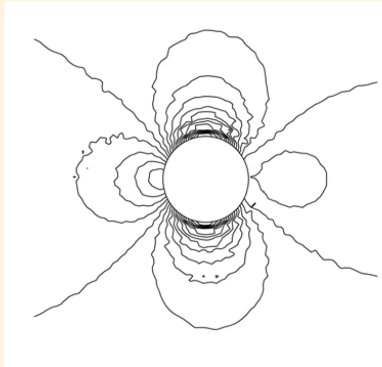 | 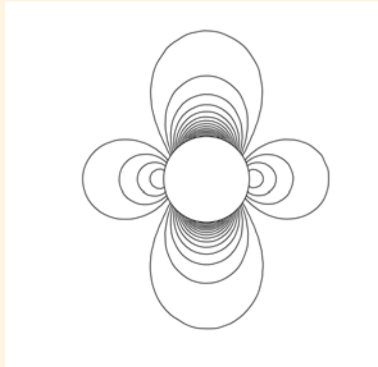 |
| $4^{th}$ RUSANOV+Li and Gu's fix | 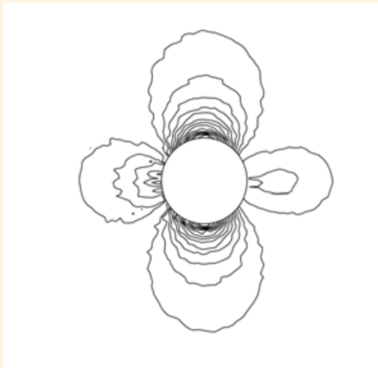 | 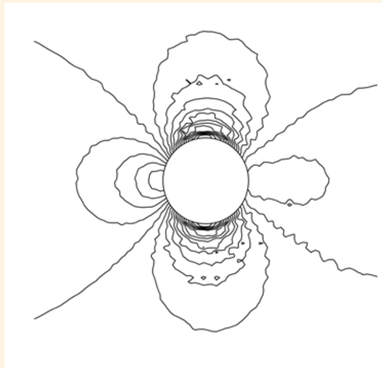 | 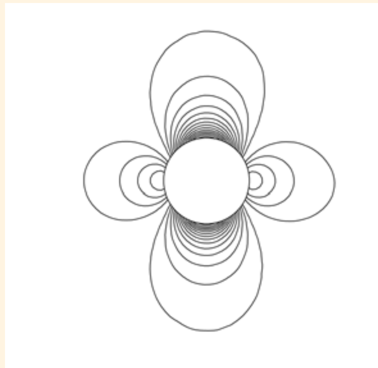 |

# Slope limiters

| Method | Van Albada | Van Albada + MLS-based sensor |
|---|---|---|
| $4^{th}$ROE+ Rieper's fix | 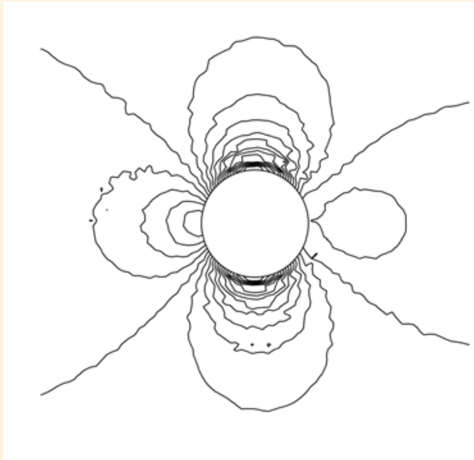 | 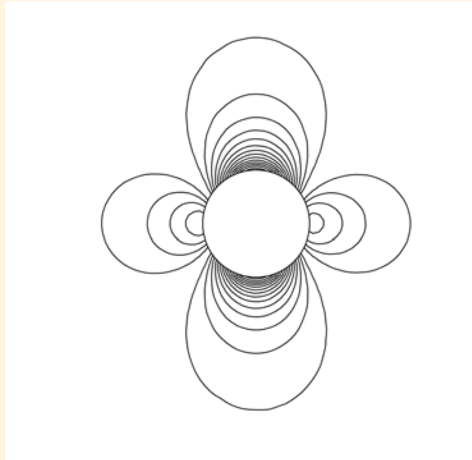 |
| $4^{th}$ RUSANOV+Li and Gu's fix | 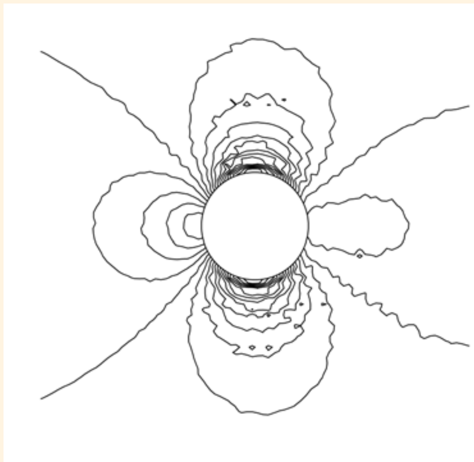 | 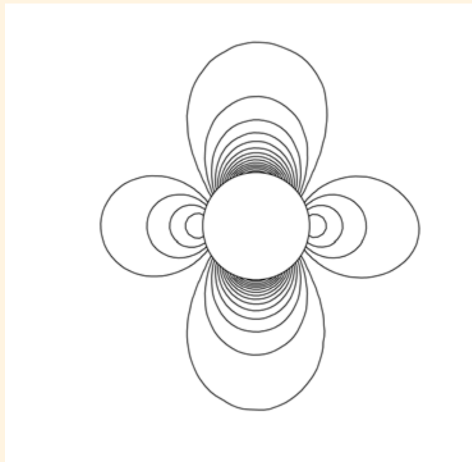 |

SHARK-FV 2015 Conference
SHARING HIGHER-ORDER ADVANCED RESEARCH KNOW-HOW on FINITE VOLUME
Ofir, Portugal
May 18 - 22, 2015

- 3D decay of compressible isotropic turbulence
  - Domain: $\Omega_T = [-\pi, \pi]^3 \rightarrow 32^3$ elements.
  - Periodic boundary conditions.
  - $3^{rd}$ order ROE-FV-MLS with Rieper's fix.
  - Van Albada limiter with the MLS-based sensor.
  - Reference solution: $6^{th}$ order FD + LES.

# Numerical Examples



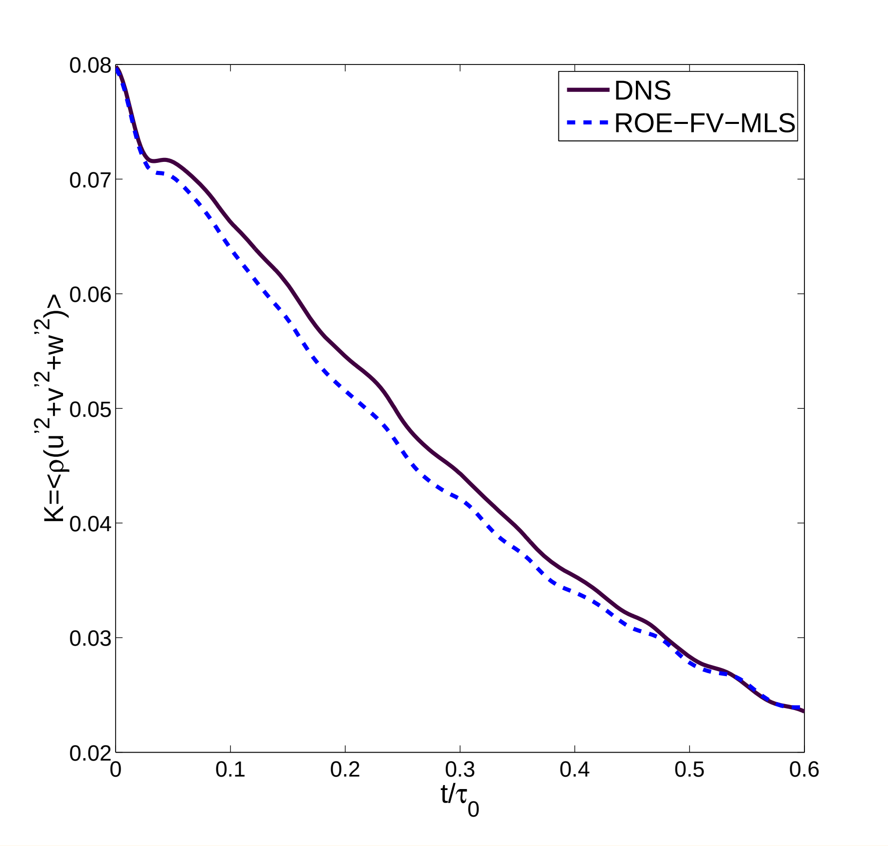


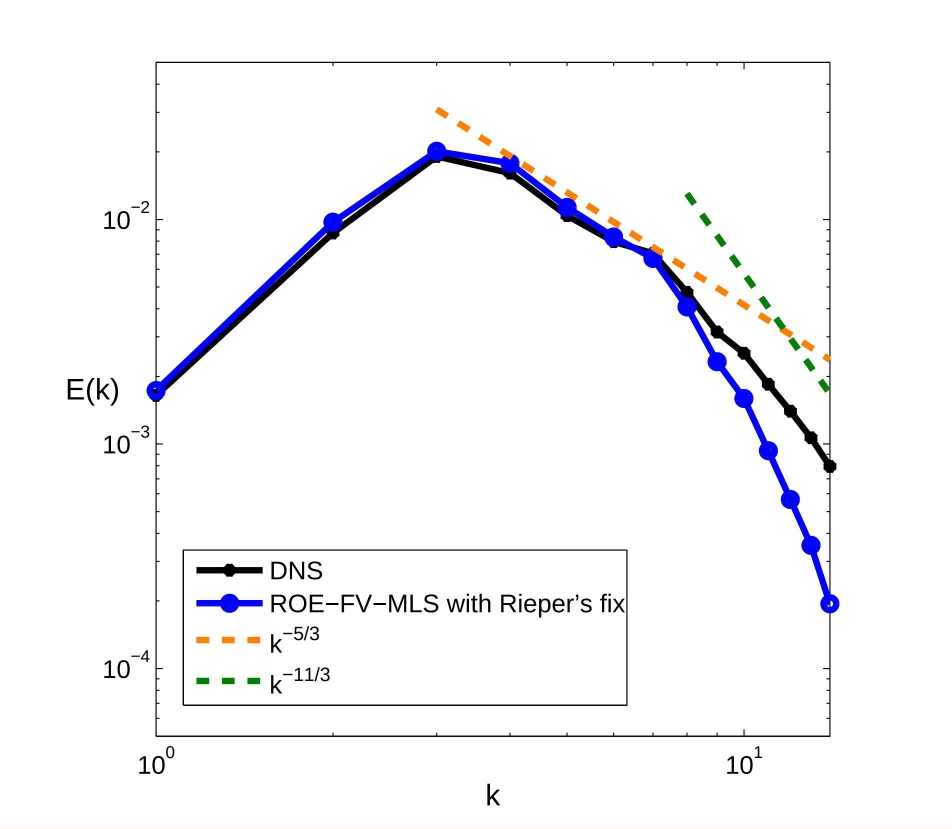


$$t/\tau_0 = 0.3$$

## Numerical Examples

- Unsteady transonic viscous flow over a circular cylinder
  - $M_\infty = 0.80$. $Re = 166.000$.
  - $3^{rd}$ ROE-FV-MLS with Rieper's Fix.

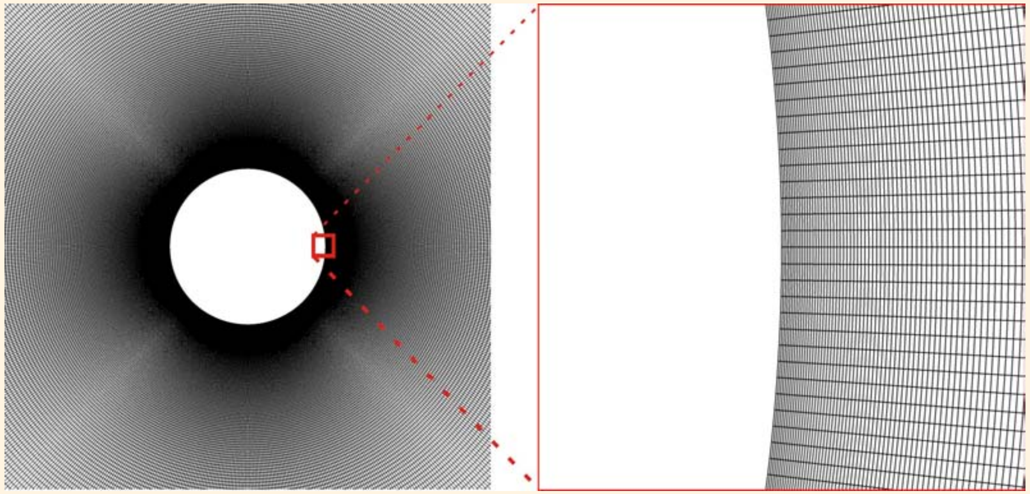

- 720 CV around the cylinder.
- $y_n = 2.85 \times 10^{-4} D$
- Total: $206.150$ CV.

SHARK-FV 2015 Conference
SHARING HIGHER-ORDER ADVANCED RESEARCH KNOW-HOW on FINITE VOLUME
Ofir, Portugal
May 18 - 22, 2015

## Numerical Examples

- Unsteady transonic viscous flow over a circular cylinder

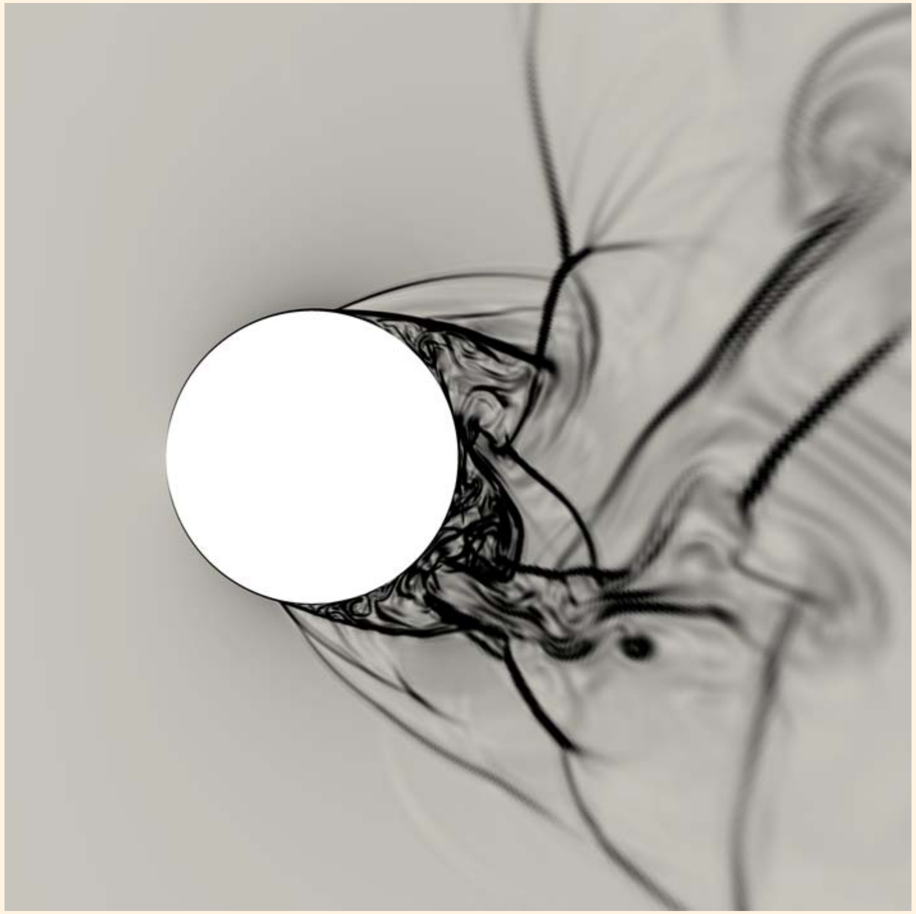

# Numerical Examples

- Unsteady transonic viscous flow over a circular cylinder

| Method | $C_{DRAG}$ |
|---|---|
| Reference 2D computations | 1.86 |
| FV-MLS Van Albada | 1.82 |
| FV-MLS Venkatakrishnan | 1.84 |
| FV-MLS Van Albada+MLS-based sensor | 1.81 |
| Experimental | 1.50 |

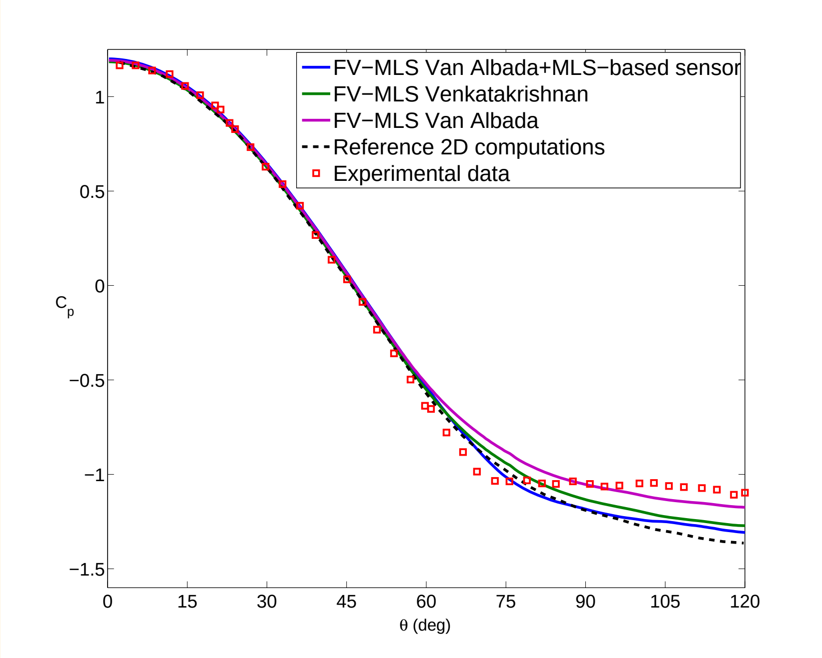


Experimental reference: Murthy, V.S., Rose, W.C., *Detailed Measurements on a Circular Cylinder in Cross Flow*, AIAA Journal, $57$, 549–550, 1978.

2D reference: Garcia, R., Bobenrieth, R.F., *Dettached Eddy simulation of the transonic flow over a circular cylinder*, Proceedings of COBEM, 2005.

- Introduction
- The FV-MLS method
- Multiscale properties of MLS: MLS-based shock detection
- A formulation for all-speed flows
- A MLS-based sliding mesh technique
- Application to Navier-Stokes-Korteweg equations
- Conclusions

- Two different approaches
  - 1. MLS-based sliding mesh with intersections.
  - 2. Interface halo-cell sliding mesh.

# MLS-based sliding mesh with intersections

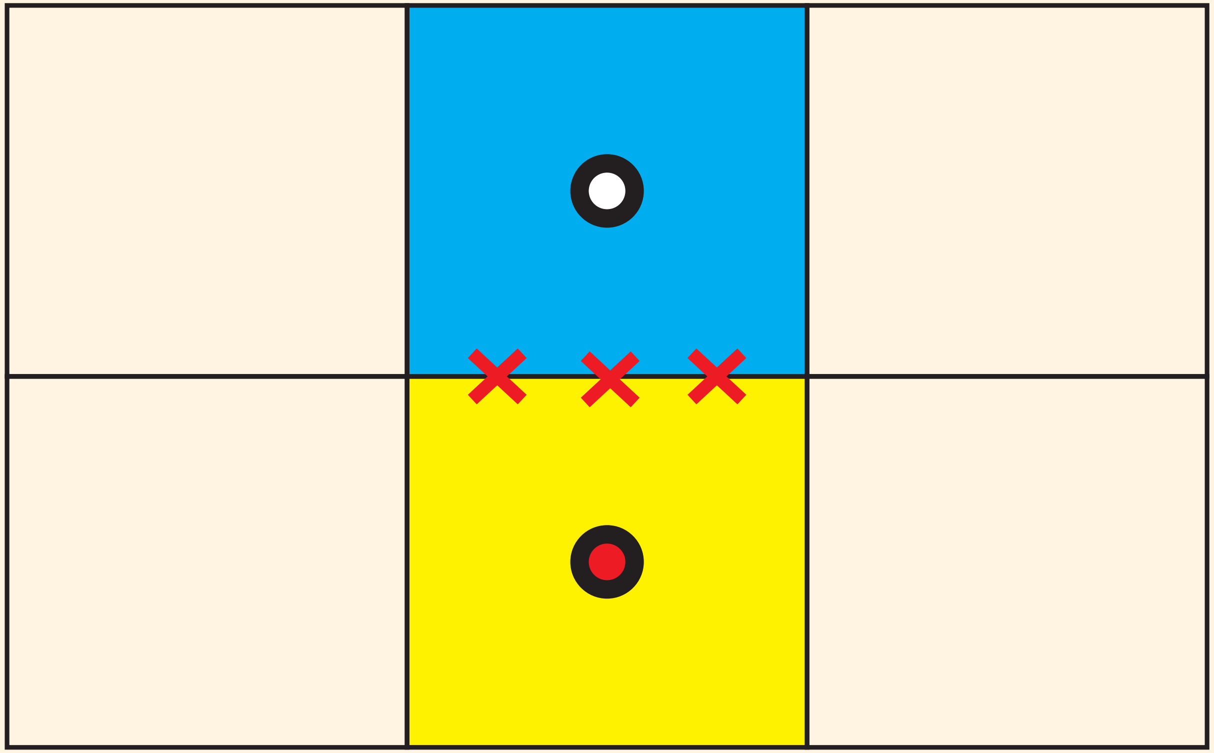

# MLS-based sliding mesh with intersections

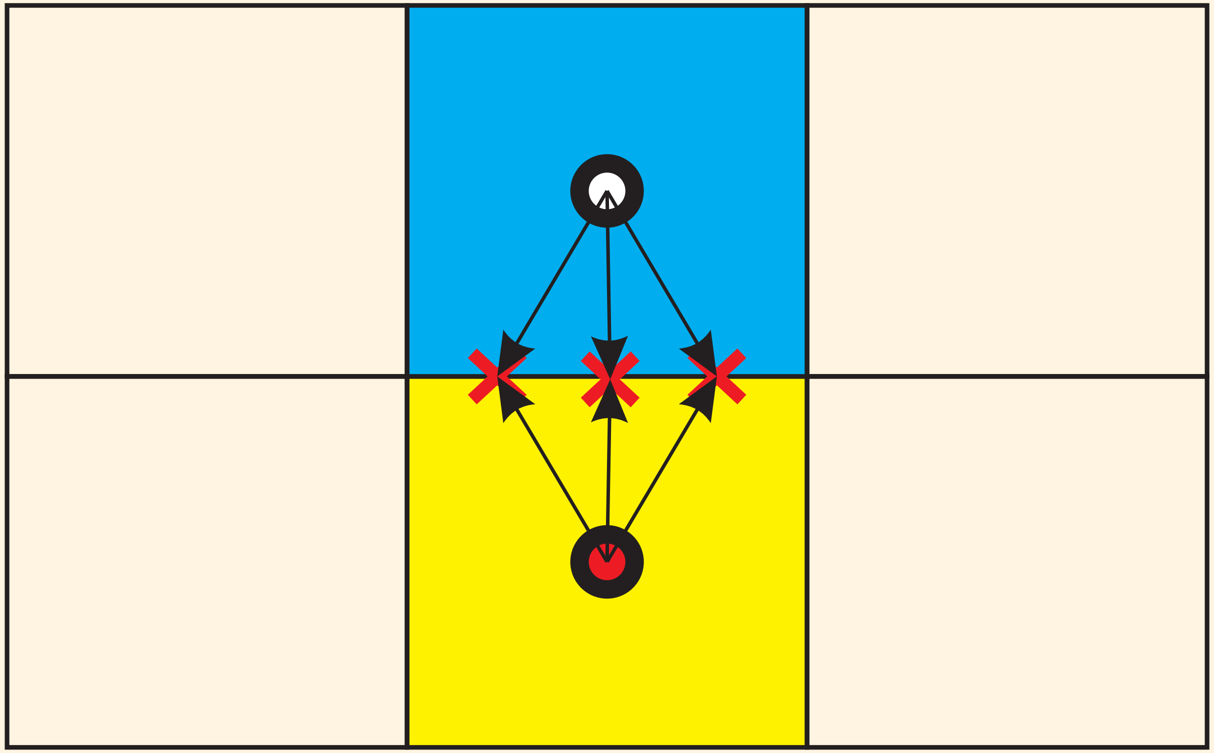

# MLS-based sliding mesh with intersections

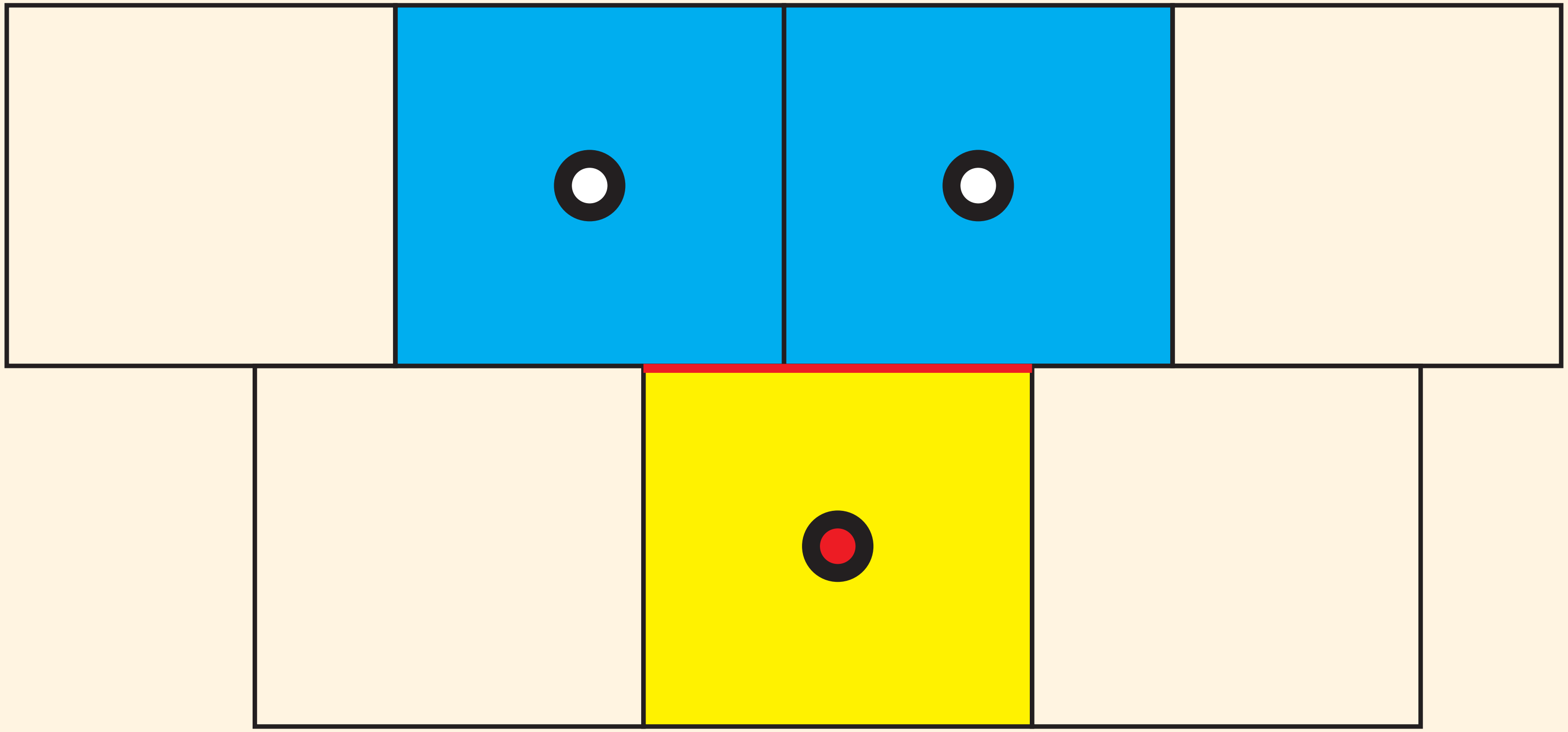

# MLS-based sliding mesh with intersections

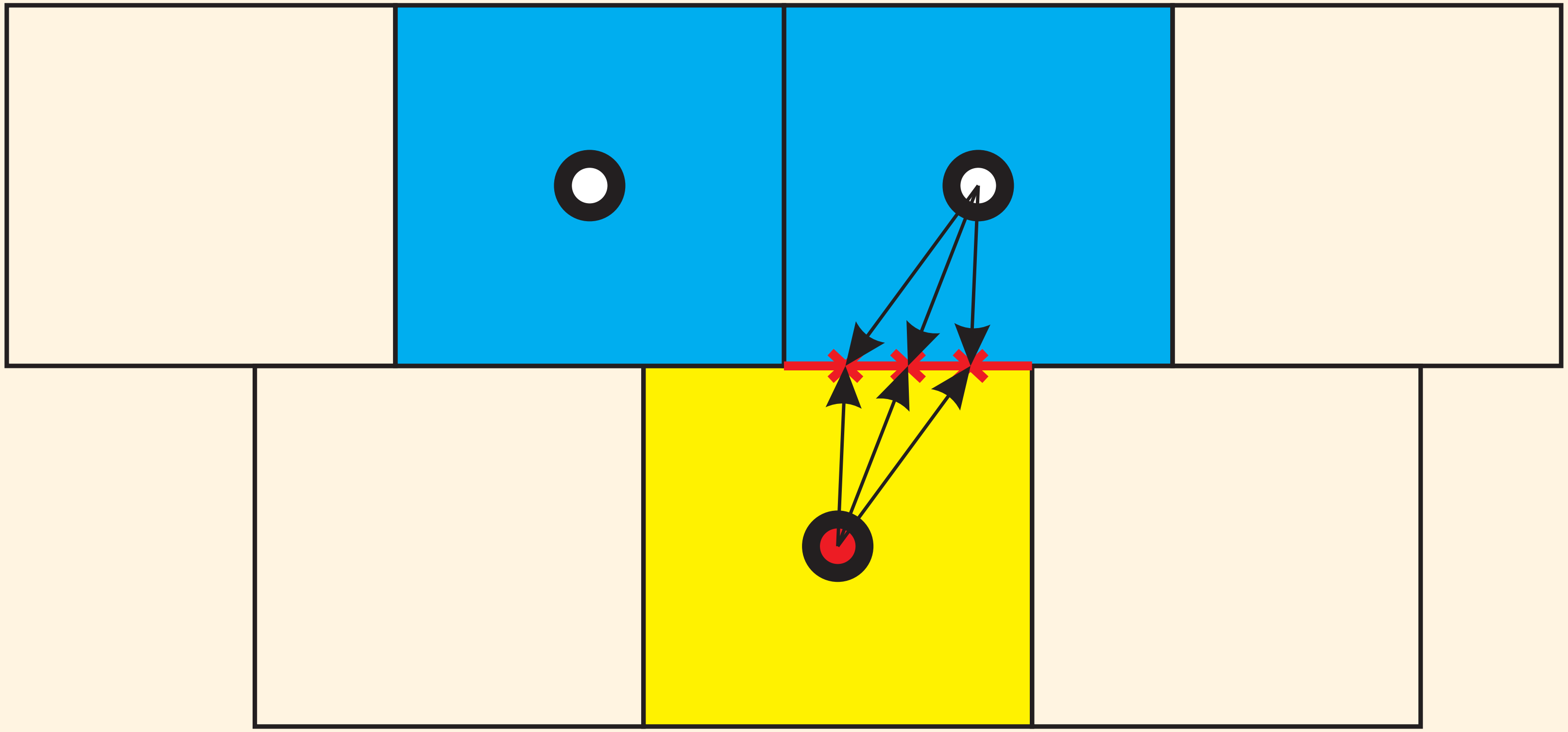

# MLS-based sliding mesh with intersections



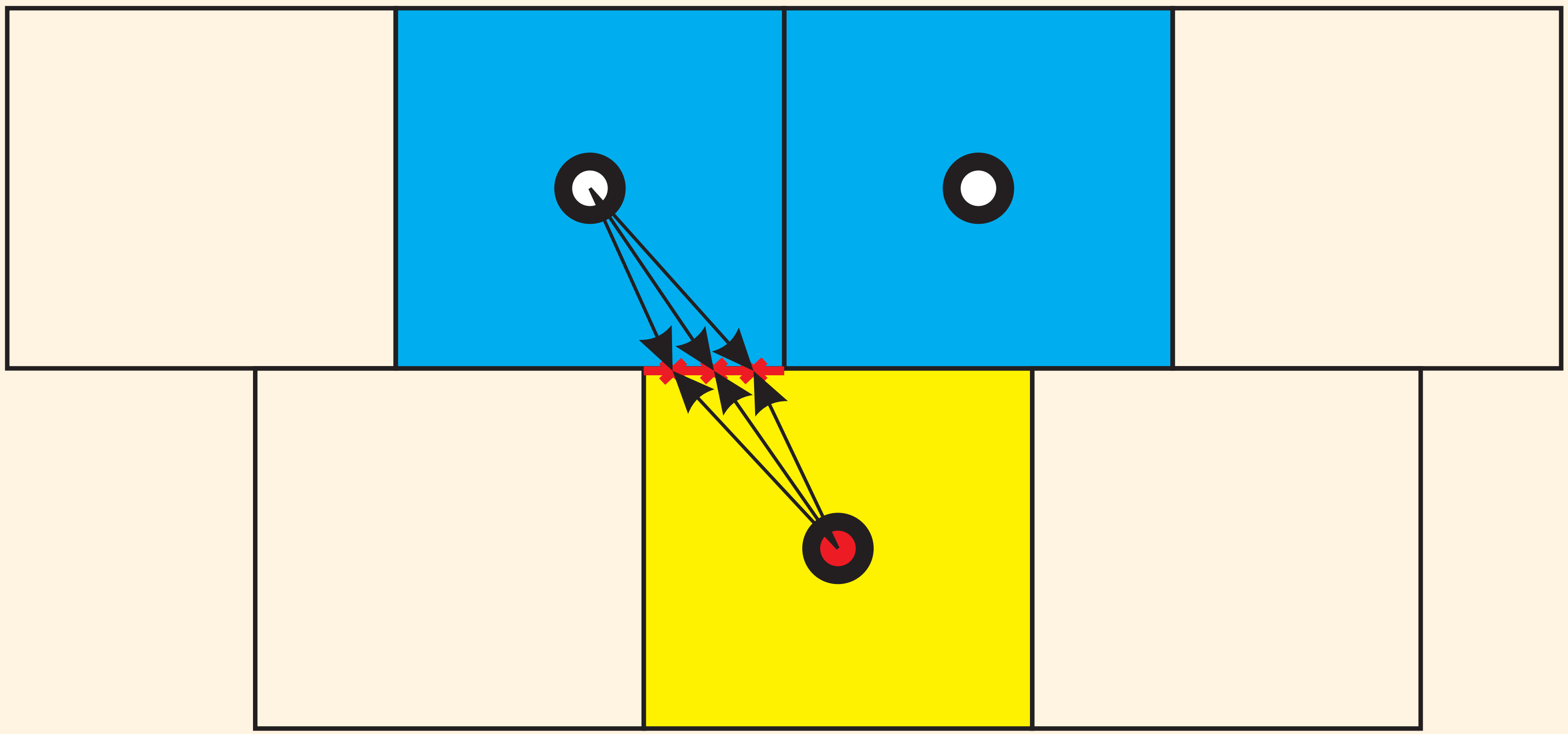

- MLS-based sliding mesh with intersections.
  - Recursive searching of intersection nodes.
  - Computation of the numerical flux at interface.

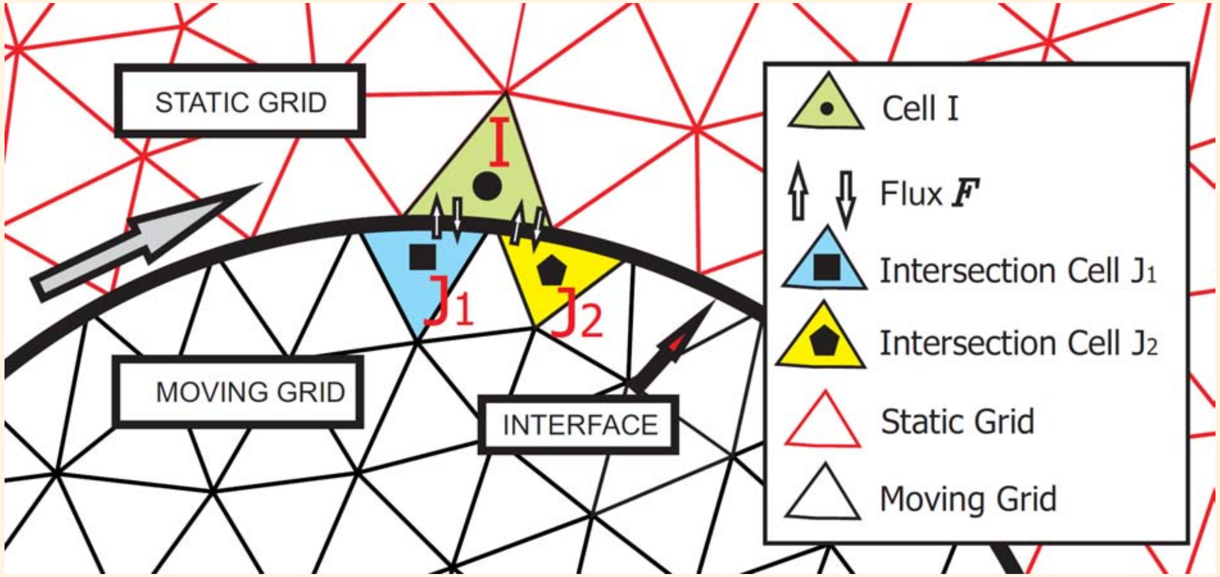

- MLS-based sliding mesh with intersections.
  - The stencil can be defined as:

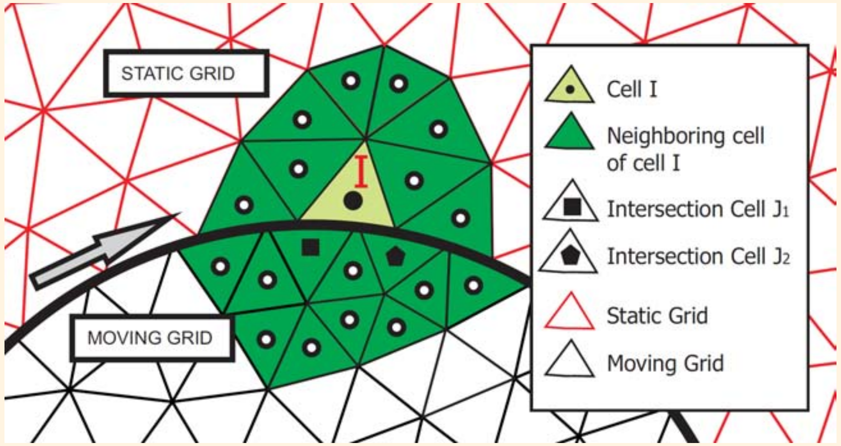


Full Stencil

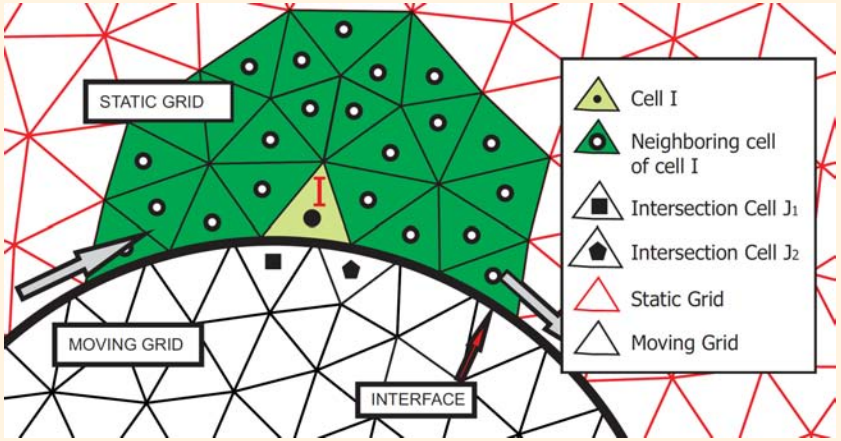


Half Stencil

- Interface halo cell sliding mesh.
  - Create a halo cell.
  - Computation of the numerical flux at interface.

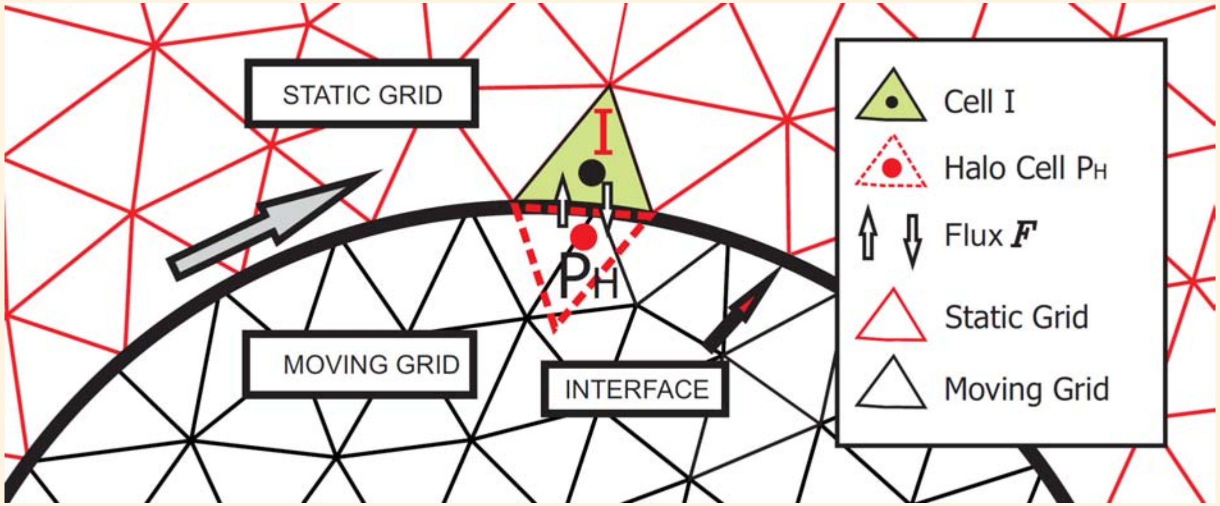

# A MLS-based sliding mesh technique

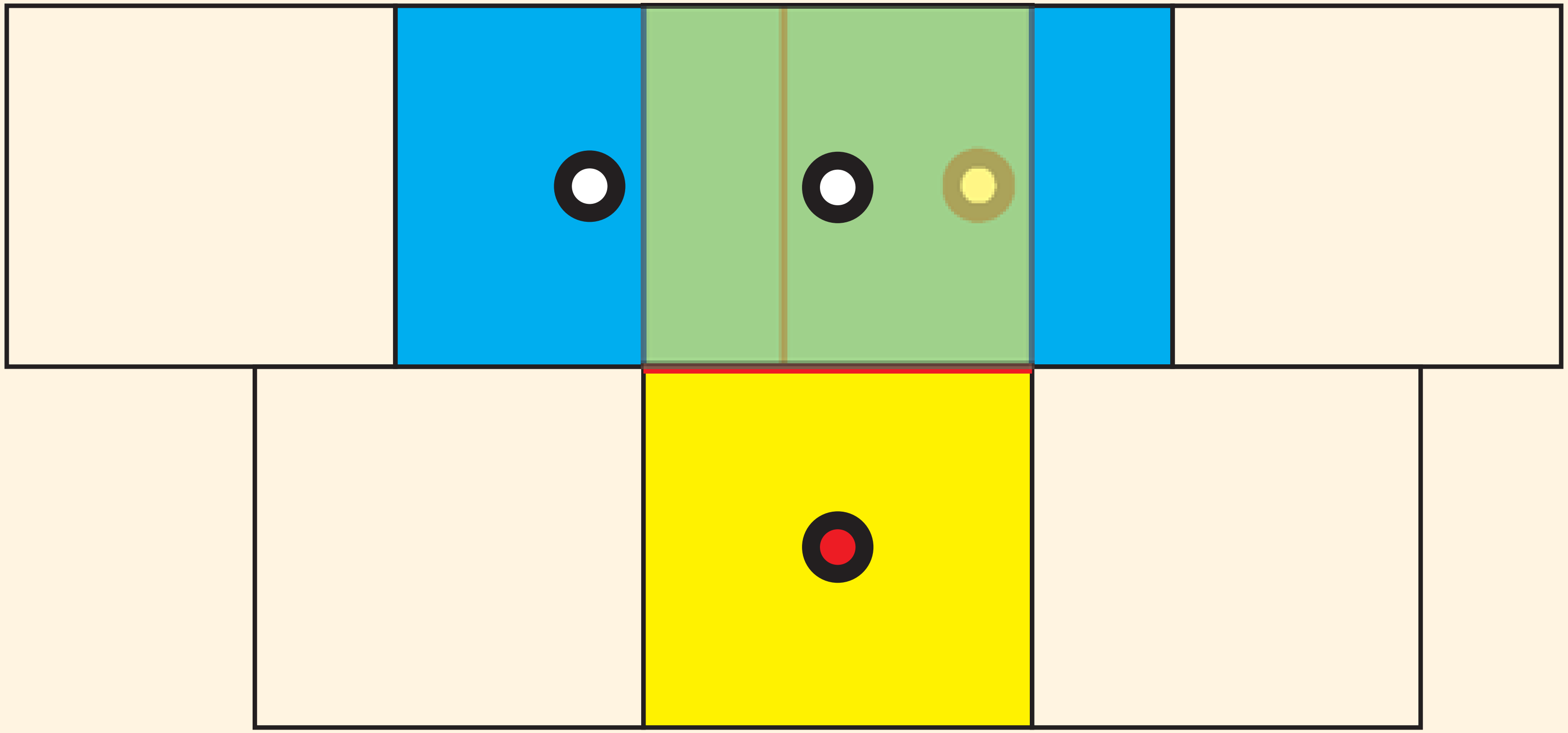

# A MLS-based sliding mesh technique

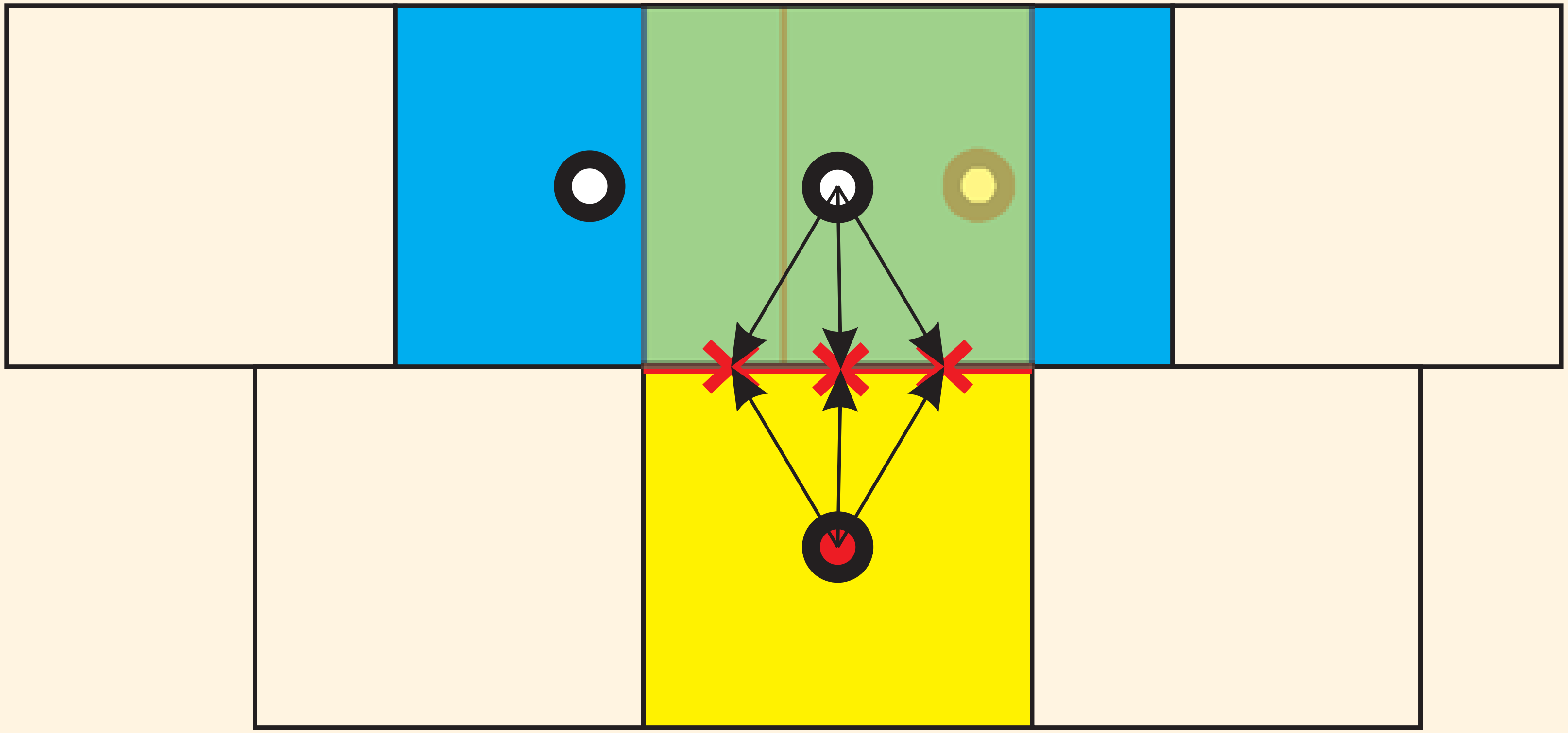

# A MLS-based sliding mesh technique



- $\boldsymbol{U}_{P_H}$ is defined as

$$\boldsymbol{U}_{P_H} = \frac{1}{A_{P_H}} \int \boldsymbol{U} dA = \frac{1}{A_{P_H}} \int \sum_{j=1}^{n_x} N_j(\boldsymbol{x}_{P_H}) U_j dA$$

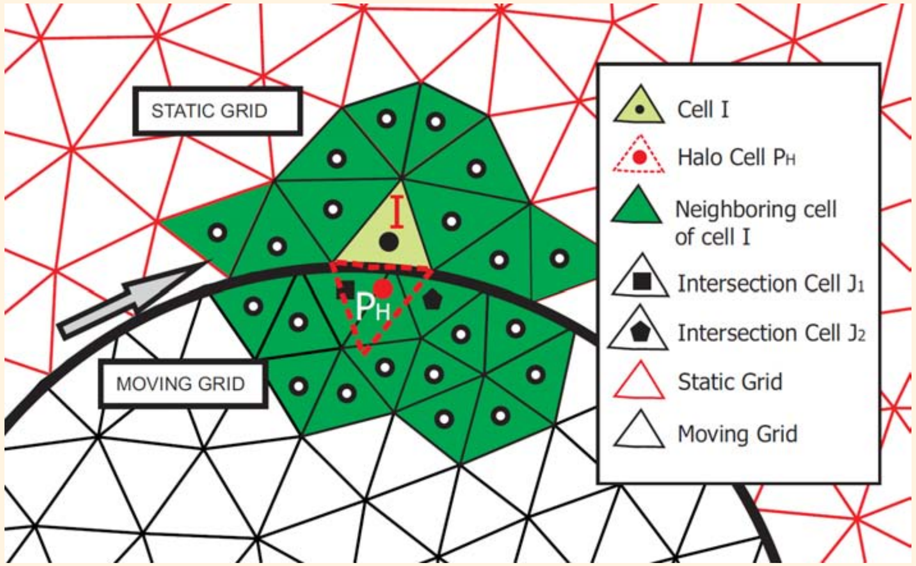


- It avoids the computation of intersection points!

- 1D Steady Shock
  - Initial Conditions

$$\begin{aligned} \rho_L &= 1, & \rho_R &= 1.8621 \\ u_L &= 1.5, & u_R &= 0.8055 \\ p_L &= 0.71429, & p_R &= 1.7559 \end{aligned}$$

  - Computational domain $0 \leq x \leq 10$ discretized in two regions of $25$ elements
  - The Interface is located at $x = 5.0$

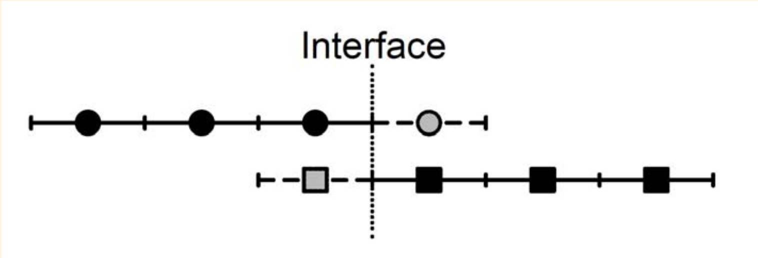


Z.J.Wang et al.. Recent development on the conservation property of chimera. IJCFD, 15,265-278,2001.

- 1D Steady Shock

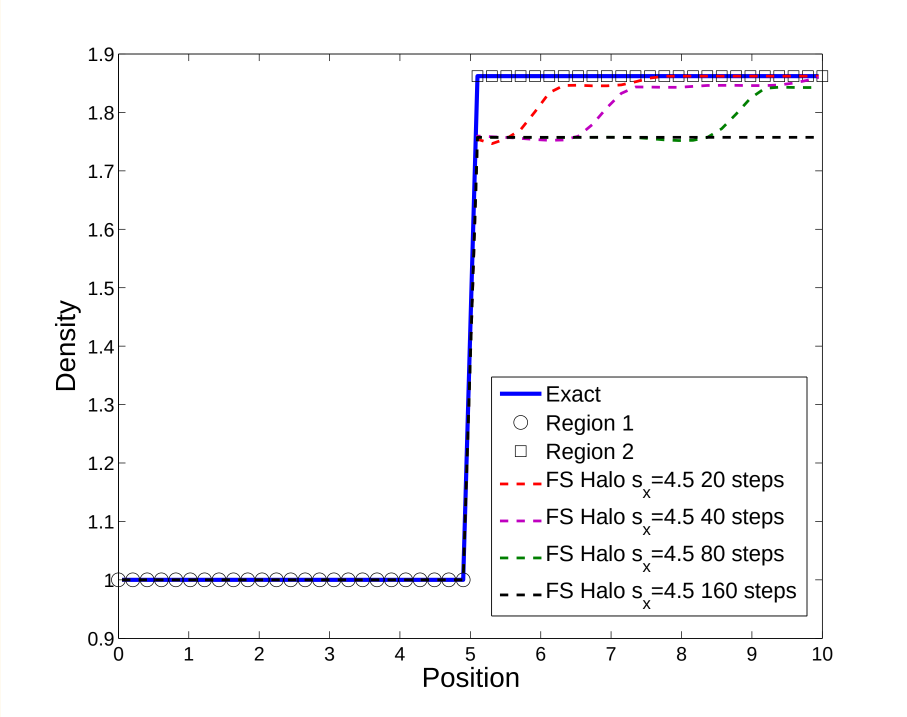


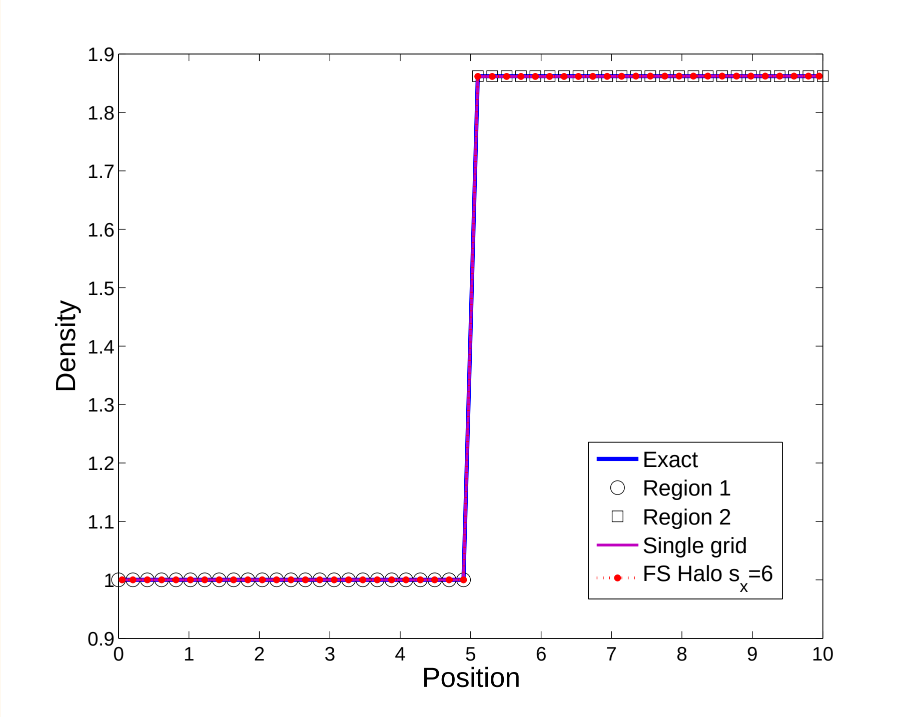

## 1D Unsteady Shock

- First test case of: *Riemann solvers and numerical methods for fluid dynamics. A practical introduction. Springer,1999.*
- Initial Conditions

$$\begin{array}{rr} \rho_L = 1.0, & \rho_R = 0.125 \\ u_L = 0.75, & u_R = 0.0 \\ p_L = 1.0, & p_R = 0.1 \end{array}$$

- Computational domain $0 \leq x \leq 1$ discretized in two regions of $150$ elements
- The Interface is located at $x = 0.5$

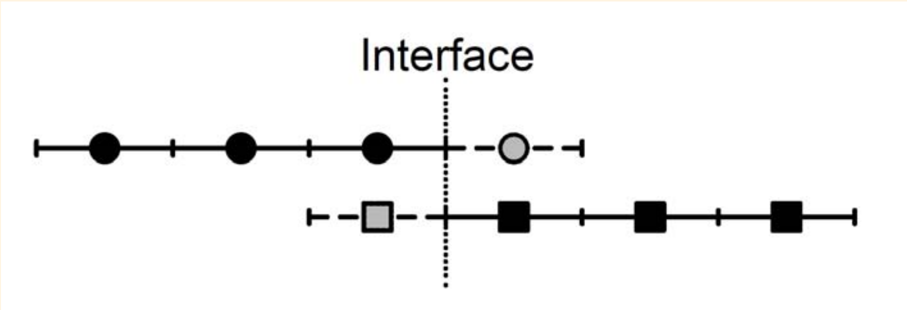

- 1D Unsteady Shock

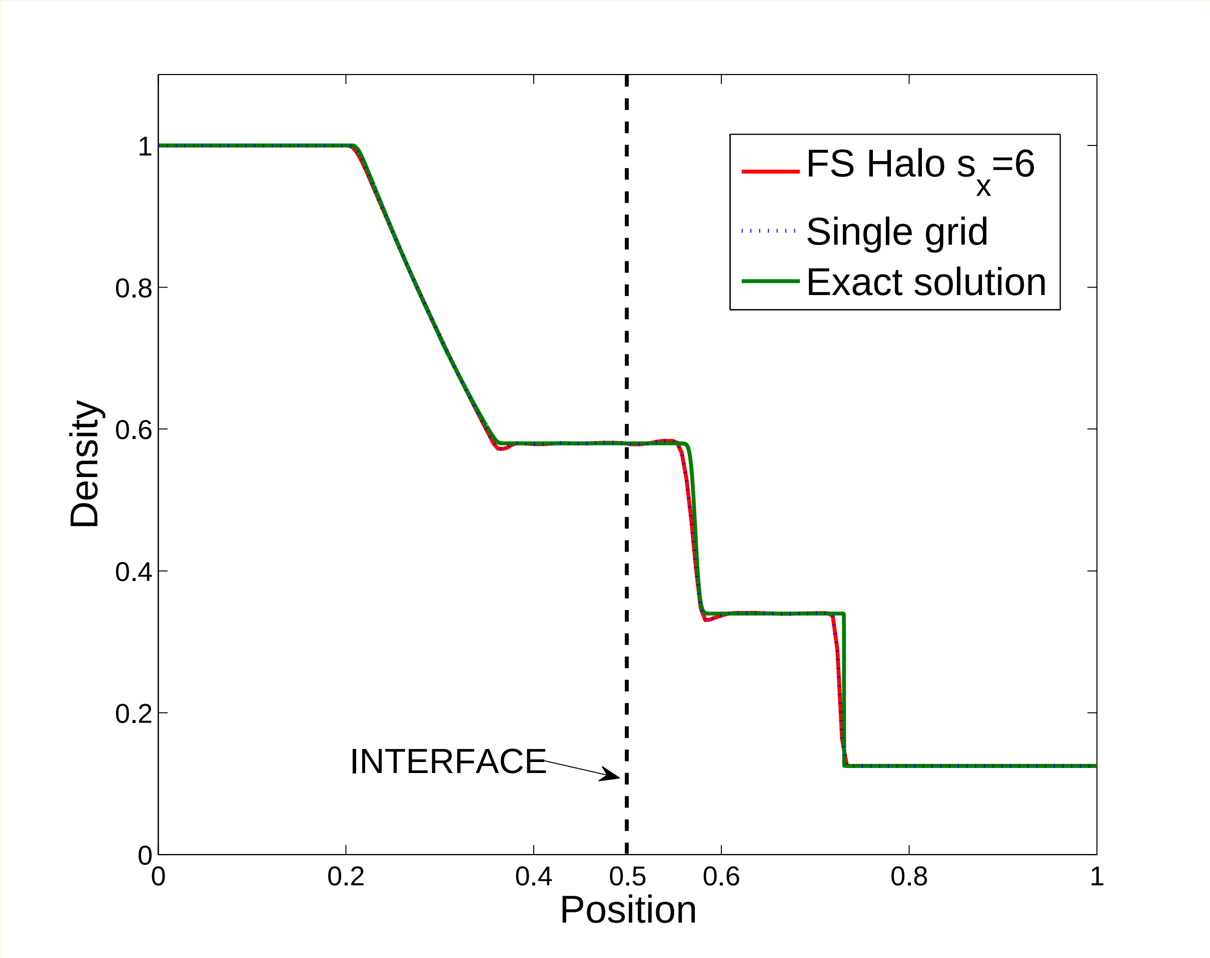

- 1D Unsteady Shock

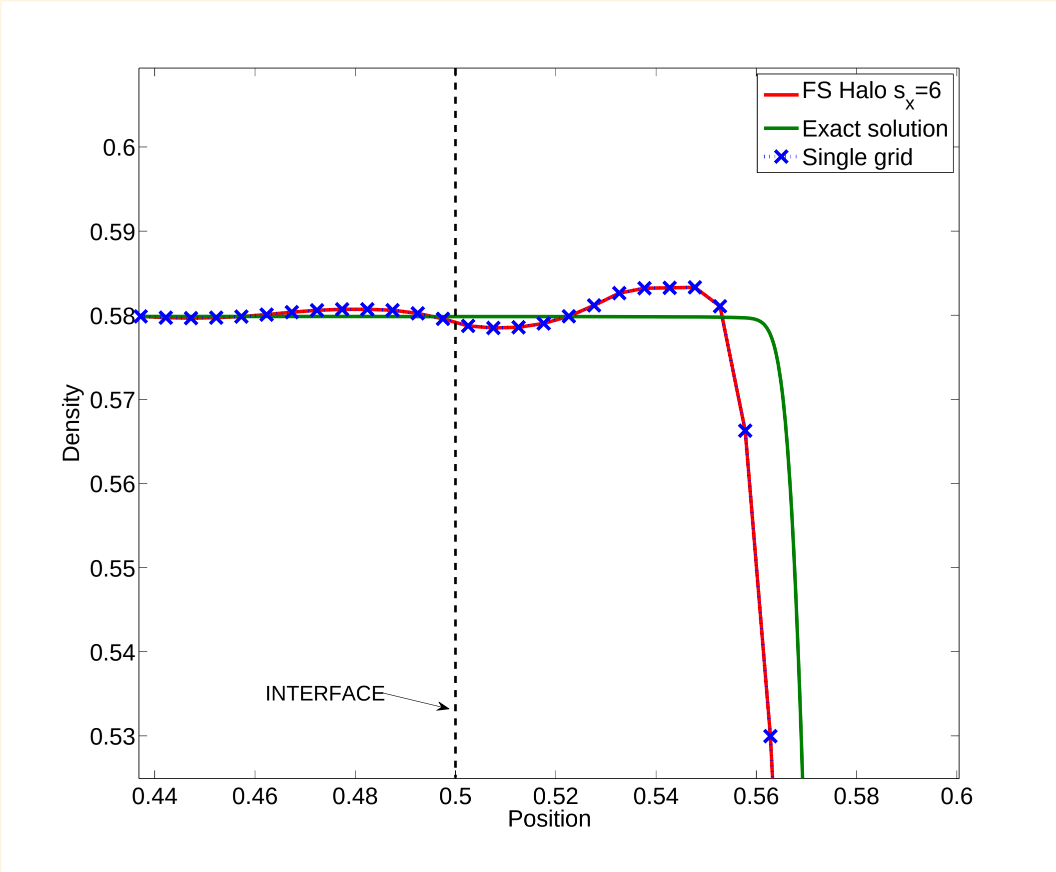

- Ringleb flow test case

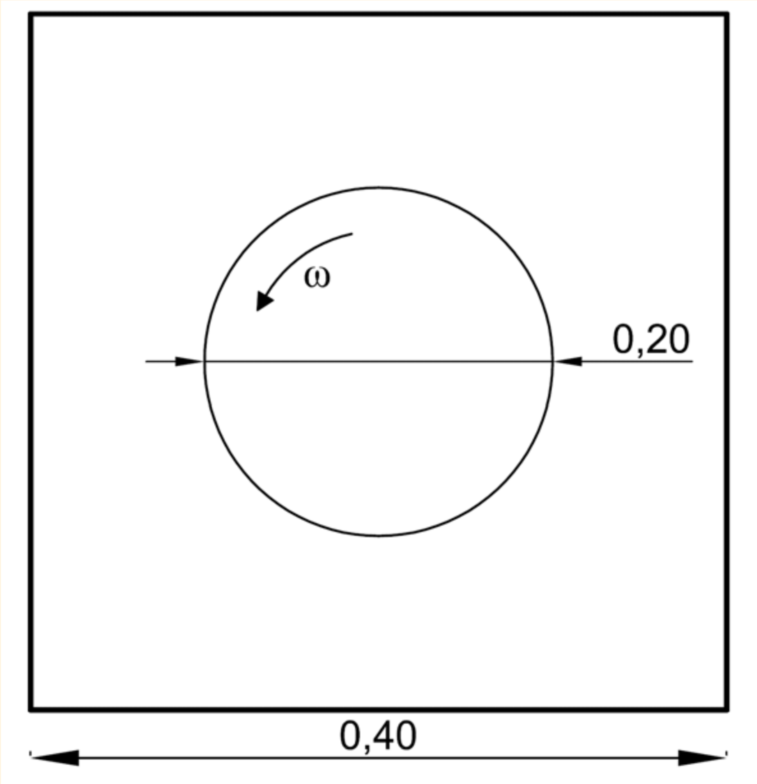


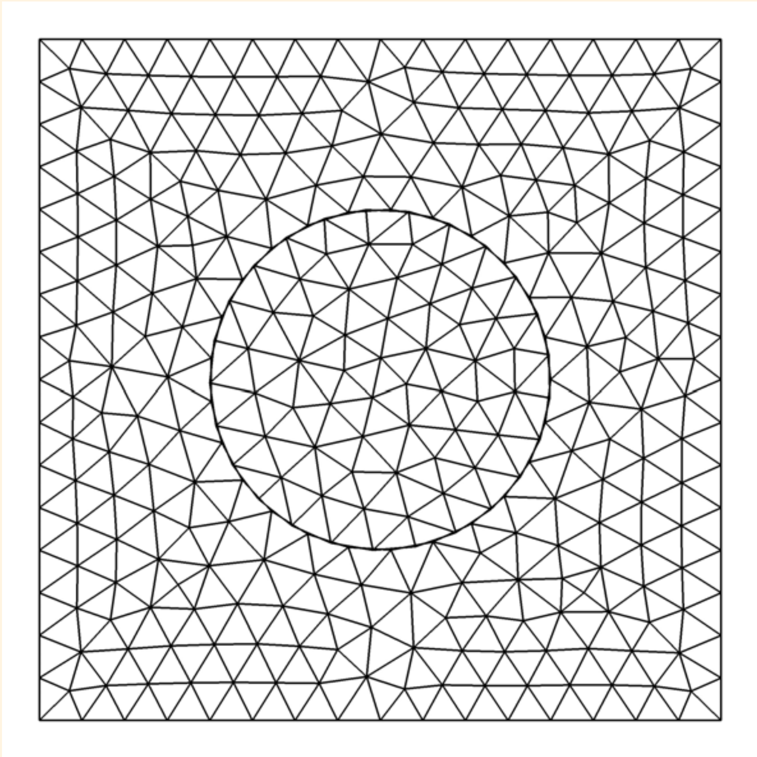

- Ringleb flow test case
  - Third order FV-MLS

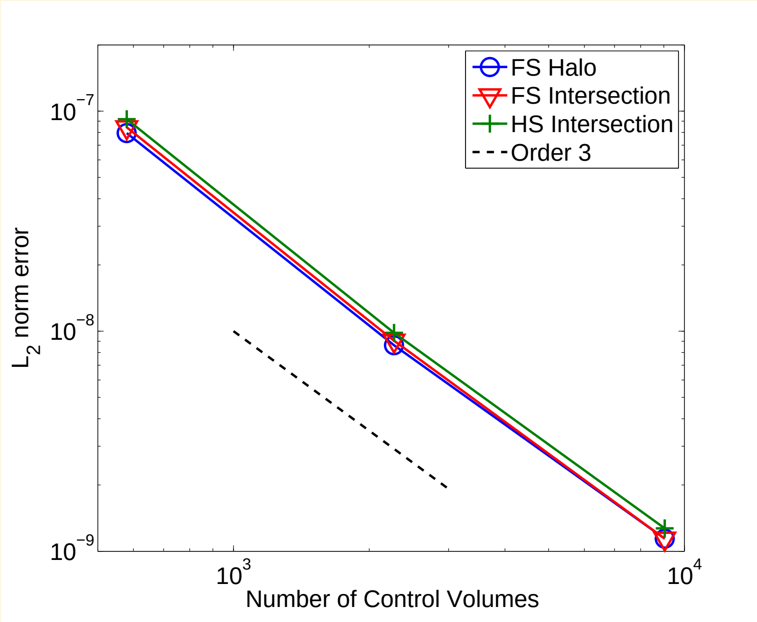


$\omega = 0$ rad/s

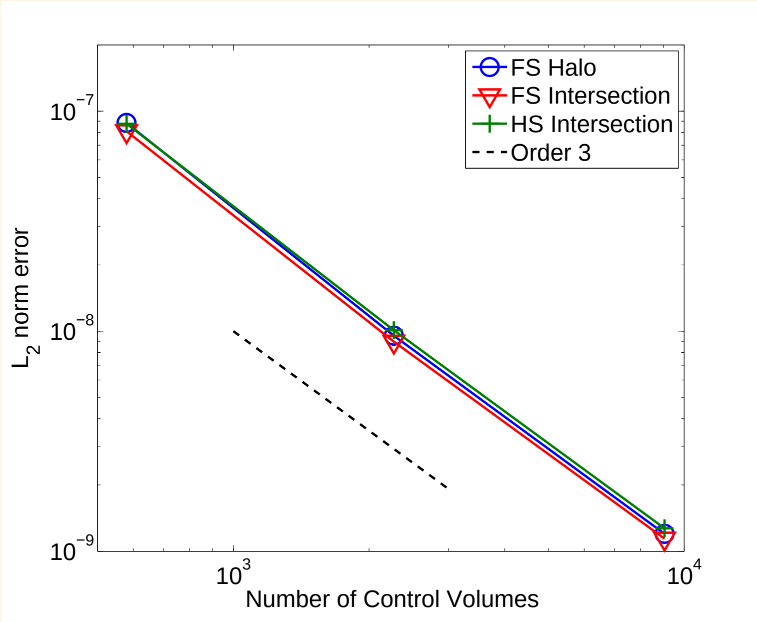


$\omega = 0.01$ rad/s

SHARK-FV 2015 Conference
SHARING HIGHER-ORDER ADVANCED RESEARCH KNOW-HOW on FINITE VOLUME
Ofir, Portugal
May 18 - 22, 2015

- Ringleb flow test case
  - Fourth order FV-MLS

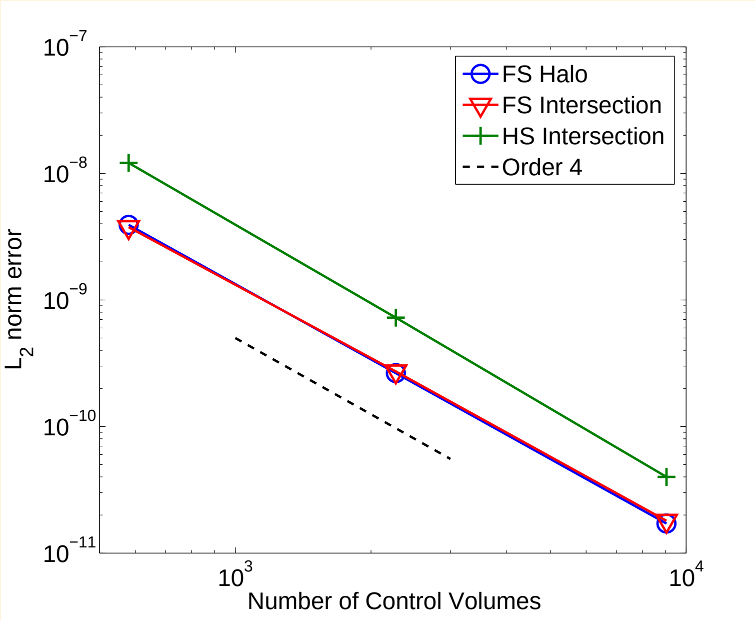


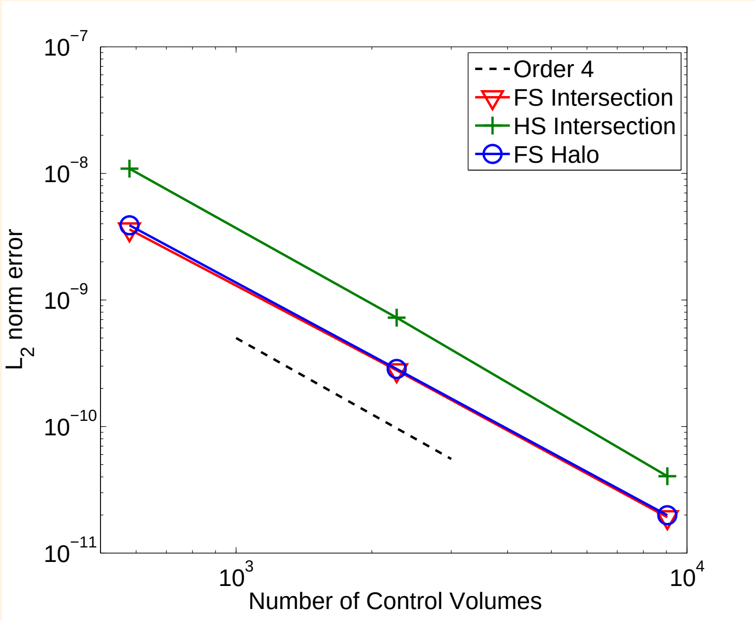


$\omega = 0$ rad/s $\qquad$ $\omega = 0.01$ rad/s

# Numerical Examples

- Ringleb flow test case
  - Conservation Error

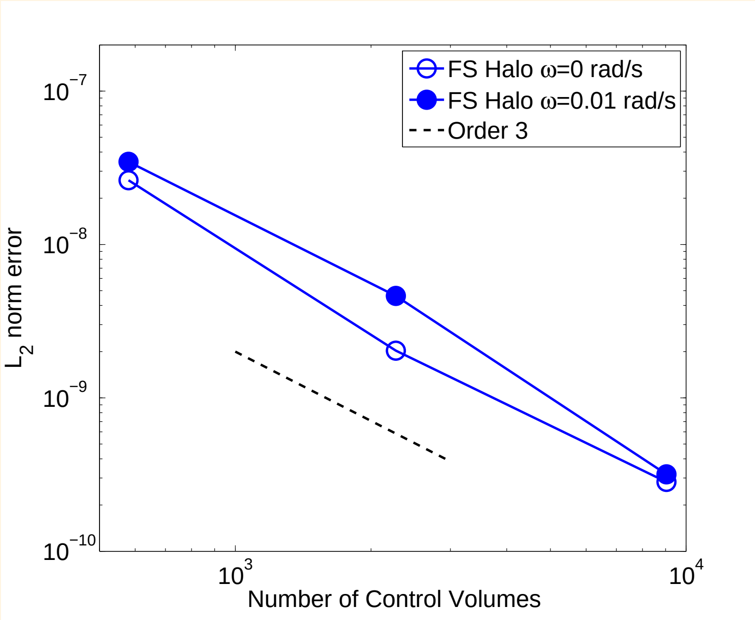


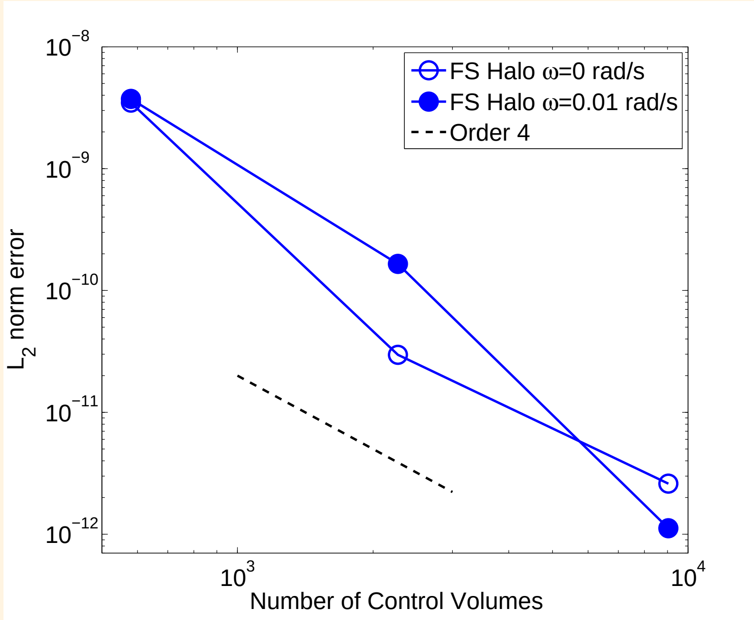


Third order

Fourth order

# Numerical Examples

- 2D Vortex Convection

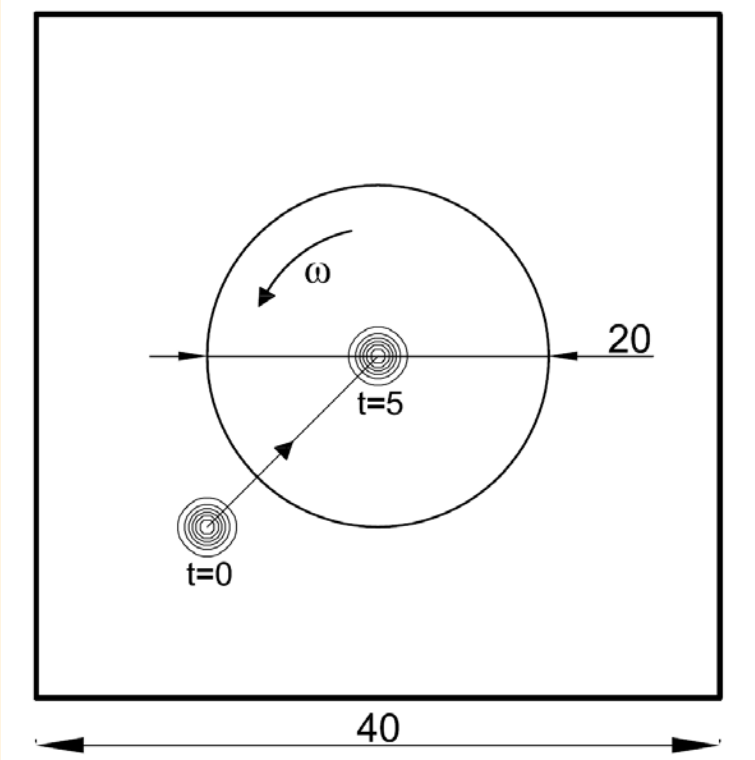


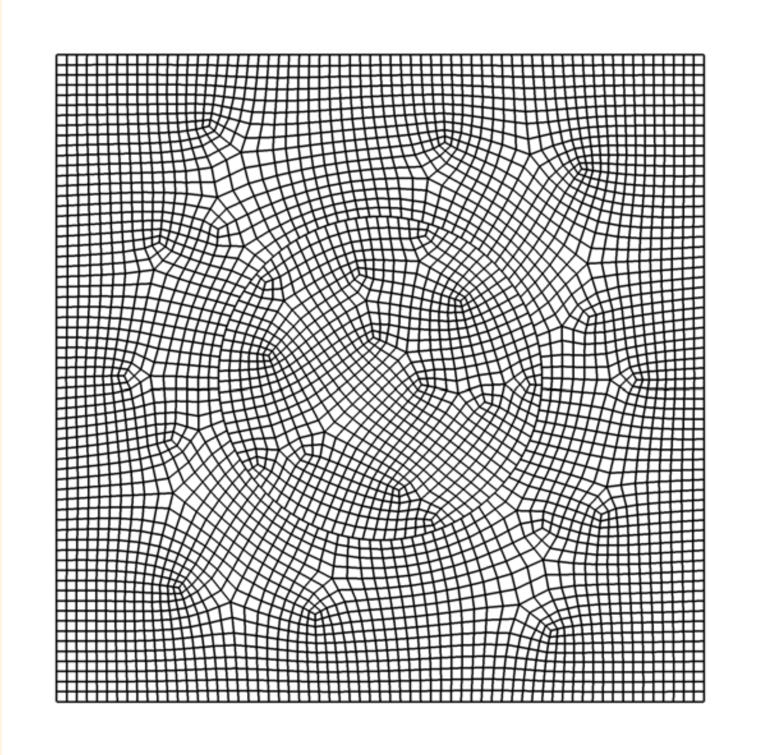

- 2D Vortex Convection
  - Third order FV-MLS

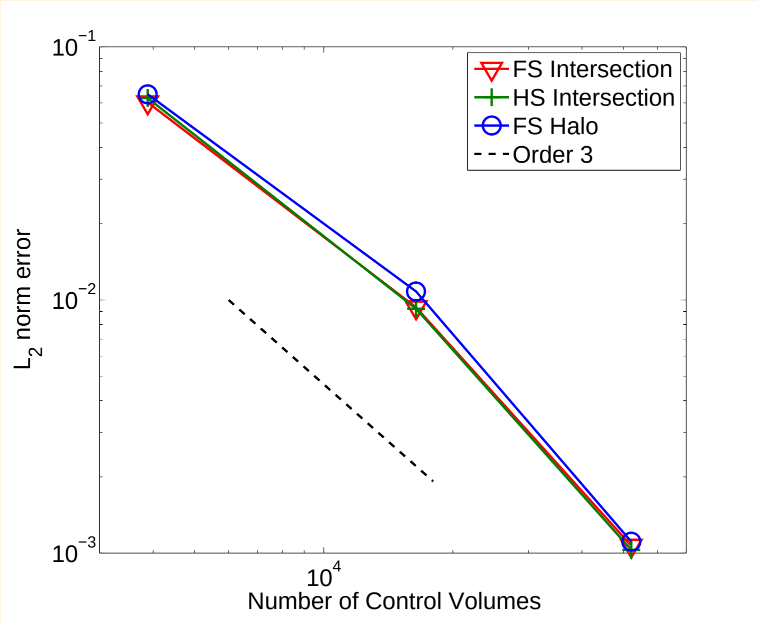


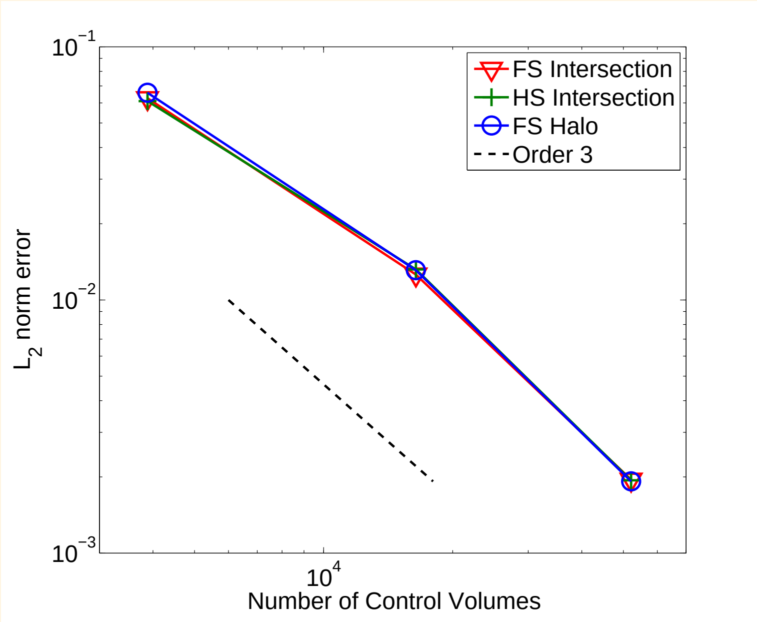


$\omega = 0$ rad/s

$\omega = 1.00$ rad/s

- 2D Vortex Convection
  - Conservation Error

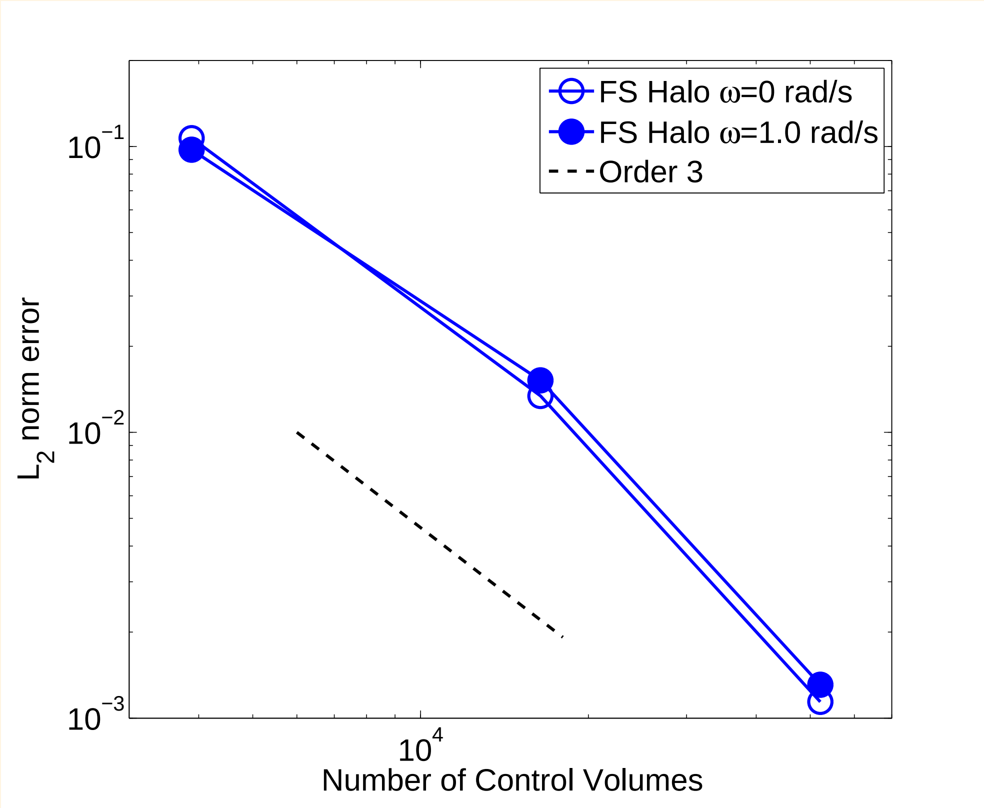


Third order

- Supersonic inviscid Flow over a cylinder. Mach 3

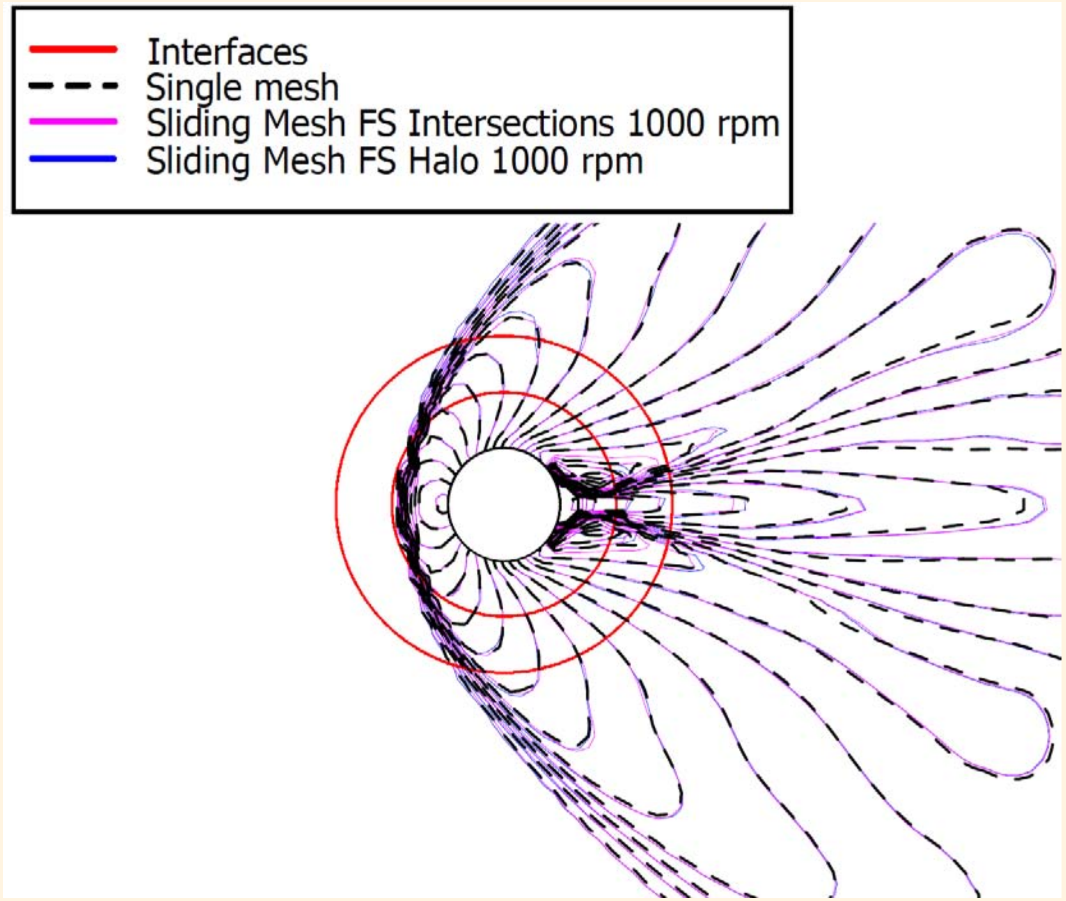

- Supersonic Flow over a cylinder. Mach 3

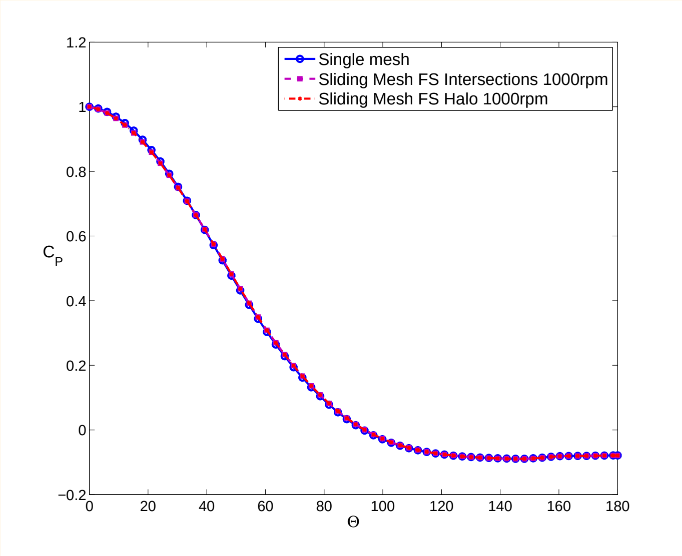


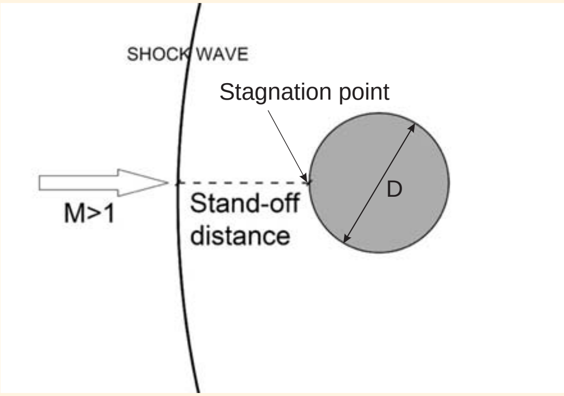


| Method | $p_0/(p)_\infty$ | Stand-off distance/D |
|---|---|---|
| Single mesh | 0.327 | 0.405 |
| Sliding Mesh FS Halo 0 rpm | 0.324 | 0.407 |
| Sliding Mesh FS Halo 1000 rpm | 0.324 | 0.408 |
| Sliding Mesh FS Intersections 1000 rpm | 0.324 | 0.408 |
| Reference solution | 0.328 | — |

- Incompressible flow around a cross-flow turbine.

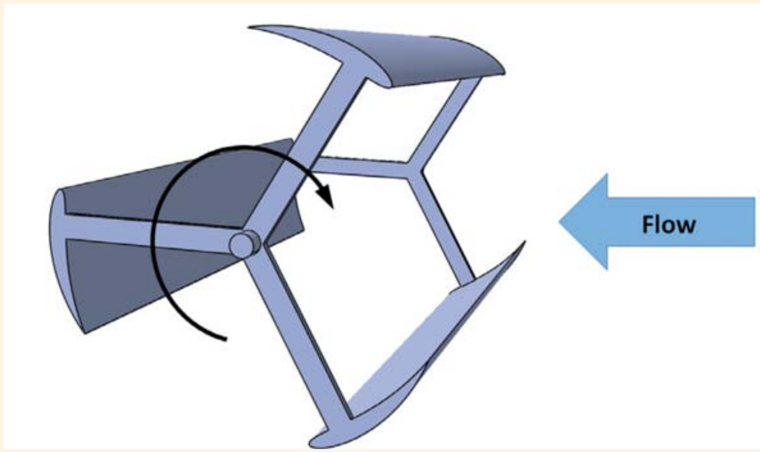


- Two test cases:
  - Single-bladed cross-flow turbine
  - Three-bladed cross-flow turbine

Problems Setup: E. Ferrer et al. A high order discontinuous galerkin fourier incompressible 3D Navier-Stokes solver with rotating sliding meshes. JCP, 231:7037-7056, 2012.

- Incompressible flow around a cross-flow turbine.

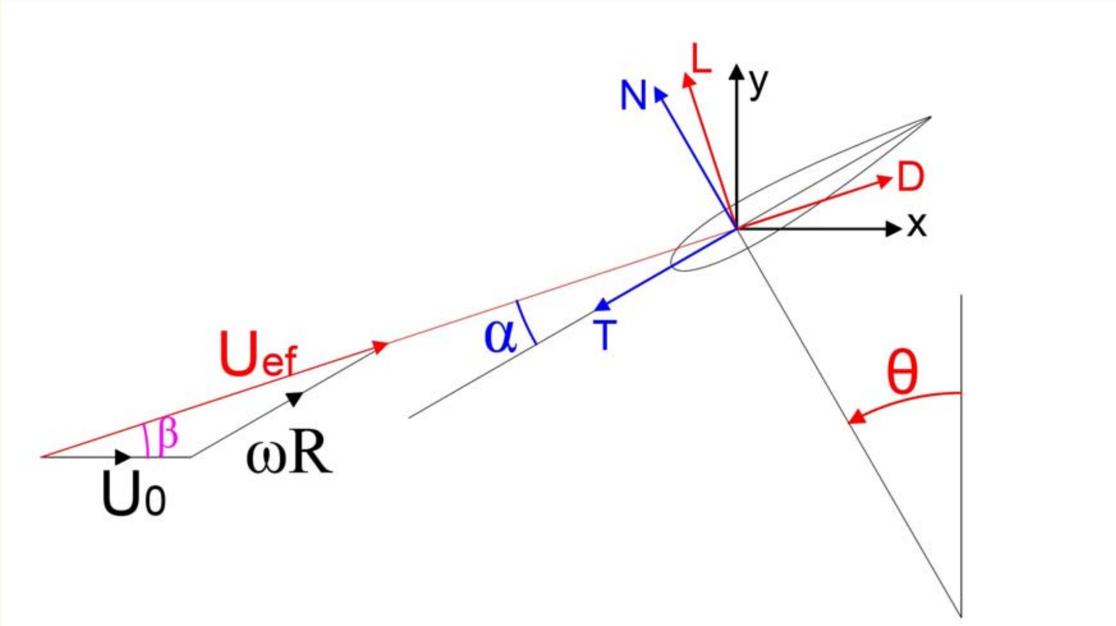


$$\vec{f} = \left\{ \begin{array}{c} f_x \\ f_y \end{array} \right\} = \oint (p\vec{n} - \nu(\nabla\vec{U}\cdot\vec{n}))d\Gamma$$

$$f_N = f_y \cos\theta - f_x \sin\theta \quad f_T = -f_x \cos\theta - f_y \sin\theta$$

- Single-bladed cross-flow turbine
  - Problem setup:

| Free-stream velocity $U_0$ | Rotational Speed $\omega$ | Tip Speed Ratio $\lambda = \omega R / U_0$ |
|---|---|---|
| $0.2$ | $0.5$ | $5$ |
| $0.5$ | $0.5$ | $2$ |
| $1.0$ | $0.5$ | $1$ |

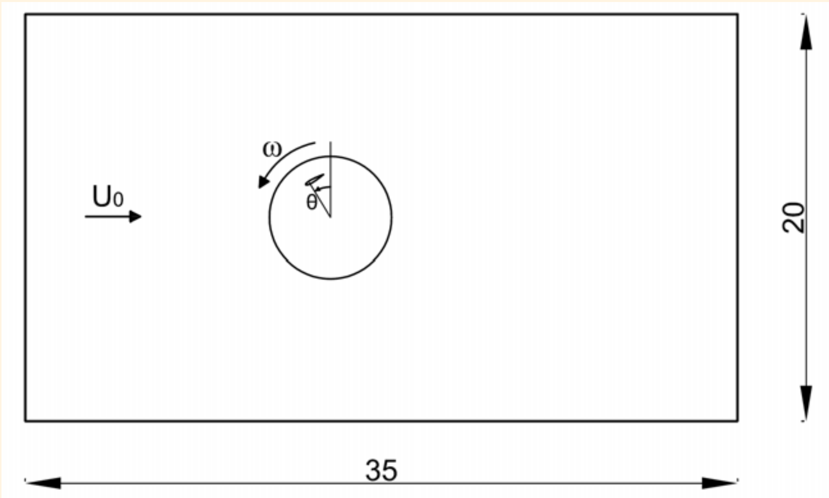

- Single-bladed cross-flow turbine

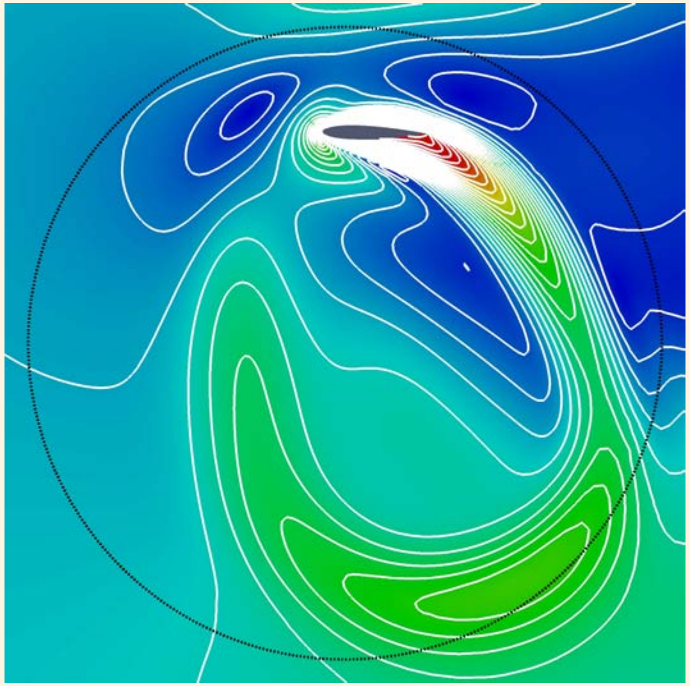

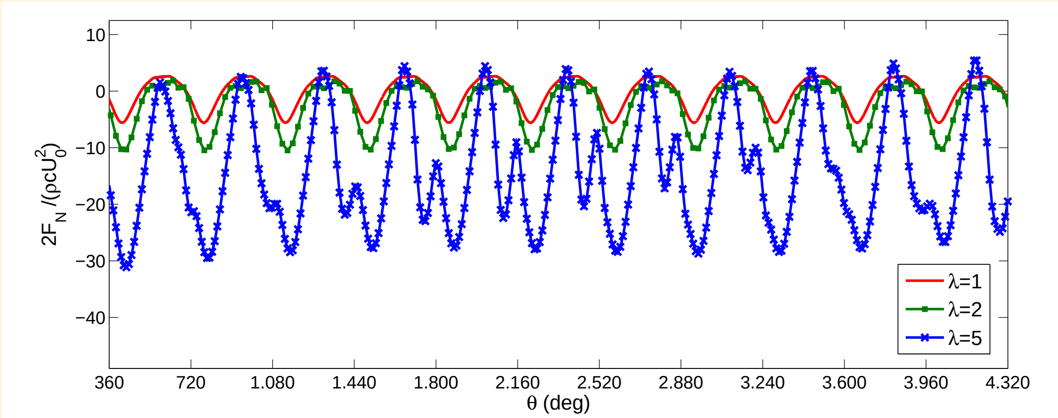


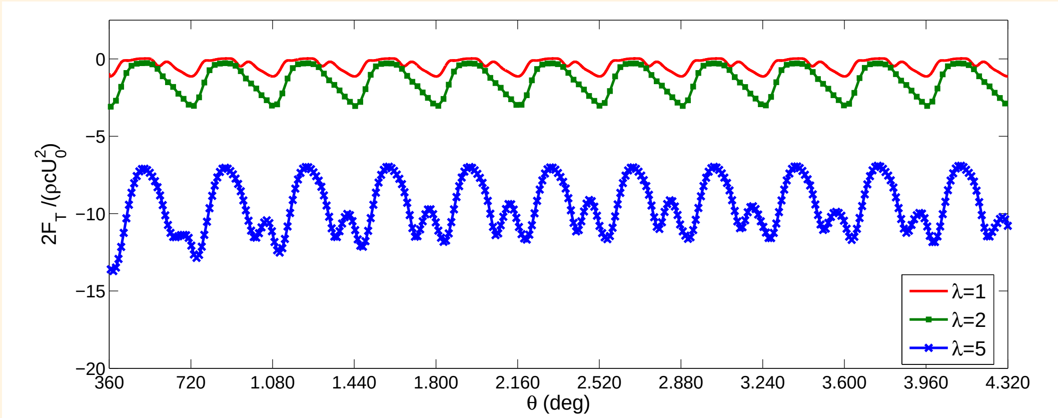

- Three bladed cross-flow turbine
  - Problem setup:
    - $U_0 = 0.5$ m/s
    - $Re = 50$
    - $\omega = 0.5$ rad/s $\rightarrow$ Tip-Speed Ratio (TSR)$= \frac{\omega R}{U_0} = 2$

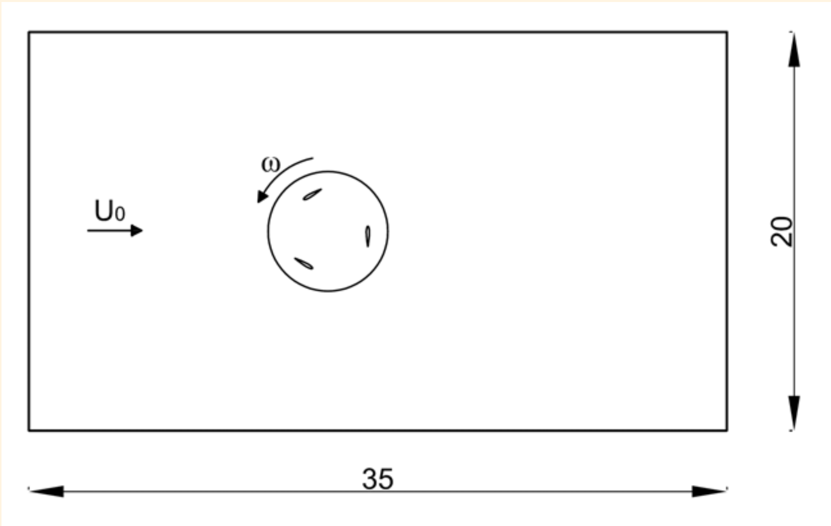


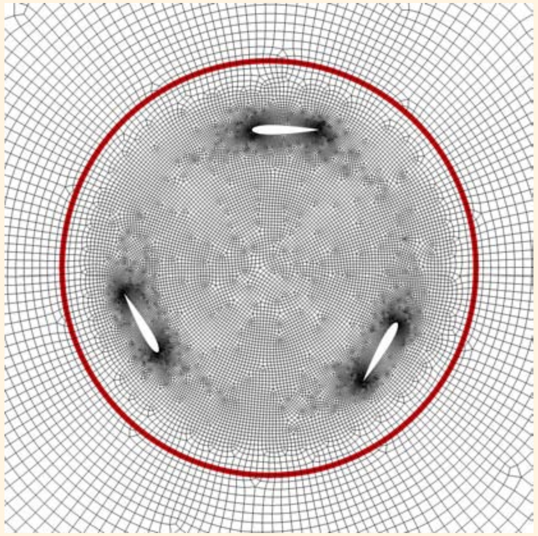

- Three bladed cross-flow turbine

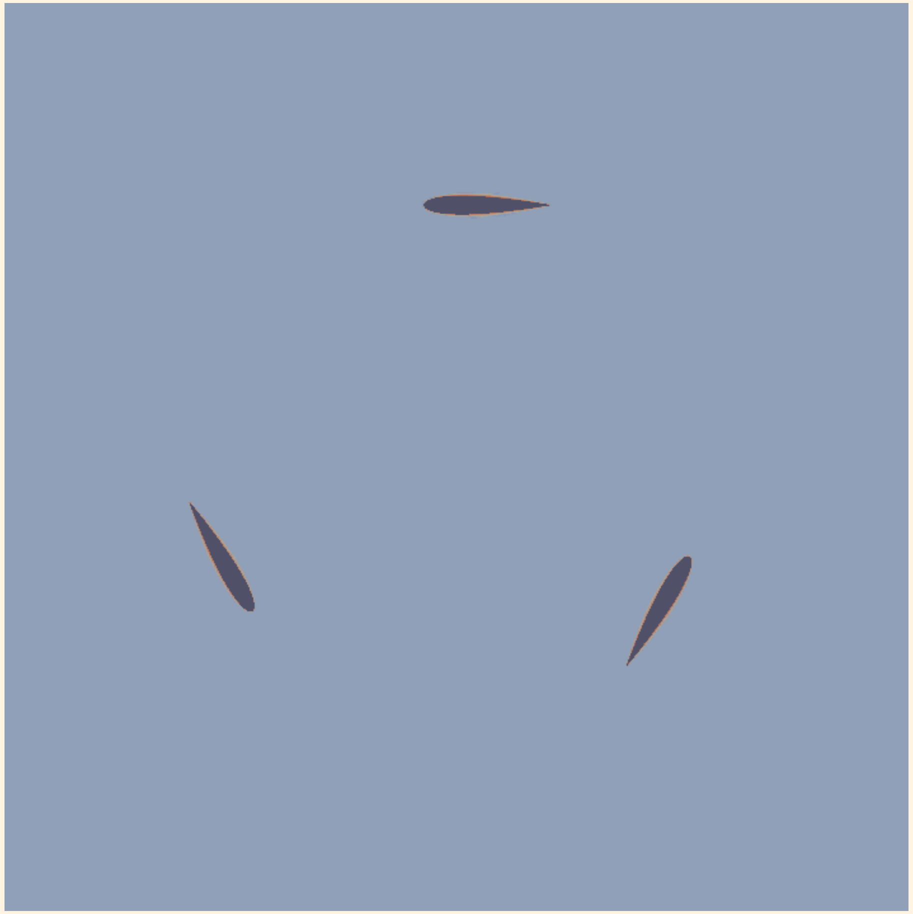

# Numerical Examples

- Three bladed cross-flow turbine

Normalized Normal Force

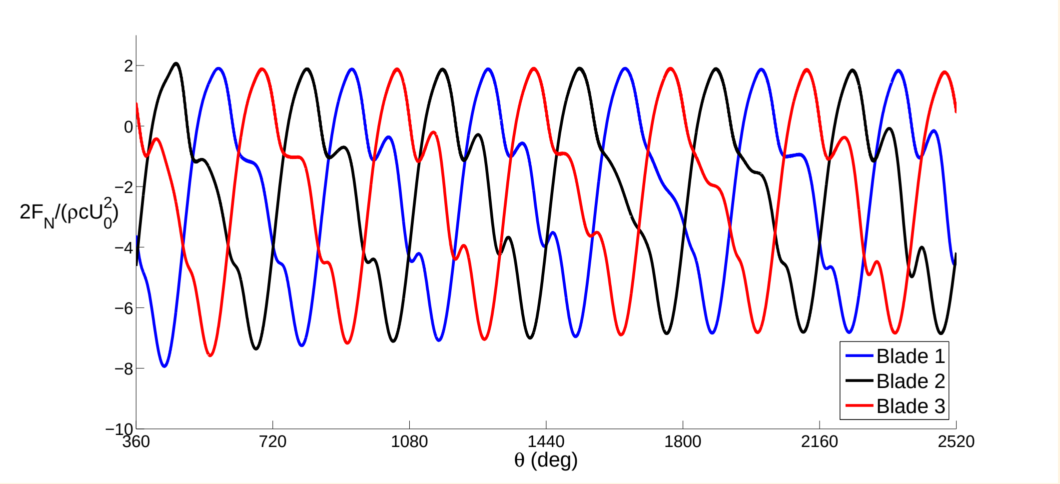


Normalized Tangential Force

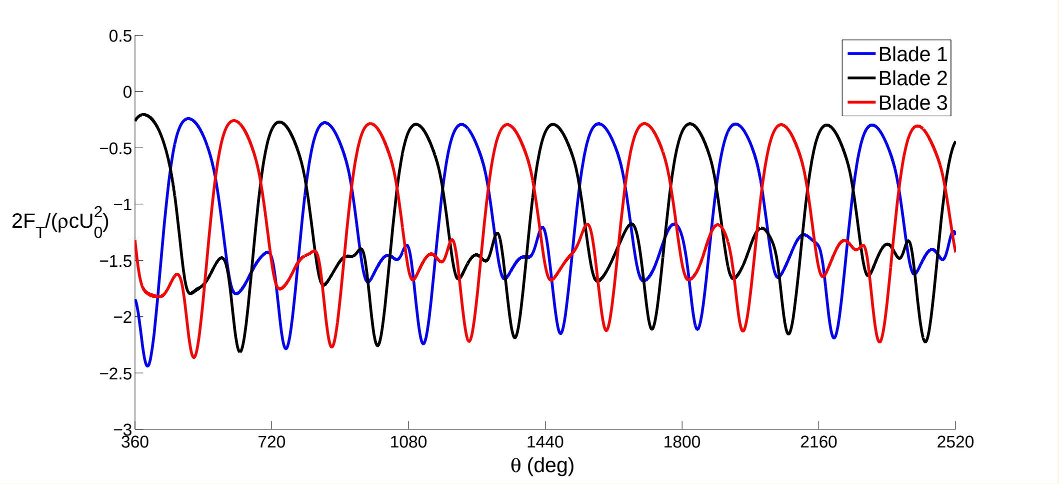

- Introduction
- The FV-MLS method
- Multiscale properties of MLS: MLS-based shock detection
- A formulation for all-speed flows
- A MLS-based sliding mesh technique
- Application to Navier-Stokes-Korteweg equations
- Conclusions

# Application to Navier-Stokes-Korteweg equations

- Navier-Stokes-Korteweg equations:
  - Density is the phase-field parameter
  - Simplest model for vaporization is the isothermal version
  - Spatial derivatives of order three
  - Very few numerical solutions (see D. Diehl, PhD. Thesis)

# Application to Navier-Stokes-Korteweg equations

- Phase-field modeling:
  - Initiated for phase evolution/transition problems
    - Phase separation of immiscible fluids
    - Vaporization and condensation
    - Solidification
  - Sound mathematics and thermodynamics
  - Successfully applied to other phenomena
    - Crack propagation
    - Thin liquid films
    - Porous media flow
    - Cancer growth

- Phase-field modeling

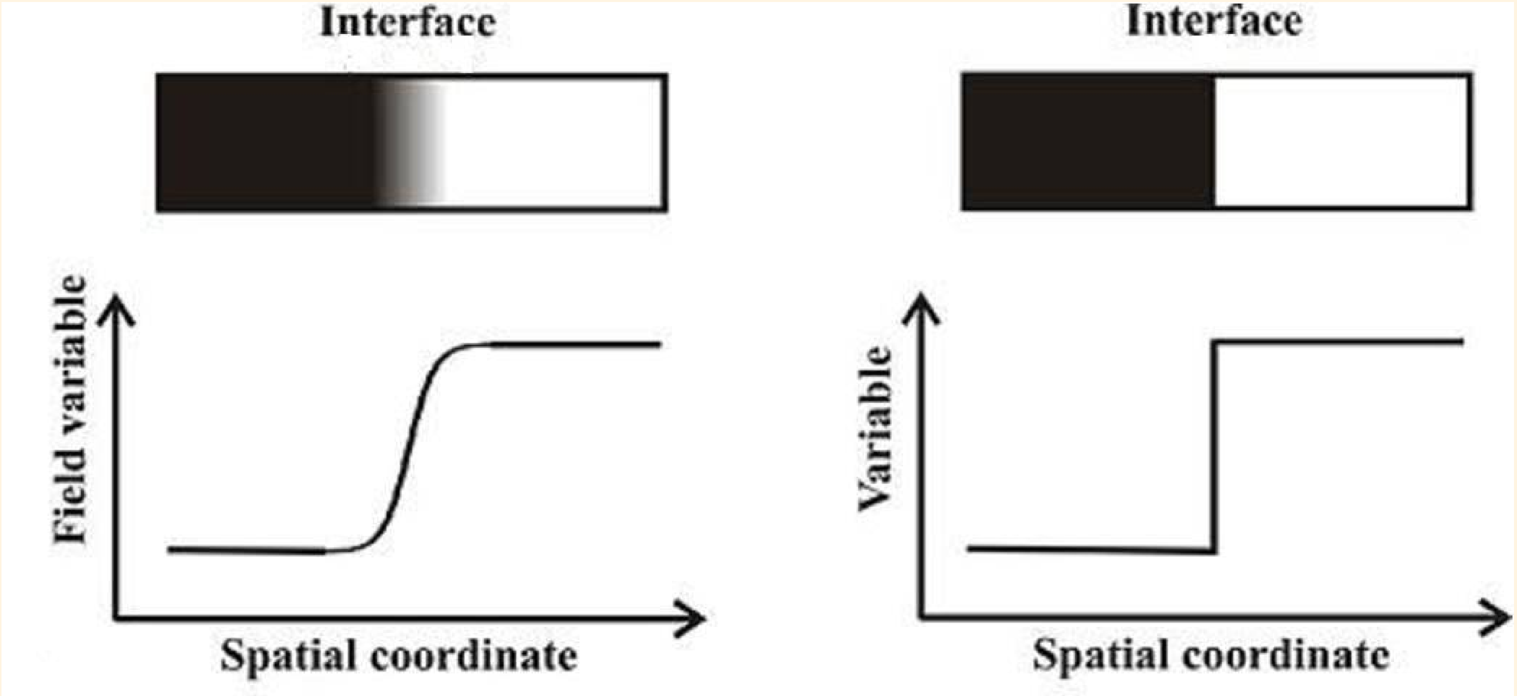

# Application to Navier-Stokes-Korteweg equations



- Sharp-interface models
  - Partial differential equations of the individual phases are coupled through interface boundary conditions
  - Very difficult numerically
- Phase-field models
  - Sharp interfaces approximated by thin layers described by higher-order differential operators
  - All variables are continuous across the interface
  - Examples:
    - Cahn-Hilliard equation
    - Navier-Stokes-Korteweg equations

# Application to Navier-Stokes-Korteweg equations

- Navier-Stokes-Korteweg equations

$$\frac{\partial \rho}{\partial t} + \nabla \cdot (\rho u) = 0$$

$$\frac{\partial \rho u}{\partial t} + \nabla \cdot (\rho u \otimes u) + \nabla p - \nabla \cdot \tau - \nabla \cdot \varsigma = S_b$$

where

$$\tau = \overline{\mu}(\nabla u + \nabla u^T) + \overline{\lambda} \nabla \cdot u \boldsymbol{I}$$

$$\varsigma = \lambda(\rho \nabla \rho + \frac{1}{2}|\nabla \rho|)\boldsymbol{I} - \lambda \nabla \rho \otimes \nabla \rho$$

The capillarity term may be written in non conservative form:

$$\nabla \cdot \varsigma = \lambda \rho \nabla (\Delta \rho)$$

- Model based on van der Waals equations

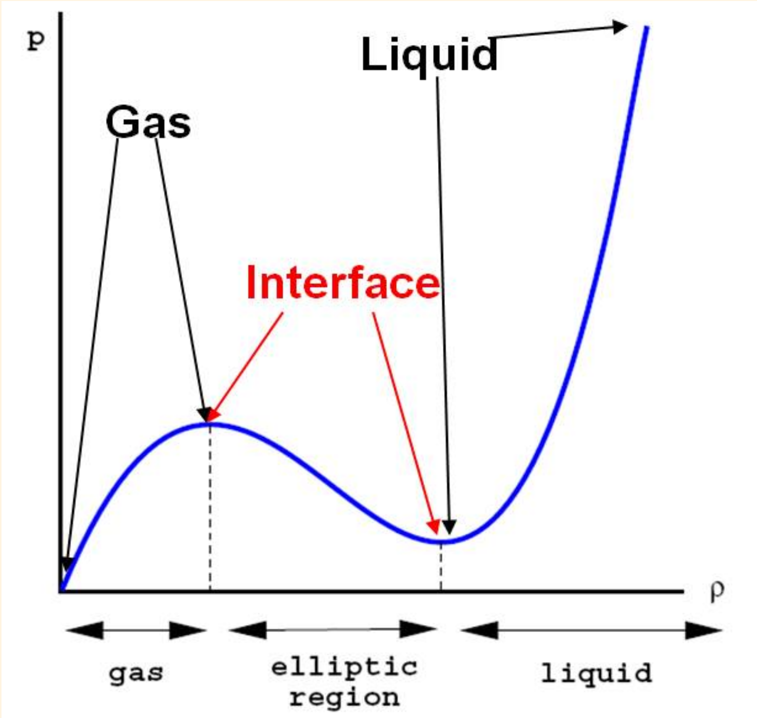


$$p(\rho) = Rb\frac{\rho\theta}{b - rho} - a\rho^2$$

$\theta$ is the temperature, $a, b$ are the van der Waals constants and $R$ is the universal gas constant

## Application to Navier-Stokes-Korteweg equations



- Convective term: Rusanov flux with Li and Gu's fix
- Korteweg term: Direct computation at Gauss points using MLS
- Interface upscaling
  - There is a very limited number of numerical solutions to the Navier–Stokes–Korteweg equations in the literature.
  - One of the main reasons is that NSK equations are only a realistic model if the thickness of the interfaces is extremely small.
  - The interfaces must be resolved by the computational mesh, which imposes severe restrictions on any numerical method.
  - We use a scaling according to which the thickness of the interfaces is adapted to the computational mesh[1].

[1] H. Gomez,T.J.R. Hughes, X. Nogueira, V. Calo *Isogeometric analysis of the isothermal Navier–Stokes–Korteweg equations*, CMAME, 199, 2010

# Application to Navier-Stokes-Korteweg equations



## ▶ Refinement methodology

- $Ca$ expresses the ratio between a characteristic length scale of the NSK equations and the arbitrary length scale $L_0$
- $Ca$ scales as the thickness of the interfaces.
- We propose to scale the capillarity number as:

$$Ca = \frac{h}{L_0}$$

- From dimensional analysis the product of $Re$ and $Ca$ must be a constant.

$$Re = \alpha \frac{L_0}{h}$$

$$L = 1,\ \alpha = 2,\ h = \max(V_i)^{1/d}$$

# Application to Navier-Stokes-Korteweg equations

- Two bubbles coalescence: $256^2$ grid

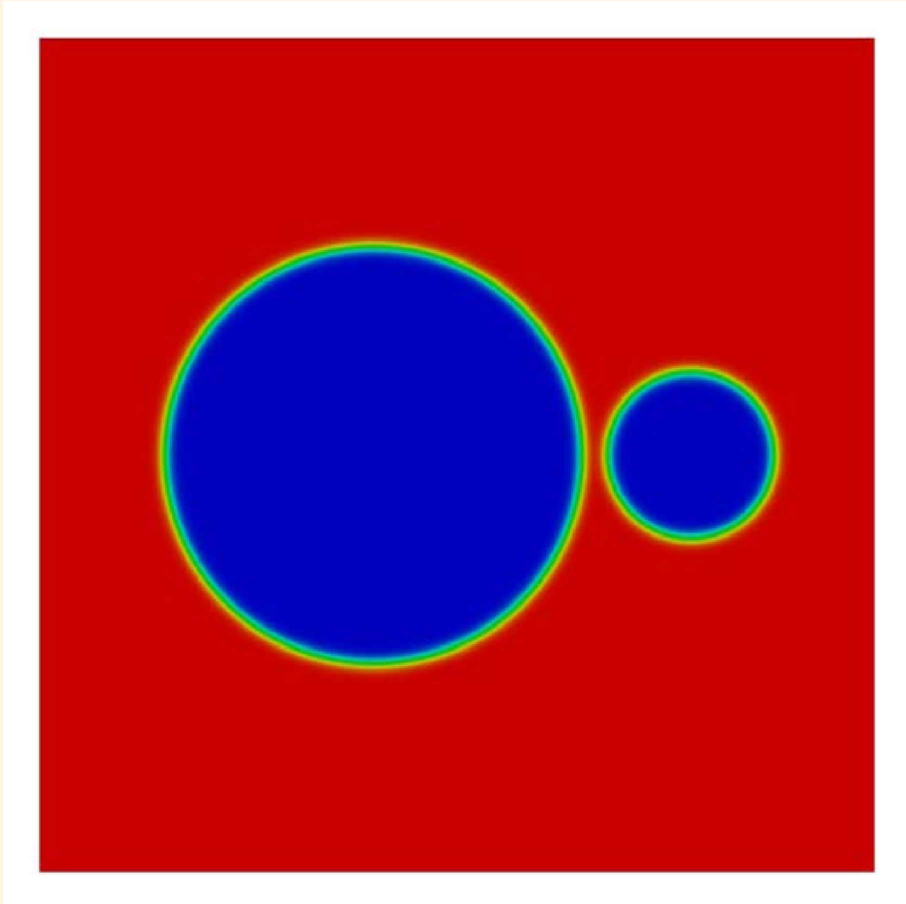

- Two bubbles coalescence: $256^2$ grid

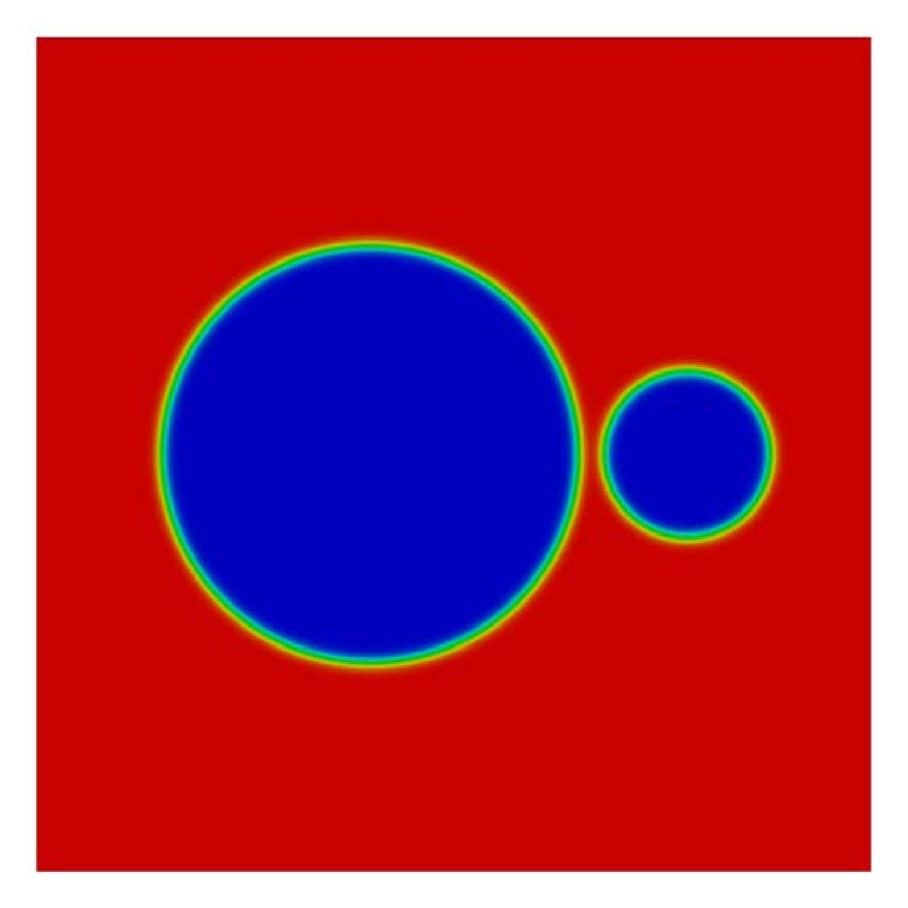

- Two bubbles coalescence: $256^2$ grid

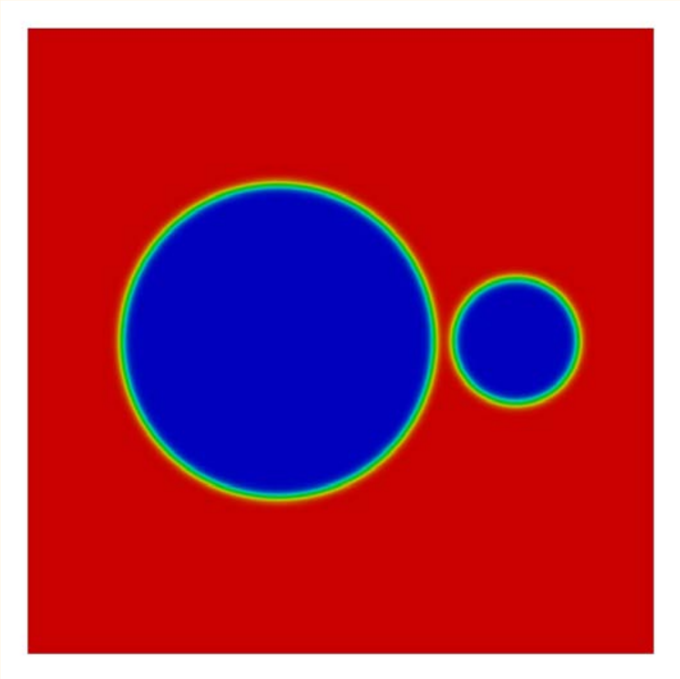

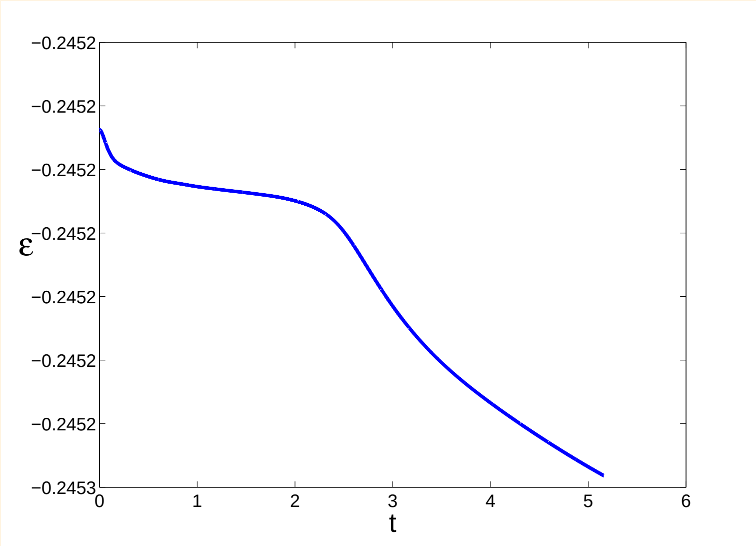

- Wet-wall boundary condition: $64^2$ grid

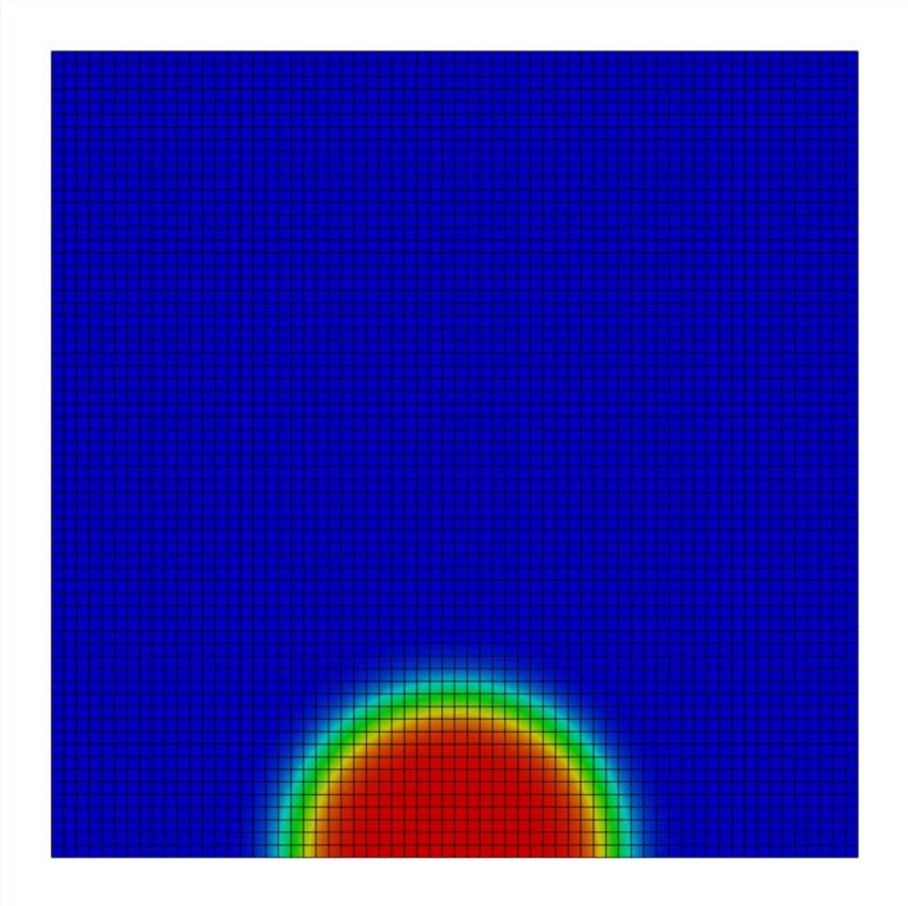

- Wet-wall boundary condition (intense gravity): $64^2$ grid

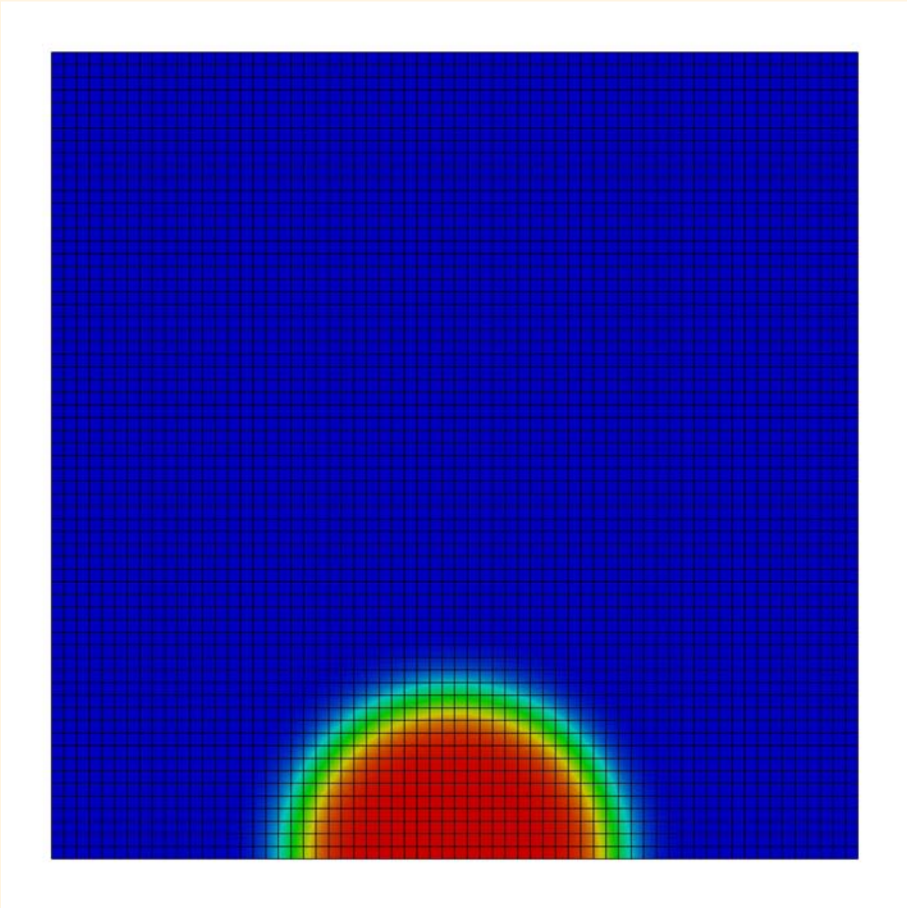

- Droplet falling interacting with an obstacle: $64^2$ grid

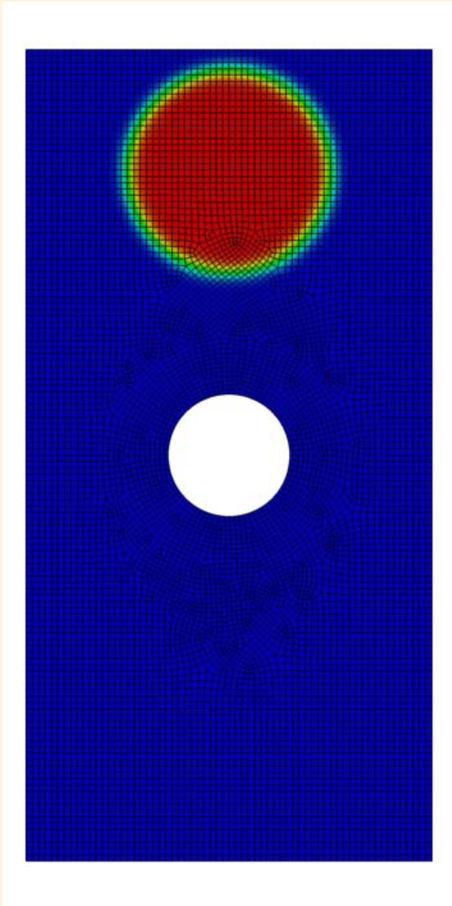

# Application to Navier-Stokes-Korteweg equations

- Two-phase spinodal decomposition with obstacles: $64^2$ grid

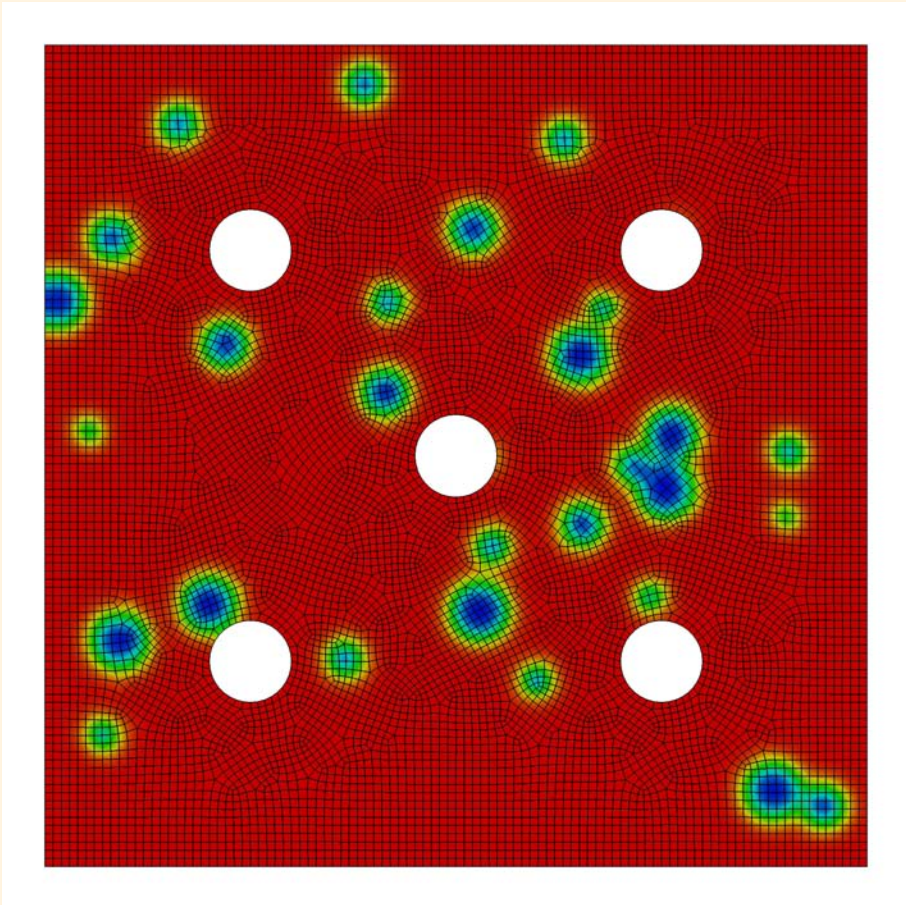

# Outline

- Introduction
- The FV-MLS method
- Multiscale properties of MLS: MLS-based shock detection
- A formulation for all-speed flows
- A MLS-based sliding mesh technique
- Application to Navier-Stokes-Korteweg equations
- Conclusions

# Conclusions



- Many numerical applications using MLS with FV schemes have been presented.
- The accuracy and robustness of the new methodologies have been shown with different numerical test cases.
- MLS allows increasing the accuracy and capabilities of current FV codes.
- FV-MLS is a good method for phase field models.


# HIGHER-ORDER FINITE VOLUME METHODS WITH MOVING LEAST SQUARES APPROXIMATIONS

Xesús Nogueira

email: xnogueira@udc.es

Thank you

—

# Acknowledgments


- This work has been partially supported by:
  - The *Ministerio de Educación y Ciencia* of the Spanish Government,
  - *Dirección Xeral de I+D* of the *Consellería de Innovación, Industria e Comercio* of the *Xunta de Galicia*,
  - the *Universidade da Coruña (UDC)*, and
  - the *Group of Numerical Methods in Engineering - GMNI*

# Some FV-MLS references


- L. Cueto-Felgueroso, I. Colominas, X. Nogueira, F. Navarrina, and M. Casteleiro, *Finite-volume solvers and moving least-squares approximations for the compressible Navier-Stokes equations on unstructured grids*, CMAME, 2007
- X. Nogueira, I. Colominas, L. Cueto-Felgueroso, and S. Khelladi, *On the simulation of wave propagation with a higher-order finite volume scheme based on reproducing kernel methods*, CMAME, 2010
- X. Nogueira, L. Cueto-Felgueroso, I. Colominas, F. Navarrina, and M. Casteleiro, *A new shock-capturing technique based on moving least squares for higher-order numerical schemes on unstructured grids*, CMAME, 2010
- X. Nogueira, L. Cueto-Felgueroso, I. Colominas, H.Gómez,*Implicit Large Eddy Simulation of non-wall-bounded turbulent flows based on the multiscale properties of a high-order finite volume method*, CMAME, 2010
- X. Nogueira, S. Khelladi, I. Colominas, L. Cueto-Felgueroso, J. París, and H. Gómez, *High-resolution finite volume methods on unstructured grids for turbulence and aeroacoustics*, ARCME, 2011
- S. Khelladi, X. Nogueira, F. Bakir, and I. Colominas, *Toward a higher-order unsteady finite volume solver based on reproducing kernel particle method*, CMAME, 2011.
- J.C. Chassaing, S. Khelladi, and X.Nogueira, *Accuracy assesment of a high-order moving least squares finite volume method for compressible flows*, C&F, 2013
- L. Ramirez, X. Nogueira, S. Khelladi, J.C. Chassaing, and I. Colominas, *A new higher-order finite volume method based on moving least squares for the resolution of the incompressible Navier-Stokes equations on unstructured grids*, CMAME, 2014